

Distinguish modular categories and 2+1D topological orders beyond modular data: Mapping class group of higher genus manifold

Xueda Wen¹ and Xiao-Gang Wen¹

¹*Department of Physics, Massachusetts Institute of Technology, Cambridge, MA 02139, USA*

(Dated: August 29, 2019)

It was believed that modular data are enough to distinguish different modular categories (and topological orders in 2+1-dimensions). Then counterexamples to this conjecture were found by Mignard and Schauenburg in 2017. In this work, we show that the simplest counterexamples can be distinguished by studying the representations of mapping class groups of a punctured torus or a genus-2 closed manifold.

CONTENTS

| | | |
|---|--|----|
| | 3. Mapping class group of genus-2 surface and knot/link invariants | 39 |
| I. Introduction | 1 | |
| A. Main results | 3 | |
| B. Mapping class group | 4 | |
| C. Representation of mapping class group | 5 | |
| D. Topological invariants | 6 | |
| II. MS modular categories | 7 | |
| A. Anyons | 7 | |
| B. Modular data | 8 | |
| 1. Equivalence of modular data | 9 | |
| III. Representations of mapping class group: quasi-particle basis | 10 | |
| A. MS modular categories with $G = \mathbb{Z}_{11} \times \mathbb{Z}_5$ | 10 | |
| 1. Simple currents | 13 | |
| B. Punctured S and T matrices | 14 | |
| 1. Gauge freedom and patterns in the solutions | 15 | |
| C. Distinguish MS MTCs with $S^{(z)}$ and T | 17 | |
| D. Topological invariants: Trace of words and link invariants | 18 | |
| 1. Punctured torus | 19 | |
| 2. Genus two | 21 | |
| IV. Topological lattice gauge theory | 22 | |
| A. Exactly solvable model | 22 | |
| B. Modular transformation | 24 | |
| 1. Genus one | 24 | |
| 2. Punctured torus | 26 | |
| 3. Genus two | 27 | |
| C. Topological invariants | 29 | |
| V. Discussion and conclusion | 31 | |
| Acknowledgement | 32 | |
| A. More on twisted quantum double of $G = \mathbb{Z}_q \times_n \mathbb{Z}_p$ | 32 | |
| 1. Basic property of $G = \mathbb{Z}_q \times_n \mathbb{Z}_p$ | 32 | |
| 2. More on modular S matrix | 33 | |
| B. On algebraic theory of anyons and others | 34 | |
| 1. Properties of punctured S matrix | 35 | |
| a. Other punctured S matrices | 37 | |
| 2. More on representations of mapping class group | 38 | |
| C. More on topological lattice gauge theory | 39 | |
| 1. Topological invariants based on a punctured torus | 39 | |
| 2. More punctures | 41 | |
| 3. Twisted quantum double of $G = \mathbb{Z}_p$ | 41 | |
| 4. Some path integrals on 3-simplices | 42 | |
| D. Galois symmetry in the modular data | 43 | |
| References | 44 | |

I. INTRODUCTION

Landau pointed out the reason that two states of matter belong to different phases is that they have different symmetries.¹ In last 30 years, we started to realize that two quantum states of matter with identical symmetry can still belong to different phases.² Those quantum states are complicated many-body states. Beside characterize them as messy and complex, it is hard to describe their internal structure, not to mention to distinguish them as different phases of matter. In 1989, a method to probe the internal structures of those messy complex many-body states was discovered: we put the many-body system on closed spatial manifold M^d with different topologies, and then measure the ground state degeneracy $GSD(M^d)$.^{2,3} Such topology dependent ground state degeneracy $GSD(M^d)$ reveal the universal internal structures of the many-body state. A concept of *topological order* was introduced to describe such an internal structure which is beyond the Landau symmetry breaking order.

If one accepts such topological order as a new kind of order, one may ask if the ground state degeneracy $GSD(M^d)$ for different spatial topologies fully characterize topological order or not? It turns what that the answer is no. So finding physical quantities that can fully characterize topological order is a key central question in developing a comprehensive theory of topological order. In early days, it was proposed to use non-Abelian geometric phases⁴ of the degenerate ground states induced by deforming the space, to further characterize topological order.^{5,6} Since the non-Abelian geometric phases lead to a representations of mapping-class-group (MCG) of the space M^d : $\mathcal{R}(g)$, $g \in \text{MCG}(M^d)$, it was proposed⁵ to use

those representations $R(g)$ of $\text{MCG}(M^d)$ to fully characterize topological order, and to develop a comprehensive theory of topological order.

For 2+1D topological order, the MCG for a torus is $\text{MCG}(S^1 \times S^1) \cong \text{SL}(2, \mathbb{Z})$. Also there is natural way to choose a canonical basis for the degenerate ground states on torus.^{7,8} The representation of $\text{SL}(2, \mathbb{Z})$ in the canonical basis is generated by S and T matrices, which are called the modular data. It turns out that S and T matrices in the canonical basis contain a lot of information about the 2+1D topological order. For a long time people speculate that modular data (*i.e.* representations of $\text{MCG}(T^2)$), plus the central charge of the edge states,⁹ can fully characterize 2+1D topological order.¹⁰⁻¹² However, recently in Ref. 13, Mignard and Schauenburg (MS) found some topological orders that have the same modular data and central charge. Thus, modular data and central charge are not enough to fully characterize topological order. In this paper, we will show that representations of genus-2 mapping class group $\text{MCG}(\Sigma_2)$ can distinguish those topological orders discovered in Ref. 13.

To understand why some topological orders cannot be distinguished by modular data, let us introduce another way to characterize topological orders. Instead of using the general ground states on closed spatial manifold M^d with various topologies, we may also consider the ground states on punctured sphere S_{punc}^d with various punctures to characterize 2+1D topological orders. This leads to the unitary modular tensor category (MTC) theory for 2+1D topological orders, where the punctures correspond to the objects in the MTC. MTC are algebraic models of anyons (*i.e.* the punctures) in 2+1D topological phases of matter.^{10,11} It is suggested that the data of a modular category should be supported on the punctured sphere up to 4 punctures, the torus, and the once-punctured torus, with consistency relations supported on the 5-punctured sphere and twice-punctured torus^{14,15} (See also the related discussions in the content of conformal field theory¹⁶⁻²⁰).

The modular data of a modular tensor category \mathcal{C} , also named S and T matrices, are square matrices indexed by the simple objects or anyons. They can be viewed as the representation of the modular group of a genus-one closed surface T^2 , realized by the modular action on the quasi-particle basis. In fact, this is how the name of ‘modular data’ comes. Alternatively, these two matrices can be considered as topological invariants in the framework of topological quantum field theory (TQFT): S matrix is related to the Hopf-link invariants colored by two simple objects, and T matrix can be viewed as a single loop with a twist. Practically, S matrix determines the fusion rules of anyons through Verlinde formula. With a properly chosen basis, the modular T matrix is a diagonal matrix with entries θ_a , where θ_a is the topological spin for anyon a . The modular T matrix is of finite order due to Vafa’s theorem.¹⁹ Physicists proposed to use S and T matrices as order parameters for the classification of topological phases of matter.²¹ It was believed/conjectured that a modular category is fully determined by the modular data.^{5,6,22} In a computer-based work,²³ it is found that the modular data are a complete invariant for $D^\omega(G)$, which are twisted Drinfeld doubles of

finite groups G , when the group order $|G|$ is smaller than 32.

Later in 2017, in the work by Mignard and Schauenburg,¹³ a family of counterexamples were discovered showing that arbitrarily many inequivalent modular categories can share the same modular data. These counterexamples are found among the quite accessible class of MTCs, *i.e.*, twisted quantum doubles of finite groups. These counterexamples are defined over the same non-abelian finite group but twisted with different cocycles.

Then one question arises naturally: How to distinguish these counterexamples? In the original paper by MS,¹³ the authors found these categories to be distinct by proving the inexistence of suitable equivalences, but not by finding extra topological invariants to distinguish them. It is desirable to find certain physical quantities to distinguish these different categories.

There may be two ways to study this problem. One way is based on the fact that modular S and T matrices are associated with the Hopf-link and a twisted unknot invariants, respectively. We know there are infinite types of links (with two components or multi components) and knots. It is natural to search for other link or knot invariants beyond the Hopf-link and the twisted unknot. This is the method used in Refs.15, 24, and 25. In Ref.15, it is found that all the knots that are two-braid closures colored by $a \in \Pi_{\mathcal{C}}$ and all the links that are two-braid closures with the two components colored by $a, b \in \Pi_{\mathcal{C}}$ are determined by the modular data, where $\Pi_{\mathcal{C}}$ represents the collection of anyons in the modular tensor category \mathcal{C} . Therefore, the next candidates to distinguish the MS MTCs may be found among the links and knots which are at least three-braid closures.

Then in Ref.15, it is found that the whitehead link invariant together with the T matrix can be used to distinguish the simplest counterexamples in MS MTCs. Later in Ref.24, based on a computer search, it is found that many link and knot invariants together with T matrix can fulfill the same aim. Remarkably, in Ref.25, it is *proved* that the Borromean ring together with T matrix are enough to distinguish *all* the counterexamples in MS MTCs. One common feature of these non-trivial link/knot invariants that go beyond modular data is that they are the closure of braids with more than two strands. In fact, all the nontrivial link/knot invariants mentioned above are the closure of three-strand braids. Note that the inverse is not true, *i.e.*, a closure of braids with more than two strands may not be able to distinguish the counterexamples in MS MTCs.

The other way is based on the fact that modular S and T matrices correspond to the representations of mapping class group of a torus. Since the modular data on a torus is not enough, it is natural to study the MCG representations of higher-genus surface⁵ with or without punctures. With the representations of the MCG of higher genus manifold, one may define topological invariants to distinguish the counterexamples in MS-MTCs. This is the main aim of this work.

One may wonder if we can distinguish different counterexamples in MS MTCs by using the full algebraic data $\{N_{ab}^c, R_a^{bc}, F_d^{abc}\}$, which represent the fusion multiplicities, R -matrix, and F -matrix, respectively.^{10,16,26} The problem is

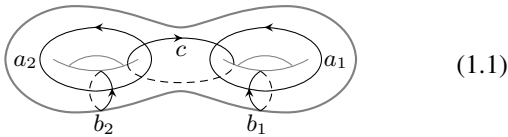
that one needs to solve the pentagon and hexagon equations, which is a hard problem even for MTCs with a small number of simple objects. As will be seen shortly, the simplest counterexamples in MS MTCs are non-abelian theories with 49 anyons, and it is a formidable task to solve for the corresponding F and R matrices. In addition, there is too much information in F and R matrices including the gauge redundancy. It is desirable for us to find a minimal set of gauge invariant data to fully determine different MS MTCs.

A. Main results

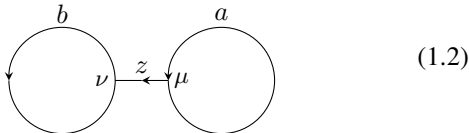
We have seen that the modular data from a torus is not enough to characterize 2+1D topological orders. To find more data, it is natural to consider MCG representations for a genus-2 surface. We find that MCG representations for a genus-2 surface indeed add extra data, beyond that of representations for the genus-1 surface. This points to a direction to build a quantitative theory of topological order in any dimensions based on MCG representations.

In this paper, we concentrate on 2+1D topological orders. We study the representations of the MCG of a punctured torus $\Sigma_{1,1}$ and a closed manifold of genus two $\Sigma_{2,0}$ for a MTC. This is used to distinguish the simplest counterexamples in MS MTCs with $G = \mathbb{Z}_{11} \rtimes \mathbb{Z}_5$ twisted by the 3-cocycles $\omega \in H^3(G, U(1))$. There are in total 5 different categories \mathcal{C}_u with $u = 0, 1, 2, 3, 4$, but only 3 inequivalent modular data. In particular, the categories $\mathcal{C}_{u=1}$ and $\mathcal{C}_{u=4}$ share the same modular data, $\mathcal{C}_{u=2}$ and $\mathcal{C}_{u=3}$ share the same modular data, and $u = 5$ has another set of modular data.

For a closed genus-2 surface $\Sigma_{2,0}$, the five generators of $\text{MCG}(\Sigma_{2,0})$ may be considered as the Dehn twists along the five closed curves a_1, a_2, b_1, b_2 , and c as follows:



The basis vectors for the degenerate ground states of a topological order on a genus-2 surface $\Sigma_{2,0}$ can be chosen as



where a, b , and z denote anyon types, and μ and ν denote the fusion channels. By studying how the modular transformations act on the basis vectors, one can define the representations of $\text{MCG}(\Sigma_{2,0})$ for the five generators (Dehn twists) as $T_{a_1}, T_{b_1}, T_{a_2}, T_{b_2}$, and T_c . Alternatively, we can define the S matrix as $S_i = T_{b_i} \cdot T_{a_i}^{-1} \cdot T_{b_i} = T_{a_i}^{-1} \cdot T_{b_i} \cdot T_{a_i}^{-1}$. Then by rewriting $T_i := T_{a_i}$ ($i = 1, 2$), the representations of the five generators of $\text{MCG}(\Sigma_{2,0})$ are denoted as T_1, S_1, T_2, S_2 , and T_c . It is found that T_i and S_i ($i = 1, 2$) are also the representations of the generators of $\text{MCG}(\Sigma_{1,1})$, where $\Sigma_{1,1}$ is a punctured torus. For this reason, we may call S_i the punctured

S matrix, in comparison to the modular S matrix for a torus without puncture.

In this work, we solve the punctured matrices S_i and T_i ($i = 1, 2$) explicitly. With these data, we can distinguish the 5 different categories in MS MTCs in the following different ways:

(i) *Punctured S matrix together with modular T matrix.*

There are gauge freedoms in the punctured S matrix. However, the diagonal parts of a punctured S -matrix are gauge invariant, and can be used to distinguish the counterexamples in MS MTCs. More explicitly, by relabeling anyons, the modular T matrix for $\mathcal{C}_{u=1(2)}$ is sent to T for $\mathcal{C}_{u=4(3)}$. Then one can find that with the same way of relabeling anyons, one can not send the diagonal parts of punctured S matrix for $\mathcal{C}_{u=1(2)}$ to those for $\mathcal{C}_{u=4(3)}$. That is, the diagonal parts of punctured S matrix together with the modular T matrix can be used to distinguish the 5 different categories.

(ii) *Topological invariants.*

We propose an efficient and simple way to distinguish the MS MTCs. We construct the topological invariants based on the trace of *words* as follows:

$$W_{\Sigma_{2,0}} = \text{Tr}(D_1^{n_1} \cdots D_i^{n_i} \cdots) \quad (1.3)$$

where the *letters* D_i can be arbitrarily chosen among the representations of the five generators in $\text{MCG}(\Sigma_{2,0})$, and n_i is an arbitrary integer. Here the trace is taken over the Hilbert space of degenerate ground states on genus-2 surface $\Sigma_{2,0}$.

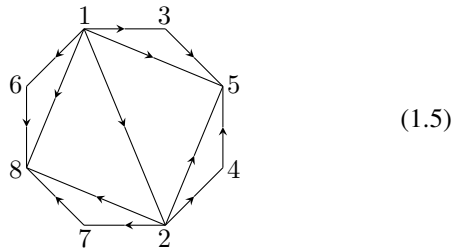
There are infinite number of words that can be used to distinguish the MS MTCs. As a simple example, we can choose $W_{\Sigma_{2,0}} = \text{Tr}[(T_1)^7(S_1)^{-7}]$, and the result of topological invariants for the 5 different MS MTCs is:

$$W_{\Sigma_{2,0}} = \begin{cases} a_0 + b \cdot e^{\frac{i2\pi}{5} \times 0}, & u = 0, \\ a_1 + b \cdot e^{\frac{i2\pi}{5} \times 1}, & u = 1, \\ a_2 + b \cdot e^{\frac{i2\pi}{5} \times 2}, & u = 2, \\ a_2 + b \cdot e^{\frac{i2\pi}{5} \times 3}, & u = 3, \\ a_1 + b \cdot e^{\frac{i2\pi}{5} \times 4}, & u = 4, \end{cases} \quad (1.4)$$

where a_i and b are certain constants (see Table XII). It is found a single topological invariant can be used to distinguish different categories. This is in contrast to Refs.15, 24, and 25 where one needs to track how the link/knot invariant changes by permuting anyons. The topological invariant defined above is independent of the permutation or relabeling of anyons. Furthermore, we show that each topological invariant in (1.3) is related to a specific link invariant.

As an alternative approach, we study the representation of $\text{MCG}(\Sigma_{2,0})$ for a general Dijkgraaf-Witten theory with a finite group G and three-cocycle $\omega \in H^3(G, U(1))$ on the lattice. We consider the minimal triangulation of a genus-2 sur-

face as follows:



where we identify the edges [24] with [35], [45] with [13], [27] with [68], and [78] with [16]. This triangulation has six triangle faces and only one vertex. By defining the ground state wavefunction on the above triangulated lattice, we can perform Dehn twists on this lattice, and study how the basis vectors transform into each other. Then we can obtain the representations of these generators. The only input are the finite group G and the 3-cocycle ω .

We apply this lattice gauge theory approach to MS MTCs with $G = \mathbb{Z}_{11} \times \mathbb{Z}_5$. Since the ground state bases we choose are different from the quasi-particle bases, the matrices S_i and T_i (which are basis dependent) look totally different from those obtained in the quasi-particle bases. But the topological invariants obtained from these two different approaches are the same, as expressed in (1.4). More topological invariants are presented in Sec.IV.

The methods discussed above also apply to the punctured torus (see more detail in the main text) and a higher-genus surface.

In short, by considering the MS MTCs on the genus-2 surface and a punctured torus, we use both the quasi-particle basis calculation and the lattice gauge theory approach to obtain the representations S_i and T_i in $\text{MCG}(\Sigma_{2,0})$ and $\text{MCG}(\Sigma_{1,1})$. With these representations S_i and T_i , we construct the topological invariants to distinguish the simplest counterexamples in MS MTCs that cannot be distinguished by the modular data.

The rest of this work is organized as follows. We introduce the basic properties of mapping class group (MCG) of a surface of genus g with n punctures, and then introduce how to construct the topological invariants based on the representations of MCG in the rest of the introduction. In Sec.II, we give a brief review of the MS modular categories, including the types of anyons and the modular data. Then in Sec.III, by focusing on the simplest counterexamples in MS MTCs, we study the representations of the mapping class group of a punctured torus and a genus-two surface. With these representations, we construct topological invariants to distinguish different MS MTCs. In Sec.IV, with an independent method on the topological lattice gauge theory, we study the representations of MCG on a genus-2 manifold and a punctured torus for a general Dijkgraaf-Witten theory. We apply the general results to the MS MTCs, and obtain the same results of topological invariants as those in Sec.III. We give some discussions and conclude in Sec.V. We also give several appendices on the properties of MS MTCs, algebraic theory of anyons and its application in the MCG representations, and further details on the lattice gauge theory approach and so on.

B. Mapping class group

In this subsection, we give a brief introduction to the mapping class group (MCG) of a connected and orientable two-dimensional surface with and without punctures.

We denote the connected and orientable surface of genus g with n punctures as $\Sigma_{g,n}$, where the genus g is the number of handles as shown in Fig.1, and the n punctures are obtained by removing n individual points from the surface. It is usually convenient to think of the punctures as marked points on the surface.

For simplicity, we start from a closed oriented manifold $\Sigma_{g,0}$ of genus g without punctures. Its topology is completely classified by the Euler number $\chi(\Sigma_{g,0}) = 2 - 2g$. The first homology group $H_1(\Sigma_{g,0})$ has the dimension $\dim H_1(\Sigma_{g,0}) = 2g$, and we can choose a canonical homology basis $\{a_i, b_i\}$ ($i = 1, \dots, g$) as shown in Fig.1. That is, the first homology group $H_1(\Sigma_{g,0})$ is generated by the $2g$ loops a_i and b_i in Fig.1.

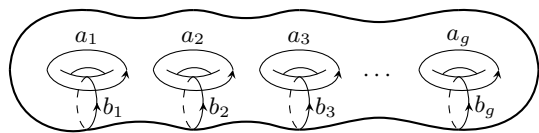


FIG. 1. Homology basis for a surface of genus g .

Once the homology basis $\{a_i, b_i\}$ ($i = 1, \dots, g$) is chosen, it is useful to represent the manifold $\Sigma_{g,0}$ in terms of a $4g$ -side polygon in the following way. We choose a basepoint x_0 on $\Sigma_{g,0}$, and cut the surface along the $2g$ curves that are homologous to the canonical basis. Then the Riemann surface unfolds into a $4g$ polygon (see Fig.2 for the example of $\Sigma_{2,0}$). Note that that all the $4g$ vertices of the polygon are identified to a single point (which is the basepoint x_0 here) on the Riemann surface. Equivalently, a Riemann surface $\Sigma_{g,0}$ can be considered as the quotient space of a polygon with the edges identified in pairs. To indicate which paired edges are to be identified, we start at a definite vertex, proceed around the boundary of the polygon, and record the letters assigned to the different sides in succession. If the arrow on the side points in the same (opposite) direction that we go around the boundary, then we write the letter for that side with exponent 1 (-1). For the case of $g = 2$ in Fig.2, the identifications of edges are indicated by the symbols $b_2^{-1}a_2^{-1}b_2a_2b_1^{-1}a_1^{-1}b_1a_1$, where the symbols are read from right to left. Similarly, for $\Sigma_{g,0}$ in Fig.1, the symbols representing the identification of edges for a $4g$ -sided polygon is $b_g^{-1}a_g^{-1}b_ga_g \cdots b_2^{-1}a_2^{-1}b_2a_2b_1^{-1}a_1^{-1}b_1a_1$. Representing a Riemann surface Σ by a polygon will be useful in studying a topological lattice gauge theory in Sec.IV.

Now let us introduce the mapping class group of a two-dimensional manifold. Let $\text{Diff}(\Sigma)$ be the group of orientation-preserving diffeomorphisms of Σ , and let $\text{Diff}_0(\Sigma)$ be the normal subgroup of diffeomorphisms homotopic to the identity. Then the mapping class group, sometimes called the modular group, is defined by

$$\text{MCG}(\Sigma) = \text{Diff}(\Sigma)/\text{Diff}_0(\Sigma). \quad (1.6)$$

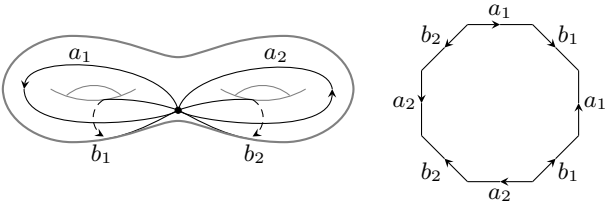


FIG. 2. A manifold $\Sigma_{2,0}$ of genus $g = 2$ (left). We cut the Riemann surface along the canonical curves (a_i and b_i cycles) to obtain a connected $4g$ -gon, which is an octagon here (right).

For a closed manifold of genus g (with $g > 1$), the mapping class group can be generated by $(2g + 1)$ Dehn twists along the $(2g + 1)$ simple closed curves as depicted in Fig.3.²⁷ In general, a Dehn twist along a closed curve means that we cut out an annulus around the curve and rotate the two boundaries of the annulus relative to each other by 2π , and then glue it back. It is noted that if one is not limited to Dehn twists, the number of generators needs not to grow with the complexity of the surface. For an orientable surface of genus g , either closed or with one puncture, its mapping class group can be generated by only two elements.²⁸

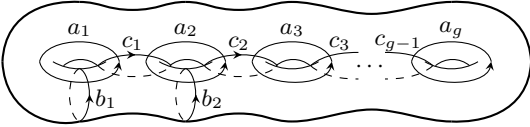


FIG. 3. Generators of $\text{MCG}(\Sigma_{g,0})$. Dehn twists around the $(2g + 1)$ simple closed curves generate $\text{MCG}(\Sigma_{g,0})$.

The relations of the $(2g + 1)$ Dehn twists that generate $\text{MCG}(\Sigma_{g,0})$ have been well studied, and one may refer to Ref.29 for more details. It is useful to consider how a nontrivial diffeomorphism acts on the homology basis in Fig.1. For example, the Dehn twist around a_1 induces the transformation on the homology basis $b_1 \rightarrow b_1 + a_1$, with other homology bases unaffected. The Dehn twist along c_1 induces the transformation $a_1 \rightarrow a_1 - b_1 + b_2$ and $a_2 \rightarrow a_2 + b_1 - b_2$, with other bases unaffected.

One basic example of $\text{MCG}(\Sigma_{g,0})$ is for $g = 1$, *i.e.*, a torus without any puncture/boundary. One can find that $\text{MCG}(\Sigma_{1,0}) \cong \text{SL}(2, \mathbb{Z})$, with the explicit expression:

$$\text{MCG}(\Sigma_{1,0}) \cong \langle \mathfrak{s}, \mathfrak{t} | \mathfrak{s}^4 = 1, (\mathfrak{st})^3 = \mathfrak{s}^2 \rangle, \quad (1.7)$$

where \mathfrak{t} can be considered as the Dehn twist \mathfrak{t}_{a_1} around a_1 in Fig.1, and \mathfrak{s} , the so-called S transformation, is a proper combination of the two Dehn twists around a_1 and b_1 as $\mathfrak{s} = \mathfrak{t}_{b_1} \cdot \mathfrak{t}_{a_1}^{-1} \cdot \mathfrak{t}_{b_1} = \mathfrak{t}_{a_1}^{-1} \cdot \mathfrak{t}_{b_1} \cdot \mathfrak{t}_{a_1}^{-1}$. Apparently, $\text{MCG}(\Sigma_{1,0})$ can be alternatively generated by the two Dehn twists \mathfrak{t}_{a_1} and \mathfrak{t}_{b_1} .

Now we consider adding punctures on the manifold. For the surface $\Sigma_{g,n}$ as introduced at the beginning of the introduction, it can be viewed as removing n distinct points from the compact manifold $\Sigma_{g,0}$. $\text{MCG}(\Sigma_{g,n})$ is generated by Dehn twists along the curves as in the closed manifold, except that now we have more curves. For example, we consider a closed

curve that includes a puncture in its interior, then doing a Dehn twist along this curve is nontrivial now.

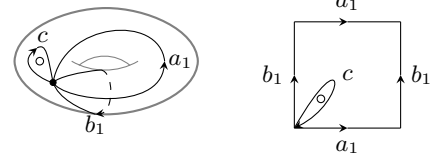


FIG. 4. A punctured torus $\Sigma_{1,1}$ (left), where \circ denotes the puncture where a point is removed, and its unfolding by cutting along a_1 and b_1 (right).

For later use, let us consider the punctured torus $\Sigma_{1,1}$, as depicted in Fig.4. One can find that $\text{MCG}(\Sigma_{1,1})$ is a central extension of $\text{SL}(2, \mathbb{Z})$, with the explicit expression:

$$\text{MCG}(\Sigma_{1,1}) \cong \langle \mathfrak{s}, \mathfrak{t} | \mathfrak{s}^4 = \mathfrak{r}^{-1}, (\mathfrak{st})^3 = \mathfrak{s}^2 \rangle, \quad (1.8)$$

where \mathfrak{r} represents the 2π rotation around the puncture or equivalently the Dehn twist around the closed curve c in Fig.4. That is, $\text{MCG}(\Sigma_{1,1})$ is still generated by \mathfrak{s} and \mathfrak{t} , or equivalently the Dehn twists \mathfrak{t}_{a_1} and \mathfrak{t}_{a_2} around the closed curves a_1 and a_2 in Fig.4. But the modular relation is modified because of the introduction of the puncture.

For a manifold $\Sigma_{g,n}$ with $n > 1$, $\text{MCG}(\Sigma_{g,n})$ is allowed to permute punctures, and one needs to introduce the operation of ‘half twist’ which exchanges two punctures. It can be proved that for any $g, n \geq 0$, the group $\text{MCG}(\Sigma_{g,n})$ is generated by a finite number of Dehn twists and half-twists. One may refer to, *e.g.*, Ref.30, for more details on $\text{MCG}(\Sigma_{g,n})$.

C. Representation of mapping class group

Now given a unitary modular category, we introduce the construction of Hilbert space of states and the representations of mapping class group. Let us give a general picture first. It is known that a modular category gives rise to a $(2+1)$ dimensional topological field theories (TQFTs). For a $(2+1)$ dimensional TQFT, the two dimensional surface Σ bounds a three dimensional open manifold. The path integral on this 3-manifold can be viewed as a wavefunction in the Hilbert space $\mathcal{H}(\Sigma)$ associated with Σ .³¹ Considering a diffeomorphism $f : \Sigma \rightarrow \Sigma$, then there is a corresponding automorphism $f_* : \mathcal{H}(\Sigma) \rightarrow \mathcal{H}(\Sigma)$, so that composition of diffeomorphisms of Σ corresponds to composition of vector-space isomorphisms. That is, the mapping class group of Σ acts as automorphisms of $\mathcal{H}(\Sigma)$. It therefore provides a (possibly) representation of MCG.

Now we give a more precise description. Let us start from a two dimensional closed oriented surfaces $\Sigma_{g,0}$, which can be considered as the boundaries of three dimensional manifold H_g in \mathbb{R}^3 . For example, the two dimensional surface $\Sigma_{1,0} = S_1 \times S_1$ bounds a three dimensional solid torus $D_2 \times S_1$ or $S^1 \times D^2$. Following 32 (see also Refs.33–35), we assign a trivalent graph at the core of the 3-manifold H_g (More rigorously, the trivalent graph here is called a ribbon graph in

literature³²). That is, the neighborhood of this trivalent graph is H_g . Then, we color this trivalent graph by different anyons $a \in \Pi_{\mathcal{C}}$ in the modular category \mathcal{C} . Here $\Pi_{\mathcal{C}}$ represents the collection of anyons in the modular category. One canonical choice of the colored trivalent graph for $\Sigma_{g,0}$ is:

$$(1.9)$$

where a_i , b_i , and c_i denote the anyon types. Note that at the vertices we need to specify the fusion channel u_i where a_i and b_{i+1} fuse into c_{i+1} , and v_i where b_i and c_i fuse into a_i . Then the Hilbert space $\mathcal{H}(\Sigma_{g,0})$ is spanned by the basis $|a_i, b_i, c_i; \mu_i, \nu_i\rangle$ with $i = 1, \dots, g$, corresponding to different ways of coloring of the trivalent graph in (1.9). For an Abelian theory, it can be found that a_1, \dots, a_{g-1} all become identity anyons, and the configuration in (1.9) decomposes into g isolated circles. The dimension of the Hilbert space $\mathcal{H}(\Sigma_{g,0})$, or the ground state degeneracy (GSD) on a closed manifold $\Sigma_{g,0}$, can be expressed in terms of the modular S matrix as³⁶

$$\dim \mathcal{H}(\Sigma_{g,0}) = \sum_{a \in \Pi_{\mathcal{C}}} \left(\frac{1}{S_{0a}} \right)^{2(g-1)}. \quad (1.10)$$

Now if we consider an oriented manifold $\Sigma_{g,n}$ of genus g with n punctures, then the basis in (1.9) is modified as

$$(1.11)$$

which span the Hilbert space $\mathcal{H}(\Sigma_{g,n})$. Here i_1, \dots, i_n in (1.11) denote the anyon types at the punctures. The dimension of Hilbert space with *fixed* anyon types i_1, \dots, i_n at the punctures is expressed in terms of the modular S matrix as¹⁶

$$\dim \mathcal{H}(\Sigma_{g,n}; i_1, \dots, i_n) = \sum_{a \in \Pi_{\mathcal{C}}} \left(\frac{1}{S_{0a}} \right)^{2(g-1)} \frac{S_{i_1 a}}{S_{0a}} \dots \frac{S_{i_n a}}{S_{0a}}, \quad (1.12)$$

which reduces to the result in Eq.(1.10) when i_1, \dots, i_n at the punctures are all identity anyons. It is remarked that by gluing the punctured-torus bases (see the left plot in (3.3)) to the punctures i_m ($m = 1, \dots, n$) in (1.11), one can obtain the basis in a closed manifold of higher genus.

Now we construct the representations of mapping class groups with the basis vectors $|v_\alpha\rangle \in \mathcal{H}(\Sigma_{g,n})$, where $\alpha = 1, \dots, \dim \mathcal{H}(\Sigma_{g,n})$. The general procedures are as follows. For an orientation preserving diffeomorphism $f : \Sigma_{g,n} \rightarrow \Sigma_{g,n}$, we consider a mapping cylinder $\Sigma_{g,n} \times [0, 1]$, with $\Sigma_{g,n} \times \{0\}$ parametrized by identity, and $\Sigma_{g,n} \times \{1\}$ parametrized by f . Now we glue the 3-manifold H_g with a specified coloring α in (1.11) to the surface $\Sigma_{g,n} \times \{0\}$ with the identity operation, and glue another 3-manifold H_g with coloring β to the surface $\Sigma_{g,n} \times \{1\}$ with f . Then we obtain a 3 dimensional manifold M with a certain ribbon graph denoted by Ω . The path integral on the manifold M with coloring Ω corresponds to the amplitude $\langle v_\beta | f_* | v_\alpha \rangle$, which defines

the action of the mapping class group on the Hilbert space, $f_* : \mathcal{H}(\Sigma_{g,n}) \rightarrow \mathcal{H}(\Sigma_{g,n})$. Then we obtain the representation of $\text{MCG}(\Sigma_{g,n})$.

Note that the manifold M and the coloring Ω depend on both f and the choice of α (β). As an illustration, we consider the example of $\Sigma_{1,0}$.³¹ The basis $|v_{\alpha(\beta)}\rangle$ in $\mathcal{H}(\Sigma_{1,0})$ can be viewed as an anyon loop carrying anyon charge α (β) threading through a solid torus. Repeating the gluing procedure above, one can find that if $f = \mathfrak{s}$, then we obtain a three manifold $M = S^3$, with Ω being a Hopf link of two anyon loops carrying anyon charges α and β , respectively. On the other hand, if $f = \mathfrak{t}$, we have $M = S^2 \times S^1$, and Ω corresponds to two parallel anyon loops carrying anyon charge α and β threading along S^1 direction, with the loop β twisted by 2π . Evaluating the path integral on the closed manifold M , one can obtain the modular data S and T matrices, corresponding to the representation of \mathfrak{s} and \mathfrak{t} , respectively.³¹ For a unitary modular category, the modular data (S, T) satisfy the following conditions:

$$(ST)^3 = S^2, \quad S^2 = C, \quad C^2 = I, \quad (1.13)$$

where d_a is the quantum dimension of anyon a , and \mathcal{D} is the total quantum dimension, and $C = (\delta_{a\bar{b}})_{a,b \in \Pi_{\mathcal{C}}}$ is called the charge conjugation matrix of \mathcal{C} . With the quasi-particle basis chosen in (1.9) and $g = 1$, T is a diagonal matrix with the diagonal elements related to the topological spin θ_a of anyon a as follows

$$e^{i\theta_a} = e^{i2\pi \frac{c}{24}} T_{aa}, \quad (1.14)$$

where c is the chiral central charge, which is 0 in the MS MTCs. Moreover, S is a unitary matrix and has the following symmetries $S_{ab} = S_{ba} = S_{\bar{a}\bar{b}}^* = S_{\bar{a}\bar{b}}^* = S_{\bar{a}\bar{b}} = S_{\bar{b}\bar{a}}$.

For a punctured torus $\Sigma_{1,1}$, recall that $\text{MCG}(\Sigma_{1,1})$ in Eq.(1.8) is still generated by \mathfrak{s} and \mathfrak{t} . We denote the corresponding representations as $S^{(z)}$ and $T^{(z)}$, where z denotes the anyon type at the puncture. Then $S^{(z)}$ and $T^{(z)}$ satisfy the following modular relations¹⁰

$$(S^{(z)} T^{(z)})^3 = (S^{(z)})^2, \quad (S^{(z)})^2 = C^{(z)}, \quad (C^{(z)})^2 = \theta_z^*, \quad (1.15)$$

where $C^{(z)}$ may be viewed as the punctured charge conjugation, and θ_z is the topological spin of anyon z at the puncture. More details on the modular relations in (1.15) will be discussed in Sec.III B.

For $\Sigma_{g,0}$, a general computation of the representations of the $(2g + 1)$ generators in Fig.3 is performed in Ref.35. Therein, the representations are expressed in terms of F and R matrices. The challenging problem is that, as we mentioned in the introduction, it is hard to calculate the F and R matrices even for a modular category with a small number of anyons.

D. Topological invariants

Based on the representations of mapping class groups on a two dimensional manifold $\Sigma_{g,n}$ of genus g with n punctures, one may construct different *words*: $w := D_{i_1}^{n_1} \dots$

$D_{i_2}^{n_2} \cdots D_{i_N}^{n_N}$, where the letters D_{i_m} denote the representations of $\text{MCG}(\Sigma_{g,n})$, and the power n_m in $D_{i_m}^{n_m}$ is an arbitrary (positive or negative) integer. Then the topological invariants we construct are of the form

$$W := \text{Tr}(w) = \text{Tr} \left(D_{i_1}^{n_1} \cdot D_{i_2}^{n_2} \cdots D_{i_j}^{n_j} \cdots \right). \quad (1.16)$$

Here the trace is over $\mathcal{H}(\Sigma_{g,n})$ as introduced in the previous subsection. The physical meaning of the topological invariant in Eq.(1.16) can be understood as the partition function on a closed 3 dimensional manifold of certain (possibly complicate) topology. A well known example is that for the torus $\Sigma_{1,0}$, $\text{Tr}[(TST)^n]$ can be understood as the partition function on the special Lens space $L_{n,1} = S^3/\mathbb{Z}_n$, where S and T are the modular matrices.

We want to emphasize that it is possible to choose a specific basis $|v_a\rangle$ in $\mathcal{H}(\Sigma_{g,n})$, and define the topological invariant as $\langle v_a | D_{i_1}^{n_1} \cdot D_{i_2}^{n_2} \cdots D_{i_N}^{n_N} | v_a \rangle$. For example, for the torus $\Sigma_{1,0}$, $\langle v_a | S | v_a \rangle$ corresponds to a Hopf link invariants of two loops labeled by anyons a in S^3 . This kind of topological invariant, however, depends on the choice of anyon charge a . In MS MTCs, by permuting the anyons, the modular data can be mapped to each other among different categories. To distinguish the MS MTCs, we want to design a topological invariant which is independent of the permutation of anyons. This is one of the underlying reasons why we use ‘‘Tr’’ over the whole Hilbert space $\mathcal{H}(\Sigma_{g,n})$ in the definition in Eq.(1.16).

II. MS MODULAR CATEGORIES

In this section we give a brief review of the basic properties of MS modular categories.¹³ The modular data of MS MTCs will be used in constructing the representations of modular groups of higher-genus manifolds in Sec.III.

The MS modular categories (MS-MCs) are modular categories that go beyond the modular data. They are representation categories of quantum doubles $D^\omega(G)$ of $G = \mathbb{Z}_q \rtimes_n \mathbb{Z}_p$, twisted by the three-cocycles $\omega \in H^3(\mathbb{Z}_q \rtimes_n \mathbb{Z}_p, U(1))$. In the following we will always consider the normalized cocycles, *i.e.*, the value of cocycle is 1 when one of arguments equals to identity. Here ω satisfy the 3-cocycle condition

$$\begin{aligned} & \omega(g_1, g_2, g_3) \cdot \omega(g_0 \cdot g_1, g_2, g_3)^{-1} \cdot \omega(g_0, g_1 \cdot g_2, g_3) \\ & \cdot \omega(g_0, g_1, g_2 \cdot g_3)^{-1} \cdot \omega(g_0, g_1, g_2) = 1. \end{aligned} \quad (2.1)$$

For the finite nonabelian gauge group $G = \mathbb{Z}_q \rtimes_n \mathbb{Z}_p$, p and q are primes with $p|(q-1)$. \mathbb{Z}_p acts on \mathbb{Z}_q as multiplication by an element n of multiplicative order p in \mathbb{Z}_q . To be concrete, the group G has the presentation

$$G = \{(a^l, b^m) | a^q = b^p = 1, bab^{-1} = a^n\}, \quad (2.2)$$

with $l \in \{0, 1, \dots, q-1\}$, $m \in \{0, 1, \dots, p-1\}$, $n^p = 1$ mod q , and $n \neq 1$.³⁷ All such choices of n give rise to isomorphic groups, *i.e.*, the group does not depend on the choice of n . The multiplication of two group elements are $(a^l, b^m) \cdot (a^{l'}, b^{m'}) = (a^l b^m a^{l'} b^{-m}), b^{m+m'}) = (a^{l+n^m l'}, b^{m+m'})$.

For the cohomology group of G , one can consider the following short exact sequence:^{13,38}

$$0 \rightarrow H^3(\mathbb{Z}_p, U(1)) \rightarrow H^3(G, U(1)) \rightarrow H^3(\mathbb{Z}_q, U(1))^{\mathbb{Z}_p} \rightarrow 0. \quad (2.3)$$

Denote $\kappa : \mathbb{Z}_p^3 \rightarrow U(1)$ as the generator of the cohomology group $H^3(\mathbb{Z}_p, U(1)) \cong \mathbb{Z}_p$. We can take κ as the p -th roots of unity. Then $\omega \in H^3(G, U(1))$ can be considered as the inflation of κ to G , *i.e.*, $\omega = \text{Inf}_{\mathbb{Z}_p}^G \kappa$. Then we can define p modular categories of twisted quantum double of G by $\mathcal{C}_u = D^{\omega^u}(G)$, with $u = 0, 1, \dots, p-1$, and $\omega \in H^3(\mathbb{Z}_q \rtimes_n \mathbb{Z}_p, U(1)) \cong \mathbb{Z}_p$. To be concrete, the 3-cocycles for MS MTCs are

$$\omega^u(g, h, k) = \exp \left[\frac{2\pi i}{p^2} u \cdot [kb]_p \cdot ([gb]_p + [hb]_p - [g+h]_p) \right], \quad (2.4)$$

with $u = 0, \dots, p-1$ characterizing inequivalent cocycles. where we have denoted the group elements as

$$g := (a^{g_a}, b^{g_b}), \quad (2.5)$$

and $[x]_p := x \bmod p$. In general, different equivalent classes of cocycles give rise to different modular data, but this is not the case for MS MTCs. For this family of modular categories with $p > 3$, MS found that there are p inequivalent modular categories. However, there are only three sets of distinct modular data.

Before introducing the modular data for the p inequivalent modular categories, let us emphasize the meaning of ‘equivalence’ (or ‘inequivalence’) of two modular categories of $D^\omega(G)$. Two cocycles ω and ν on a group G give the same category not only if they are cohomologous, but also if their cohomology classes are mapped to each other under the action of the automorphism group of G . Alternatively, $D^\omega(G)$ and $D^\nu(G)$ are equivalent as modular categories if and only if there is an automorphism f of G such that ν and $f^* \omega$ are cohomologous. For the MS MTCs with $G = \mathbb{Z}_q \rtimes \mathbb{Z}_p$, one can find that any automorphisms of G fixes the unique subgroup \mathbb{Z}_q of order q and induces the identity on the quotient \mathbb{Z}_p . Recall that the 3-cocycles ω are inflated from $H^3(\mathbb{Z}_p, U(1))$, then the p modular categories are pairwise inequivalent.

A. Anyons

In MS MTCs, there are in total $\frac{q^2-1+p^3}{p}$ anyons, including $(\frac{q-1}{p} + p)$ type- I anyons, $(\frac{q-1}{p} \times q)$ type- A anyons, and $p(p-1)$ type- B anyons. The anyons in $D^\omega(G)$ are parametrized by pairs

$$(g, \tilde{\chi}), \quad (2.6)$$

or alternatively by pairs $([g], \tilde{\chi})$, where $g \in G$ is a representative of a conjugacy class $[g]$ in G . To distinguish with the character χ of a linear representation, $\tilde{\chi}$ is denoted as the character of α_g -irreducible representation of the centralizer $C_G(g) := \{x | gx = xg\}$. Here α_g is a two cocycle on $C_G(g)$ obtained from the three cocycle ω as follows

$$\alpha_g(x, y) := \frac{\omega(g, x, y) \cdot \omega(x, y, g)}{\omega(x, g, y)}. \quad (2.7)$$

Each α_g determines a class of representations called α_g -representation $\tilde{\rho} : C_G(g) \rightarrow \text{GL}(C_G(g))$ obeying

$$\tilde{\rho}^g(x)\tilde{\rho}^g(y) = \alpha_g(x, y)\tilde{\rho}^g(x, y). \quad (2.8)$$

The two-cocycle condition for α_g corresponds to the associativity $\tilde{\rho}^g(x)[\tilde{\rho}^g(y)\tilde{\rho}^g(z)] = [\tilde{\rho}^g(x)\tilde{\rho}^g(y)]\tilde{\rho}^g(z)$. Physically, for the pairs in (2.6), we may call g or $[g]$ the flux (magnetic charge), and $\tilde{\chi}$ the charge (electric charge). Moreover, the (charge) conjugation of $(g, \tilde{\chi})$ is isomorphic to $(g^{-1}, \tilde{\chi}^*)$.

One can check there are $\frac{q-1}{p} + p$ conjugacy classes of G . Depending on the conjugacy classes, we divide the anyons into three types (See Appendix A for more details):

(i) type- I anyons: $I_i := (1, \chi_i)$.

The conjugacy class is $\{1\}$, where $1 = (a^0, b^0)$ is the identity element of G . Since the two-cocycle α_g is trivial for $g = 1$, here χ in Eq.(2.6) is the irreducible character of G . The number of irreducible representations of G are also $\frac{q-1}{p} + p$, equal to the number of conjugacy classes in G . This is the number of type- I anyons. In particular, p of them are one dimensional, and $\frac{q-1}{p}$ of them are p dimensional. Denoting the dimension of irreducible representation ρ_μ as d_μ , then one can check that $\sum_\mu d_\mu^2 = 1^2 \cdot p + p^2 \cdot \frac{q-1}{p} = pq = |G|$.

(ii) type- A anyons: $A_{l,m} := (a^l, \chi_m)$.

Here we denote $a^l := (a^l, b^0)$, where the integer l has the value

$$l \in \mathbb{Z}_q^\times / \langle n \rangle, \quad (2.9)$$

where \mathbb{Z}_q^\times is the multiplicative group of integers coprime to q . The conjugacy class that contains the group element (a^l, b^0) is $\{(a^{l'}, b^0) | l' = l \cdot n^k \text{ mod } q; k = 0, 1, \dots, p-1\}$. Note that the size of the conjugacy class $|\{(a^l, b^0)\}| = p$. The number of conjugacy classes is $|\mathbb{Z}^\times|/p = (q-1)/p$. The centralizer subgroup of the representative a^l is $C_G(a^l) = \{(a^{l'}, b^0) | l' = 0, 1, \dots, q-1\} = \mathbb{Z}_q$. One can find the 3-cocycle in Eq.(2.4) is trivial for the centralizer subgroup \mathbb{Z}_q . Therefore, $\tilde{\chi}$ reduce to χ , the linear irreducible representations in \mathbb{Z}_q , which are all one dimensional. The quantum dimensions of a type- A anyons are $p \times 1 = p$.

(iii) type- B anyons: $B_{k,n} := (b^k, \tilde{\chi}_n)$.

Here we denote $b^k := (a^0, b^k)$, where $k \in \{1, 2, \dots, p-1\}$. The conjugacy class containing the group element b^k is $\{(a^l, b^k) | l = 0, \dots, q-1\}$. Then the size of conjugacy class is q . The number of conjugacy classes is $p-1$. The centralizer subgroup of (a^l, b^k) is $C_G((a^l, b^k)) = \{(a^0, b^{k'}) | k' = 0, 1, \dots, p-1\} = \mathbb{Z}_p$. Different from the type- I and type- A anyons, now the 3-cocycle in Eq.(2.4) plays a role. One can check that the associated 2-cocycle in Eq.(2.7) now becomes

$$\alpha_{b^k}(b^{k_1}, b^{k_2}) = \omega(b^{k_1}, b^{k_2}, b^k), \quad (2.10)$$

where $k_1, k_2 \in \{0, 1, \dots, p-1\}$. It can be found that the two cocycle α_{b^k} is actually a two coboundary. This kind of twisting is sometimes called ‘‘cohomology trivial’’ (CT).³⁹ For the two-coboundary α_{b^k} , one can find a one-cochain ϵ_{b^k} such that

$$\alpha_{b^k}(g, h) = \delta\epsilon_{b^k}(g, h) = \epsilon_{b^k}(g)\epsilon_{b^k}(h)\epsilon_{b^k}^{-1}(gh). \quad (2.11)$$

Based on the definition of α_g -representations in Eq.(2.8), one can find that the representation and the linear representation are related by a phase:

$$\tilde{\rho}_n^{b^k}(x) = \epsilon_{b^k}(x)\rho_n^{b^k}(x). \quad (2.12)$$

Here n labels the n -th representation. That is, the representation is obtained from a usual representation by adding a twist ϵ_{b^k} , which is a $U(1)$ phase. Both the number and dimensions of the irreducible presentations stay the same by adding this twist, *i.e.*, a CT twisted theory has the same number and quantum dimensions of anyons as the untwisted theory. Since the irreducible presentations of the centralizer subgroup \mathbb{Z}_p are all one dimensional, the quantum dimensions of type- B anyons are $q \times 1 = q$.

A short summary for the three types of anyons: for type- I and type- A anyons, the 3-cocycle $\omega \in H^3(G, U(1))$ does not enter the definition of anyons, and only the group data of G plays a role. For type- B anyons, however, the 3-cocycle ω will twist the irreducible presentation of the centralizer subgroup. Strictly speaking, the irreducible presentation is twisted by the two-cocycle obtained from ω . This will affect the modular data as will be discussed below. In total, there are $\frac{q-1}{p} + p$ type- I anyons, with $\frac{q-1}{p}$ of them p dimensional, and p of them one dimensional, $\frac{q-1}{p} \cdot q$ type- A anyons with quantum dimension p , and $(p-1) \cdot p$ type- B anyons with quantum dimensions q . One can check explicitly that the total quantum dimension is indeed $\sum_i d_i^2 = p^2 q^2 = |G|^2$.

B. Modular data

Having defined the types of anyons, now we discuss the modular data of MS MTCs, which will be used in constructing the representations of MCG of higher-genus manifold in Sec.III. In addition, we will check explicitly there are only three sets of S and T matrices in MS MTCs, up to anyon permutation.

A general construction of modular data for a twisted quantum double of a finite group G can be found in Ref.39. Let us consider the T matrix first. The topological spin of anyon $(g, \tilde{\chi})$ is

$$\theta_{(g,\chi)} = \frac{\text{tr}\tilde{\chi}(g)}{\text{tr}\tilde{\chi}(1)}. \quad (2.13)$$

For type- I and type- A anyons, the irreducible representations are all linear. Then one simply has $\theta_{(g,\chi)} = \frac{\text{tr}\chi(g)}{\text{tr}\chi(1)}$. In particular, for type- I anyons $(1, \chi_i)$, the topological spin is trivial, *i.e.*,

$$\theta(1, \chi_i) = \frac{\text{tr}\chi_i(1)}{\text{tr}\chi_i(1)} = 1. \quad (2.14)$$

For type- A anyon (a^l, χ_m) , χ_m is the m -th linear irreducible character of \mathbb{Z}_q and is generated by $\chi(a) = e^{\frac{2\pi i a}{q}}$, where we have defined $a^l := (a^l, b^0)$. Then the topological spin of

anyon (a^l, χ_m) is

$$\theta_{(a^l, \chi_m)} = \exp\left(\frac{2\pi i}{q} lm\right). \quad (2.15)$$

Now let us check type- B anyons $(b^k, \tilde{\chi}_n)$. The irreducible representation is twisted by $\alpha_{b^k}^u$, with

$$\alpha_{b^k}^u(g, h) = \exp\left[\frac{2\pi i}{p^2} uk \cdot ([g_b]_p + [h_b]_p - [g_b + h_b]_p)\right], \quad (2.16)$$

where we have defined $g := (a^{g_a}, b^{g_b})$, and $[x]_p = x \bmod p$. Recall that $\alpha_{b^k}^u$ is a two-coboundary and can be expressed as a function of one-cochain in Eq.(2.11), with

$$\epsilon_{b^k}^u(g) = \exp\left(\frac{2\pi i}{p^2} ku \cdot [g_b]_p\right). \quad (2.17)$$

Based on Eq.(2.12), the m -th α_{b^k} - character is related with the linear character as follows:

$$\tilde{\chi}_m^{b^k}(x) = \chi_m(x) \cdot \epsilon_{b^k}(x) = (\chi(x))^m \cdot \epsilon_{b^k}(x), \quad (2.18)$$

where $m \in \{0, 1, 2, \dots, p-1\}$, and χ is the generator of linear characters, with the expression

$$\chi(b^k) := \exp\left(\frac{2i\pi}{p} k\right). \quad (2.19)$$

Then the topological spin of a type- B anyons $(b^k, \tilde{\chi}_m)$ is

$$\theta_{(b^k, \tilde{\chi}_m)}^{(u)} = \frac{\text{tr} \chi_m(b^k)}{\text{tr} \chi_m(1)} \epsilon_{b^k}^u(b^k) = \exp\left(\frac{2\pi i}{p^2} (p \cdot mk + k^2 u)\right), \quad (2.20)$$

where $k \in \{1, 2, \dots, p-1\}$.

As a short summary of the modular T matrix, or the topological spins, we have

- (i) type- I anyons: $\theta_{(1, \chi)} = 1$;
- (ii) type- A anyons: $\theta_{(a^l, \chi_m)} = e^{\frac{2\pi i}{q} lm}$;
- (iii) type- B anyons: $\theta_{(b^k, \tilde{\chi}_m)}^{(u)} = e^{\frac{2\pi i}{p^2} (pmk + k^2 u)}$.

That is, only the topological spins of type- B anyons depend on the equivalence class of 3-cocycle ω^u , where $u = 0, \dots, p-1$.

Now let us check the modular S matrix, which are indexed by two simples $(g, \tilde{\chi}_\mu)$ and $(h, \tilde{\chi}_\nu)$, as follows:³⁹

$$S_{(g, \tilde{\chi}_\mu), (h, \tilde{\chi}_\nu)} = \frac{1}{|G|} \sum_{\substack{g' \in [g], h' \in [h] \\ g' h' = h' g'}} [\tilde{\chi}_\mu^{g'}(h')]^* [\tilde{\chi}_\nu^{h'}(g')]^*. \quad (2.21)$$

One can find that $S_{a,b}$ depends on the 3-cocycle ω only when there is at least one type- B anyon in the indices. In fact, by further looking into the details of S -matrix as shown in Appendix A 2, one can find that $S_{a,b}$ depends on the 3-cocycle only when both a and b are type- B anyons. In this case, the modular S matrix has a simple expression (see Appendix A 2)

$$S_{(b^k, \tilde{\chi}_m), (b^{k'}, \tilde{\chi}_n)}^{(u)} = \frac{1}{p} \exp\left(-\frac{2\pi i}{p^2} [2uk'k' + p(kn + k'm)]\right), \quad (2.22)$$

where $u = 0, \dots, p-1$ denotes inequivalent classes of 3-cocycle ω .

One remark here: If we focus on the modular data that depend on the 3-cocycle ω^u , they are topological spins $\theta_{(b^k, \tilde{\chi}_m)}^{(u)} = e^{\frac{2\pi i}{p^2} (pmk + k^2 u)}$, and $S_{(b^k, \tilde{\chi}_m), (b^{k'}, \tilde{\chi}_n)}^{(u)}$ as expressed in Eq.(2.22). One can find they are the same as the modular data for a twisted quantum double of $G = \mathbb{Z}_p$ (see appendix C 3). For the later case, however, there are only three inequivalent categories for $p > 3$,⁴⁰ while for MS MTCs there are p inequivalent categories.¹³ This difference may be intuitively understood by considering that the twisted quantum double of $G = \mathbb{Z}_p$ is an abelian theory, and there is no more new information in the representations of MCG of higher genus manifold (Recall that for an abelian theory, the basis vector in (1.9) decomposes into disconnected loops with $a_1 = \dots = a_{g-1} = 1$, where 1 denotes the identity anyon). But MS MTCs are non-abelian, and there are new structures in the ground states on higher-genus manifolds, which introduces extra information compared to the genus-1 case.

1. Equivalence of modular data

Now we are ready to see how the modular data of different categories can be mapped to each other.¹³ Mathematically, this is based on the application of Galois group actions. There are two steps. Step 1 is to check how the modular data transform as we change the 3-cocycle from ω^ν to ω^u . Step 2 is to consider how the modular data transform as we permute anyons within the same category. One can refer to Appendix D for an introduction of the Galois symmetry in the modular data.

Step 1: For the modular category of $D^{\omega^u}(G)$, ω^u (here $u \neq 0$) is related to ω by $\omega^u = \sigma^r \omega$, where $r = 0, 1, \dots, p-2$. Mathematically, σ is an element of the absolute Galois group of abelian extensions $\Gamma := \text{Gal}(\mathbb{Q}^{ab})/\mathbb{Q}$. One can choose σ such that $\sigma(\zeta_p) = \zeta_p^m$, where m is the primitive root of the prime number p , with $m^{p-1} = 1 \bmod p$. Then by considering the mapping $\omega \xrightarrow{\sigma^r} \omega^u$ where $u = m^r$, there is a bijection p_r between the simple objects (anyons) in $D^\omega(G)$ and $D^{\omega^u}(G)$ as follows

$$p_r : (g, \tilde{\chi}) \text{ in } D^\omega(G) \longrightarrow (g, \sigma^r \tilde{\chi}) \text{ in } D^{\omega^u}(G). \quad (2.23)$$

Hereafter, in some cases we may call the bijection p_r of anyons in two categories as ‘permutation’ of anyons in two categories. This bijection can be understood in the following way. The 3-cocycle ω^u affects the definition/property of anyons through its representation of the centralizer $C_G(g)$ in (2.8). By replacing ω with $\omega^u = \sigma^r \omega = \omega^{m^r}$, α_g in Eq.(2.7) is replaced by $\sigma^r \alpha_g$. Then to obtain a $\sigma^r \alpha_g$ - representation, every matrix element in the representation $\tilde{\rho}$ of $C_G(g)$ should be acted by σ^r , which results in the replacement of $\tilde{\chi}$ by $\sigma^r \tilde{\chi}$. Then from the definition of modular S and T matrices in Eqs.(2.21) and (2.13), one can find that the modular data of $D^{\omega^u}(G)$ are related to those of $D^\omega(G)$ as

$$S_{p_r(i), p_r(j)}^{(u)} = \sigma^r(S_{ij}^{(u=1)}), \quad T_{p_r(i), p_r(i)}^{(u)} = \sigma^r(T_{ii}^{(u=1)}), \quad (2.24)$$

where $u = m^r \bmod p$. More generally, the modular data of $D^{\omega^u}(G)$ and those of $D^{\omega^v}(G)$ are related by

$$S_{p_{r,s}(i),p_{r,s}(j)}^{(u)} = \sigma^{r-s}(S_{ij}^{(v)}), \quad T_{p_{r,s}(i),p_{r,s}(i)}^{(u)} = \sigma^{r-s}(T_{ii}^{(v)}), \quad (2.25)$$

where, without loss of generality, we have assumed that $r > s$ with $\omega^u = \sigma^r \omega$ and $\omega^v = \sigma^s \omega$ (so that $u = m^r \bmod p$, and $v = m^s \bmod p$), and $p_{r,s}$ denotes the corresponding bijection between the simple objects in $D^{\omega^u}(G)$ and $D^{\omega^v}(G)$.

Step 2: Now let us check how the modular data transform by permuting anyons within the category. It is known that for the twisted quantum double $D^{\omega^u}(G)$, for each $\sigma \in \Gamma$ (see Step 1) there exists a unique permutation $\hat{\sigma}$ of simple objects in $D^{\omega^u}(G)$, so that $S_{\hat{\sigma}(i),\hat{\sigma}(j)} = \sigma^2(S_{i,j})$ and $T_{\hat{\sigma}(i),\hat{\sigma}(i)} = \sigma^2(T_{i,i})$ (See also Appendix D).^{39,41-43}

Comparing the two steps above, one can find that if $(r-s)$ is an even number, then the modular categories $D^{\omega^u}(G)$ and $D^{\omega^v}(G)$ share the same modular data. That is, the modular data only depends on the parity of r . In short, there are at most three distinct sets of modular data, corresponding to $D^{\omega^u}(G)$ with $u = 0$, $u = m^{2n}$, and $u = m^{2n+1}$, respectively.

From this point of view, as suggested in Ref.13, the different categories that share the same modular data in MS MTCs are ‘Galois twists’ of each other.

III. REPRESENTATIONS OF MAPPING CLASS GROUP: QUASI-PARTICLE BASIS

In this section, we study the representations of mapping class group for the MS MTCs on a genus-2 manifold. All the calculation is based on the simplest examples of MS MTCs with $G = \mathbb{Z}_{11} \times \mathbb{Z}_5$. We will use the quasi-particle basis, *i.e.*, the basis colored by anyons. One merit of the quasi-particle basis is that we can relate the topological invariants constructed from the MCG representations to various link invariants.

For a genus-2 manifold (without punctures), there are two choices of canonical basis as

$$\text{basis I: } \begin{array}{c} \text{b} \qquad \qquad \text{a} \\ \circ \qquad \qquad \circ \\ \nu \xleftarrow{z} \mu \end{array} \quad (3.1)$$

and

$$\text{basis II: } \begin{array}{c} \mu \\ \circ \qquad \qquad \circ \\ \text{b} \qquad \qquad \text{a} \\ \nu \end{array} \quad (3.2)$$

where a , b , and z denote anyons, and u (ν) denotes the fusion channel. For example, in basis I, there are two loops colored by anyons a and b , respectively. These two loops can be connected by a third line colored by anyon z if $N_{a\bar{a}}^z, N_{b\bar{b}}^z > 0$. The two different bases in (3.1) and (3.1) can be transformed into each other based on a F transformation (see Sec.B 2). As

the number of genus g increases, there are more choices of canonical basis. See, *e.g.*, the case of $g = 3$ in (B31).

If there are punctures on the manifold, the quasiparticle basis will have open ends corresponding to the anyons at the punctures. For example, the quasi-particle basis for a torus with one puncture and two punctures can be expressed as follows:

$$\begin{array}{c} \text{a} \\ \circ \\ \mu \end{array} \quad \begin{array}{c} \text{a} \\ \circ \\ \mu \\ \text{b} \\ \nu \\ \text{z}_1 \\ \text{z}_2 \end{array} \quad (3.3)$$

It is noted that by gluing punctured-torus bases, one may obtain the basis for a higher-genus manifold. For example, by gluing two copies of bases for the once-punctured torus (the left in (3.3)) along the puncture, one can obtain the genus-2 basis in (3.1). Hereafter we will mainly focus on genus-2 manifold and use basis I in (3.1). It is noted that the basic structure in basis I is the vertex structure:

$$\begin{array}{c} \text{a} \quad \text{z} \\ \swarrow \quad \downarrow \\ \mu \\ \uparrow \\ \text{a} \end{array} \quad (3.4)$$

which is actually the basis in the so-called splitting space V_a^{az} (whose dual space is the fusion vector space V_{az}^a) in algebraic anyon theory (see Appendix B). In the following, we will first specify the fusion rules of $a \times \bar{a}$ in (3.4), and then study how the modular transformations act on this vertex basis.

A. MS modular categories with $G = \mathbb{Z}_{11} \times \mathbb{Z}_5$

The twisted quantum double $D^\omega(G)$ of $G = \mathbb{Z}_{11} \times \mathbb{Z}_5$ are the simplest examples of MS MTCs, with group order 55, and 49 simple objects. Throughout this work, all the concrete calculation is based on these examples. In the following, we will review the basic data that are necessary for our later study on the MCG representations.

Recall that the simple objects of a twisted quantum double of a finite group are labeled by the ‘flux’ (conjugacy class) and ‘charge’ (the irreducible representation of the centralizer of conjugacy class). There are $p + \frac{q-1}{p} = 7$ conjugacy classes of $G = \mathbb{Z}_{11} \times \mathbb{Z}_5$, which we label as $[1]$, $[a^1]$, $[a^2]$, $[b^1]$, $[b^2]$, $[b^3]$, and $[b^4]$, as described in Table I.

As discussed in the previous section, depending on the conjugacy classes, there are three types of anyons. Here we denote them as type- I , type- A , and type- B anyons:

$$\begin{aligned} I_i &:= (1, \chi_i), \\ A_{l,m} &= (a^l, \omega_{11}^m), \\ B_{k,n} &= (b^k, \tilde{\omega}_5^n), \end{aligned} \quad (3.5)$$

where χ_i , ω_{11}^m , and $\tilde{\omega}_5^n$ are the corresponding character of centralizer subgroup (see the following).

– type- I anyons (pure charge): $(1, \chi_i)$

| anyons | Conjugacy class | Centralizer |
|-----------|--|--|
| type- I | $[1] = \{1\}$ | $G = \mathbb{Z}_{11} \rtimes \mathbb{Z}_5$ |
| type- A | $[a^1] = \{a, a^3, a^4, a^5, a^9\}$ | \mathbb{Z}_{11} |
| | $[a^2] = \{a^2, a^6, a^7, a^8, a^{10}\}$ | \mathbb{Z}_{11} |
| type- B | $[b^1] = \{a^0 b^1, a^1 b^1, a^2 b^1, \dots, a^{10} b^1\}$ | \mathbb{Z}_5 |
| | $[b^2] = \{a^0 b^2, a^1 b^2, a^2 b^2, \dots, a^{10} b^2\}$ | \mathbb{Z}_5 |
| | $[b^3] = \{a^0 b^3, a^1 b^3, a^2 b^3, \dots, a^{10} b^3\}$ | \mathbb{Z}_5 |
| | $[b^4] = \{a^0 b^4, a^1 b^4, a^2 b^4, \dots, a^{10} b^4\}$ | \mathbb{Z}_5 |

TABLE I. Conjugacy classes and the corresponding centralizers of $G = \mathbb{Z}_{11} \rtimes \mathbb{Z}_5$.

In this case, the flux is trivial, *i.e.*, the conjugacy class is $\{1\}$, with 1 representing the identity group element in G , and therefore type- I anyons are all pure charges. The centralizer of 1 is the total group $G = \mathbb{Z}_{11} \rtimes \mathbb{Z}_5$. The character table of G is¹⁵

| G | $[1]$ | $[a^1]$ | $[a^2]$ | $[b^1]$ | $[b^2]$ | $[b^3]$ | $[b^4]$ |
|----------|-------|------------|------------|-----------|-----------|-----------|-----------|
| χ_0 | 1 | 1 | 1 | 1 | 1 | 1 | 1 |
| χ_1 | 1 | 1 | 1 | ξ_5 | ξ_5^2 | ξ_5^3 | ξ_5^4 |
| χ_2 | 1 | 1 | 1 | ξ_5^2 | ξ_5^4 | ξ_5 | ξ_5^3 |
| χ_3 | 1 | 1 | 1 | ξ_5^3 | ξ_5 | ξ_5^4 | ξ_5^2 |
| χ_4 | 1 | 1 | 1 | ξ_5^4 | ξ_5^3 | ξ_5^2 | ξ_5 |
| χ_5 | 5 | σ | σ^* | 0 | 0 | 0 | 0 |
| χ_6 | 5 | σ^* | σ | 0 | 0 | 0 | 0 |

(3.6)

where $\xi_m = e^{\frac{2\pi i}{5}}$, and $\sigma = e^{\frac{2\pi i}{11} \cdot 1} + e^{\frac{2\pi i}{11} \cdot 3} + e^{\frac{2\pi i}{11} \cdot 4} + e^{\frac{2\pi i}{11} \cdot 5} + e^{\frac{2\pi i}{11} \cdot 9}$. One can find there are in total 7 irreducible representations for G , with five of them 1 dimensional, *i.e.*, $\chi_i(1) = 1$ and two of them 5 dimensional, *i.e.*, $\chi_i(1) = 5$. One can check that $1^2 \cdot 5 + 5^2 \cdot 2 = 55 = |G|$. Corresponding to the characters χ_i in (3.6), we denote these pure charges as

$$\begin{aligned} I_0, I_1, I_2, I_3, I_4, \quad d = 1, \\ I_5, I_6, \quad d = 5. \end{aligned} \quad (3.7)$$

The topological spins of all type- I anyons are trivial, *i.e.*, $\theta_{I_i} = 1$.

– type- A anyons: (a^l, ω_{11}^m)

These anyons correspond to conjugacy classes $[a^1]$ and $[a^2]$. As seen from Table I, the size of the conjugacy class is 5, and the centralizer is \mathbb{Z}_{11} . From Eq.(2.4), one can find the 3-cocycle in this case is trivial, and the irreducible presentations are all linear, and one dimensional. The generator of characters for \mathbb{Z}_{11} is $\omega_{11}(a) = e^{\frac{2\pi i}{11}}$, so that $\omega_{11}^m(a^l) = e^{\frac{2\pi i}{11} \cdot lm}$. There are in total $2 \times 11 = 22$ type- A anyons, with the quantum dimension $d_i = 5 \times 1 = 5$. As seen from Eq.(2.15), the topological spin for anyon (a^l, ω_{11}^m) is $e^{\frac{2\pi i}{11} \cdot lm}$, which is independent of the 3-cocycle.

– type- B anyons: $(b^k, \tilde{\omega}_5^n)$

The corresponding conjugacy classes are $[b^1]$, $[b^2]$, $[b^3]$, and $[b^4]$. As seen from Table I, the size of conjugacy class is 11. The centralizer subgroup is \mathbb{Z}_5 . The irreducible representations of \mathbb{Z}_5 are all one dimensional (see Eq.(2.18)). There are in total $4 \times 5 = 20$ type- B anyons, with quantum dimensions

| Label | d | θ |
|------------|-----|---|
| I_0 | 1 | 1 |
| I_1 | 1 | 1 |
| I_2 | 1 | 1 |
| I_3 | 1 | 1 |
| I_4 | 1 | 1 |
| I_5 | 5 | 1 |
| I_6 | 5 | 1 |
| $A_{1,0}$ | 5 | 1 |
| $A_{1,1}$ | 5 | $\exp\left(\frac{i2\pi}{11}\right)$ |
| $A_{1,2}$ | 5 | $\exp\left(\frac{i2\pi}{11} \cdot 2\right)$ |
| $A_{1,3}$ | 5 | $\exp\left(\frac{i2\pi}{11} \cdot 3\right)$ |
| $A_{1,4}$ | 5 | $\exp\left(\frac{i2\pi}{11} \cdot 4\right)$ |
| $A_{1,5}$ | 5 | $\exp\left(\frac{i2\pi}{11} \cdot 5\right)$ |
| $A_{1,6}$ | 5 | $\exp\left(\frac{i2\pi}{11} \cdot 6\right)$ |
| $A_{1,7}$ | 5 | $\exp\left(\frac{i2\pi}{11} \cdot 7\right)$ |
| $A_{1,8}$ | 5 | $\exp\left(\frac{i2\pi}{11} \cdot 8\right)$ |
| $A_{1,9}$ | 5 | $\exp\left(\frac{i2\pi}{11} \cdot 9\right)$ |
| $A_{1,10}$ | 5 | $\exp\left(\frac{i2\pi}{11} \cdot 10\right)$ |
| $A_{2,0}$ | 5 | 1 |
| $A_{2,1}$ | 5 | $\exp\left(\frac{i4\pi}{11}\right)$ |
| $A_{2,2}$ | 5 | $\exp\left(\frac{i4\pi}{11} \cdot 2\right)$ |
| $A_{2,3}$ | 5 | $\exp\left(\frac{i4\pi}{11} \cdot 3\right)$ |
| $A_{2,4}$ | 5 | $\exp\left(\frac{i4\pi}{11} \cdot 4\right)$ |
| $A_{2,5}$ | 5 | $\exp\left(\frac{i4\pi}{11} \cdot 5\right)$ |
| $A_{2,6}$ | 5 | $\exp\left(\frac{i4\pi}{11} \cdot 6\right)$ |
| $A_{2,7}$ | 5 | $\exp\left(\frac{i4\pi}{11} \cdot 7\right)$ |
| $A_{2,8}$ | 5 | $\exp\left(\frac{i4\pi}{11} \cdot 8\right)$ |
| $A_{2,9}$ | 5 | $\exp\left(\frac{i4\pi}{11} \cdot 9\right)$ |
| $A_{2,10}$ | 5 | $\exp\left(\frac{i4\pi}{11} \cdot 10\right)$ |
| $B_{1,0}$ | 11 | $\exp\left(\frac{i2\pi}{25} \cdot 1^2 u\right)$ |
| $B_{1,1}$ | 11 | $\exp\left(\frac{i2\pi}{25} (5 \cdot 1 \cdot 1 + 1^2 u)\right)$ |
| $B_{1,2}$ | 11 | $\exp\left(\frac{i2\pi}{25} (5 \cdot 1 \cdot 2 + 1^2 u)\right)$ |
| $B_{1,3}$ | 11 | $\exp\left(\frac{i2\pi}{25} (5 \cdot 1 \cdot 3 + 1^2 u)\right)$ |
| $B_{1,4}$ | 11 | $\exp\left(\frac{i2\pi}{25} (5 \cdot 1 \cdot 4 + 1^2 u)\right)$ |
| $B_{2,0}$ | 11 | $\exp\left(\frac{i2\pi}{25} \cdot 2^2 u\right)$ |
| $B_{2,1}$ | 11 | $\exp\left(\frac{i2\pi}{25} (5 \cdot 2 \cdot 1 + 2^2 u)\right)$ |
| $B_{2,2}$ | 11 | $\exp\left(\frac{i2\pi}{25} (5 \cdot 2 \cdot 2 + 2^2 u)\right)$ |
| $B_{2,3}$ | 11 | $\exp\left(\frac{i2\pi}{25} (5 \cdot 2 \cdot 3 + 2^2 u)\right)$ |
| $B_{2,4}$ | 11 | $\exp\left(\frac{i2\pi}{25} (5 \cdot 2 \cdot 4 + 2^2 u)\right)$ |
| $B_{3,0}$ | 11 | $\exp\left(\frac{i2\pi}{25} \cdot 3^2 u\right)$ |
| $B_{3,1}$ | 11 | $\exp\left(\frac{i2\pi}{25} (5 \cdot 3 \cdot 1 + 3^2 u)\right)$ |
| $B_{3,2}$ | 11 | $\exp\left(\frac{i2\pi}{25} (5 \cdot 3 \cdot 2 + 3^2 u)\right)$ |
| $B_{3,3}$ | 11 | $\exp\left(\frac{i2\pi}{25} (5 \cdot 3 \cdot 3 + 3^2 u)\right)$ |
| $B_{3,4}$ | 11 | $\exp\left(\frac{i2\pi}{25} (5 \cdot 3 \cdot 4 + 3^2 u)\right)$ |
| $B_{4,0}$ | 11 | $\exp\left(\frac{i2\pi}{25} \cdot 4^2 u\right)$ |
| $B_{4,1}$ | 11 | $\exp\left(\frac{i2\pi}{25} (5 \cdot 4 \cdot 1 + 4^2 u)\right)$ |
| $B_{4,2}$ | 11 | $\exp\left(\frac{i2\pi}{25} (5 \cdot 4 \cdot 2 + 4^2 u)\right)$ |
| $B_{4,3}$ | 11 | $\exp\left(\frac{i2\pi}{25} (5 \cdot 4 \cdot 3 + 4^2 u)\right)$ |
| $B_{4,4}$ | 11 | $\exp\left(\frac{i2\pi}{25} (5 \cdot 4 \cdot 4 + 4^2 u)\right)$ |

TABLE II. Quantum dimensions and topological spins for twisted quantum double of $G = \mathbb{Z}_{11} \rtimes \mathbb{Z}_5$. Here $u = 0, 1, 2, 3$, and 4.

$d_i = 11 \times 1 = 11$. The topological spin of anyon $(b^k, \tilde{\chi}^m)$ is $\theta_{(b^k, \tilde{\chi}^m)}^{(u)} = e^{\frac{2\pi i}{25}(5mk+k^2u)}$, where $u = 0, \dots, 4$.

In short, there are in total 49 anyons. The quantum dimensions and topological spins of these anyons are summarized in Table II, where $u = 0, 1, 2, 3, 4$ denote different categories.

For the modular S matrix, the explicit expression has been given in Appendix A 2. The elements that depend on the 3-cocycle ω^u are

$$S_{(b^k, \tilde{\chi}^m), (b^{k'}, \tilde{\chi}^n)}^{(u)} = \frac{1}{5} \exp\left(-\frac{2\pi i}{25}[2ukk' + 5(kn + k'm)]\right). \quad (3.8)$$

According to the previous section, $m = 2$ is the primitive root of the prime number $p = 5$. Then the five categories $D^{\omega^u}(G)$ are divided into three sets with $u = 0$, $u = m^{2n}$, and $u = m^{2n+1} \bmod p$. That is, one can find there are three distinct sets of modular data for (1) $u = 0$, (2) $u = 1$ and $u = 4$, and (3) $u = 2$ and $u = 3$, respectively.

As mentioned at the beginning of this section, to specify the fusion/splitting basis in Eq.(3.1), we need to know the fusion rules of $a \times \bar{a}$. With the modular S matrix in Eq.(2.21), this can be obtained via Verlinde's formula

$$N_{ab}^c = \sum_i \frac{S_{ai} S_{bi} S_{ci}^*}{S_{0i}}. \quad (3.9)$$

The explicit results are listed as follows:

$$(1) a \times \bar{a} = \sum_c N_{a\bar{a}}^c c, \text{ with } a = I_i$$

$$\begin{aligned} I_0 \times I_0 &= I_0, \\ I_1 \times I_4 &= I_0, \\ I_2 \times I_3 &= I_0, \\ I_5 \times I_6 &= I_0 + I_1 + I_2 + I_3 + I_4 + 2I_5 + 2I_6. \end{aligned} \quad (3.10)$$

$$(2) a \times \bar{a} = \sum_c N_{a\bar{a}}^c c, \text{ with } a = A_{l,m}$$

$$\begin{aligned} A_{1,0} \times A_{2,0} &= I_0 + I_1 + I_2 + I_3 + I_4 \\ &\quad + 2A_{1,0} + 2A_{2,0}, \\ A_{1,1} \times A_{2,6} &= I_0 + I_1 + I_2 + I_3 + I_4 \\ &\quad + A_{1,6} + A_{1,10} + A_{2,3} + A_{2,5}, \\ A_{1,2} \times A_{2,1} &= I_0 + I_1 + I_2 + I_3 + I_4 \\ &\quad + A_{1,1} + A_{1,9} + A_{2,6} + A_{2,10}, \\ A_{1,3} \times A_{2,7} &= I_0 + I_1 + I_2 + I_3 + I_4 \\ &\quad + A_{1,7} + A_{1,8} + A_{2,4} + A_{2,9}, \\ A_{1,4} \times A_{2,2} &= I_0 + I_1 + I_2 + I_3 + I_4 \\ &\quad + A_{1,2} + A_{1,7} + A_{2,1} + A_{2,9}, \\ A_{1,5} \times A_{2,8} &= I_0 + I_1 + I_2 + I_3 + I_4 \\ &\quad + A_{1,6} + A_{1,8} + A_{2,3} + A_{2,4}, \\ A_{1,6} \times A_{2,3} &= I_0 + I_1 + I_2 + I_3 + I_4 \\ &\quad + A_{1,3} + A_{1,5} + A_{2,7} + A_{2,8}, \\ A_{1,7} \times A_{2,9} &= I_0 + I_1 + I_2 + I_3 + I_4 \\ &\quad + A_{1,4} + A_{1,9} + A_{2,2} + A_{2,10}, \\ A_{1,8} \times A_{2,4} &= I_0 + I_1 + I_2 + I_3 + I_4 \\ &\quad + A_{1,3} + A_{1,4} + A_{2,2} + A_{2,7}, \\ A_{1,9} \times A_{2,10} &= I_0 + I_1 + I_2 + I_3 + I_4 \\ &\quad + A_{1,2} + A_{1,10} + A_{2,1} + A_{2,5}, \\ A_{1,10} \times A_{2,5} &= I_0 + I_1 + I_2 + I_3 + I_4 \\ &\quad + A_{1,1} + A_{1,5} + A_{2,6} + A_{2,8}, \end{aligned} \quad (3.11)$$

Note that the above fusion results in (3.10) and (3.11) are independent of u . This can be understood based on the fact that $S_{I_i, x}$ and $S_{A_{l,m}, x}$ are independent of u for arbitrary anyon type x . Or more essentially, the definitions of type- I and type- A anyons are independent of u .

$$(3) a \times \bar{a} = \sum_c N_{a\bar{a}}^c c, \text{ with } a = B_{k,n}$$

Now the fusion rules depend on u as follows. For different choices of u , the fusion results are the same, but the dual anyons of $B_{k,n}$ are different.

$$- u = 0:$$

$$\begin{aligned} B_{1,0} \times B_{4,0} &= I_0 + I_5 + I_6 \\ &\quad + A_{1,0} + A_{1,1} + A_{1,2} + A_{1,3} + A_{1,4} + A_{1,5} \\ &\quad + A_{1,6} + A_{1,7} + A_{1,8} + A_{1,9} + A_{1,10} \\ &\quad + A_{2,0} + A_{2,1} + A_{2,2} + A_{2,3} + A_{2,4} + A_{2,5} \\ &\quad + A_{2,6} + A_{2,7} + A_{2,8} + A_{2,9} + A_{2,10}. \end{aligned} \quad (3.12)$$

The quantum dimensions on the two sides of fusion rules satisfy the relation $11 \times 11 = 1 + 5 \times 24$. Interestingly, one can find that the fusion results for the other 9 pairs (anyons and their dual anyons) are the same as $B_{1,0} \times B_{4,0}$, *i.e.*,

$$\begin{aligned} B_{1,0} \times B_{4,0} &= B_{1,1} \times B_{4,4} = B_{1,2} \times B_{4,3} \\ &= B_{1,3} \times B_{4,2} = B_{1,4} \times B_{4,1} \\ &= B_{2,0} \times B_{3,0} = B_{2,1} \times B_{3,4} = B_{2,2} \times B_{3,3} \\ &= B_{2,3} \times B_{3,2} = B_{2,4} \times B_{3,1}. \end{aligned} \quad (3.13)$$

It is emphasized that the “=” here means the fusion results (but not the fusion rules) are the same.

$$- u = 1:$$

One can find the fusion results of the following anyons and their dual anyons are the same as that in Eq.(3.12).

$$\begin{aligned}
B_{3,0} \times B_{2,3} &= B_{3,1} \times B_{2,2} = B_{3,2} \times B_{2,1} \\
&= B_{3,3} \times B_{2,0} = B_{3,4} \times B_{2,4} \\
&= B_{4,0} \times B_{1,3} = B_{4,1} \times B_{1,2} = B_{4,2} \times B_{1,1} \\
&= B_{4,3} \times B_{1,0} = B_{4,4} \times B_{1,4}.
\end{aligned} \tag{3.14}$$

Similarly, for $u = 2, 3$, and 4, we have

- $u = 2$:

$$\begin{aligned}
B_{1,0} \times B_{4,1} &= B_{1,1} \times B_{4,0} = B_{1,2} \times B_{4,4} \\
&= B_{1,3} \times B_{4,3} = B_{1,4} \times B_{4,2} \\
&= B_{2,0} \times B_{3,1} = B_{2,1} \times B_{3,0} = B_{2,2} \times B_{3,4} \\
&= B_{2,3} \times B_{3,3} = B_{2,4} \times B_{3,2}.
\end{aligned} \tag{3.15}$$

- $u = 3$:

$$\begin{aligned}
B_{1,0} \times B_{4,4} &= B_{1,1} \times B_{4,3} = B_{1,2} \times B_{4,2} \\
&= B_{1,3} \times B_{4,1} = B_{1,4} \times B_{4,0} \\
&= B_{2,0} \times B_{3,4} = B_{2,1} \times B_{3,3} = B_{2,2} \times B_{3,2} \\
&= B_{2,3} \times B_{3,1} = B_{2,4} \times B_{3,0}.
\end{aligned} \tag{3.16}$$

- $u = 4$:

$$\begin{aligned}
B_{1,0} \times B_{4,2} &= B_{1,1} \times B_{4,1} = B_{1,2} \times B_{4,0} \\
&= B_{1,3} \times B_{4,4} = B_{1,4} \times B_{4,3} \\
&= B_{2,0} \times B_{3,2} = B_{2,1} \times B_{3,1} = B_{2,2} \times B_{3,0} \\
&= B_{2,3} \times B_{3,4} = B_{2,4} \times B_{3,3}.
\end{aligned} \tag{3.17}$$

One can find that for different 3-cocycle ω^u , the dual anyons of $B_{k,n}$ are different. This is also straightforwardly seen by looking at the topological spins in Table II, noting that $\theta_a = \theta_{\bar{a}}$. Based on these fusion rules, we can fix the basis in Eq.(3.4). For example, if we fix $z = A_{1,1}$, it is found that a can only be chosen as $A_{1,2}, A_{2,1}, A_{1,10}, A_{2,5}$, and all the 20 type- B anyons. In addition, there is only one fusion channel for these choices of a , i.e., $N_{a\bar{a}}^z = 1$. Then the Hilbert space spanned by the basis in Eq.(3.4) with fixed $z = A_{1,1}$ is 24 dimensional. It is noted that in certain cases, e.g., $z = A_{1,0}$, we may have more than one fusion channels with $N_{a\bar{a}}^z > 1$. The dimension of Hilbert space for $\bigoplus_a V_a^{az}$ with fixed z is $\sum_a N_{a\bar{a}}^z$.

1. Simple currents

There are some fine structures in the modular data due to those anyons with quantum dimension 1, which are called ‘simple currents’ in literature.⁴⁴⁻⁴⁶ Understanding such fine structures will help us in analyzing the patterns of a punctured S matrix in the next subsection.

The simple currents, which will be denoted as j here, can be defined as any $j \in \Pi_C$, with quantum dimension $d_j = S_{0j}/S_{00} = 1$. The fusion rules of j with any other simple objects $a \in \Pi_C$ are simply $j \times a = a'$, where $a' \in \Pi_C$. That is, there is only one anyon appearing in the fusion results. The effect of simple currents on modular S and T matrices have been studied in, e.g., Refs.39, 44-46. Here we focus on the simplest counterexamples in MS MTCs with $G = \mathbb{Z}_{11} \rtimes$

\mathbb{Z}_5 . From Table II, one can find there are in total five simple currents I_i , with $i = 0, \dots, 4$. Since I_0 is the identity anyon, its fusion rules with other anyons are trivial, and we will not write them down. Note that there are five different categories with $u = 0, 1, 2, 3, 4, 5$, but interestingly, the fusion rules of the simple currents with other simple objects are independent of u as follows:

$$\begin{aligned}
I_1 \times I_1 &= I_2, I_1 \times I_2 = I_3, I_1 \times I_3 = I_4, I_1 \times I_4 = I_0, \\
I_2 \times I_2 &= I_4, I_2 \times I_3 = I_0, I_2 \times I_4 = I_1, \\
I_3 \times I_3 &= I_1, I_3 \times I_4 = I_2, \\
I_4 \times I_4 &= I_3,
\end{aligned} \tag{3.18}$$

$$I_k \times A_{l,m} = A_{l,m}, \quad k = 1, 2, 3, 4, \tag{3.19}$$

and

$$\begin{aligned}
I_1 \times B_{i,j} &= B_{i,j+1}, \\
I_4 \times B_{i,j} &= B_{i,j-1}, \\
I_2 \times B_{i,j} &= B_{i,j+2}, \\
I_3 \times B_{i,j} &= B_{i,j-2},
\end{aligned} \tag{3.20}$$

where $i = 1, 2, 3, 4$ and $j = j \bmod 5$. It is noted that in the above fusion rules $B_{i,j'} = B_{i,j} \times I_k$, the index ‘ i ’ which labels the flux keeps the same, but only the index ‘ j ’ which labels the charge changes. This is because the simple currents I_k are pure charges, and fusing I_k with any other anyon $a \in \Pi_C$ can at most change the charge of anyon a .

Diagrammatically, Eq.(3.20) can be expressed as

$$B_{ij'} = B_{ij} \times I_k : \begin{array}{c} \uparrow \\ B_{ij'} \end{array} = \begin{array}{c} \uparrow \\ B_{ij} \\ \text{---} \\ \uparrow \\ I_k \end{array} \tag{3.21}$$

where the dashed line represents the world line of I_k anyons. We are interested in the effect of simple currents I_k ($k = 1, 2, 3, 4$) on $S_{B_{i,j}, B_{i',j'}}$ and $T_{B_{i,j}, B_{i,j}}$. From the fusion rules (3.20) and the modular data in Appendix (A 2), it is found that

$$\begin{cases} S_{(I_k \times B_{i,j}), B_{m,n}} = S_{B_{i,j}, B_{m,n}} \cdot e^{2\pi i Q_k(B_{m,n})}, \\ T_{(I_k \times B_{m,n}), (I_k \times B_{m,n})} = T_{B_{i,j}, B_{i,j}} \cdot e^{-2\pi i Q_k(B_{m,n})}. \end{cases} \tag{3.22}$$

where $e^{2\pi i Q_k(B_{m,n})}$ is a pure $U(1)$ phase with the expression

$$e^{2\pi i Q_k(B_{m,n})} = \frac{S_{I_k, B_{m,n}}}{S_{I_0, B_{m,n}}} = \frac{S_{B_{m,n}, I_k}}{S_{B_{m,n}, I_0}} = e^{-\frac{2\pi i}{5} \cdot k \cdot m}. \tag{3.23}$$

This phase can be viewed as the AharonovBohm phase introduced by dragging an I_k anyon ($k = 0, 1, 2, 3, 4$) around anyon $B_{m,n}$. Diagrammatically, the relations in Eq.(3.22) can be depicted as follows:

$$\begin{array}{c} \text{---} \\ \uparrow \\ B_{i,j'} \end{array} \text{---} \begin{array}{c} \uparrow \\ B_{m,n} \end{array} = \begin{array}{c} \text{---} \\ \uparrow \\ I_k \end{array} \text{---} \begin{array}{c} \uparrow \\ B_{i,j} \end{array} \text{---} \begin{array}{c} \uparrow \\ B_{m,n} \end{array} \tag{3.24}$$

where $B_{ij'} = B_{ij} \times I_k$, and

$$\begin{array}{c} \circlearrowleft \\ B_{m,n'} \uparrow \end{array} = \begin{array}{c} \circlearrowleft \\ B_{m,n} \uparrow \end{array} \begin{array}{c} I_k \\ \uparrow \end{array} \quad (3.25)$$

where $B_{m,n'} = B_{m,n} \times I_k$. Then by considering the local operation¹⁰

$$\begin{array}{c} \circlearrowleft \\ \bar{x} \end{array} \begin{array}{c} a \\ \uparrow \end{array} = \frac{S_{ax}}{S_{0x}} \begin{array}{c} \uparrow \\ \bar{x} \end{array} \quad (3.26)$$

one can remove the I_k anyon in (3.24) and (3.25) by introducing extra phases $\frac{S_{I_k, B_{m,n}}}{S_{I_0, B_{m,n}}}$ in S -matrix, and $\frac{S_{I_k, \bar{B}_{m,n}}}{S_{I_0, \bar{B}_{m,n}}} = \frac{S_{I_k, B_{m,n}}^*}{S_{I_0, B_{m,n}}^*}$ in T matrix, as expressed in Eq.(3.22).

B. Punctured S and T matrices

In this subsection, we study the properties of punctured S and T matrices, and in particular present the results for the MS MTCs with $G = \mathbb{Z}_{11} \rtimes \mathbb{Z}_5$.

First, we give an intuitive picture on how to obtain the punctured S and T matrices based on the modular transformation of a punctured torus. As introduced in Sec.I C, the canonical basis on a punctured torus can be considered as the path integral over a solid torus $D^2 \times S^1$ as follows:

$$|\psi_{a\bar{a},\mu}^{(z)}\rangle := \begin{array}{c} \circlearrowleft \\ \mu \\ \circlearrowright \\ a \end{array} \quad \text{on } D^2 \times S^1$$

where \circ denotes the puncture on the two dimensional surface $\partial(D^2 \times S^1) = S^1 \times S^1$, z denotes the anyon at the puncture, and μ denotes the channel that a and \bar{a} fuse into z . Note that when $z = 1$, $|\psi_{a\bar{a},\mu}^{(z)}\rangle$ reduces to the canonical basis on a torus T^2 without any puncture.

Then we can define the matrix element of the punctured S -matrix as

$$S_{a,\mu;b,\nu}^{(z)} := \frac{\langle \psi_{a\bar{a},\mu}^{(z)} | \hat{S} | \psi_{b\bar{b},\nu}^{(z)} \rangle}{\sqrt{\langle \psi_{a\bar{a},\mu}^{(z)} | \psi_{a\bar{a},\mu}^{(z)} \rangle \cdot \langle \psi_{b\bar{b},\nu}^{(z)} | \psi_{b\bar{b},\nu}^{(z)} \rangle}}, \quad (3.27)$$

where we have

$$\langle \psi_{a\bar{a},\mu}^{(z)} | \psi_{a\bar{a},\mu}^{(z)} \rangle = \begin{array}{c} \mu \\ \circlearrowleft \\ \mu \\ \circlearrowright \\ a \bar{a} \end{array} \quad \text{on } S^2 \times S^1,$$

and similarly for $\langle \psi_{b\bar{b},\nu}^{(z)} | \psi_{b\bar{b},\nu}^{(z)} \rangle$. They can be evaluated based on the surgery approach³¹, and the result is

$$\langle \psi_{a\bar{a},\mu}^{(z)} | \psi_{a\bar{a},\mu}^{(z)} \rangle = \langle \psi_{b\bar{b},\nu}^{(z)} | \psi_{b\bar{b},\nu}^{(z)} \rangle = \sqrt{d_z}. \quad (3.28)$$

The numerator in (3.27) is

$$\langle \psi_{a\bar{a},\mu}^{(z)} | \hat{S} | \psi_{b\bar{b},\nu}^{(z)} \rangle = \begin{array}{c} \circlearrowleft \\ \mu \\ \circlearrowright \\ a \bar{b} \end{array} \quad \text{on } S^3. \quad (3.29)$$

That is, after the S transformation, two solid torus are glued together as a S^3 , with the two punctures identified.

Hereafter, without specific explanation, all the link/knot invariants can be considered as embedded in the three manifold S^3 , and for convenience we will remove \circ which represents S^3 in Eq.(3.29).

Based on the above analysis, one can find that the punctured S -matrix can be presented as (note that an extra normalization factor $1/\mathcal{D}$ is introduced):

$$S_{a,\mu;b,\nu}^{(z)} = \frac{1}{\mathcal{D}} \cdot \frac{1}{\sqrt{d_z}} \cdot \begin{array}{c} \circlearrowleft \\ \mu \\ \circlearrowright \\ a \bar{b} \end{array} \quad (3.30)$$

One can see clearly that for the case of $z = 1$, the presentation above reduces to the conventional modular S matrix. It is noted that $S_{a,\mu;b,\nu}^{(z)}$ can also be expressed in terms of F and R symbols (also called F and R matrices)^{10,16}.

Similarly, one can define the punctured T matrix as

$$T_{a,\mu;b,\nu}^{(z)} := \frac{\langle \psi_{a\bar{a},\mu}^{(z)} | \hat{T} | \psi_{b\bar{b},\nu}^{(z)} \rangle}{\sqrt{\langle \psi_{a\bar{a},\mu}^{(z)} | \psi_{a\bar{a},\mu}^{(z)} \rangle \cdot \langle \psi_{b\bar{b},\nu}^{(z)} | \psi_{b\bar{b},\nu}^{(z)} \rangle}}, \quad (3.31)$$

where the numerator $\langle \psi_{a\bar{a},\mu}^{(z)} | \hat{T} | \psi_{b\bar{b},\nu}^{(z)} \rangle$ corresponds to a path integral over $S^2 \times S^1$. With the straightforward surgery approach³¹, one can find that

$$T_{a,\mu;b,\nu}^{(z)} = \delta_{a,b} \delta_{\mu,\nu} \theta_a, \quad (3.32)$$

with $N_{a\bar{a}}^z > 0$. For the twisted quantum double $D^\omega(G)$ of $G = \mathbb{Z}_q \rtimes \mathbb{Z}_p$, the topological spin θ_a can be straightforwardly obtained based on Eq.(2.13). That is, based on the modular data and the fusion rules (which are also determined by the modular data due to Verlinde formula), we can obtain the punctured T -matrix in (3.32).

To obtain the punctured S matrix, our strategy is to solve the modular relations for punctured S and T as follows:^{10,16}

$$\begin{cases} (S^{(z)})^2 = C^{(z)}, \\ (C^{(z)})^2 = \theta_z^*, \\ (S^{(z)}T^{(z)})^3 = (S^{(z)})^2, \end{cases} \quad (3.33)$$

$C^{(z)}$ can be understood as the ‘punctured’ charge conjugation, which will reduce to the conventional charge conjugation C when $z = 1$. In addition, $S^{(z)}$ and $T^{(z)}$ are unitary matrices. This is apparent for $T^{(z)}$ based on the expression in (3.32). The unitarity property of $S^{(z)}$ is related to the

braiding non-degeneracy of modular categories.¹⁰ Intuitively, it means that a nontrivial anyon (which is not an identity) can be detected by Aharonov-Bohm measurement by dragging a test particle around it. With the unitary property of $S^{(z)}$ and $T^{(z)}$, the last equation in Eq.(3.33) is equivalent to $(S^{(z)})^\dagger T^{(z)} (S^{(z)}) = (T^{(z)})^\dagger (S^{(z)})^\dagger (T^{(z)})^\dagger$, which is useful in solving $S^{(z)}$. Furthermore, from Eq.(3.33), one can also observe that $(S^{(z)})^4 = \theta_z^*$. This is related to MCG($\Sigma_{1,1}$) in (1.8), where $\mathfrak{s}^4 = \mathfrak{r}^{-1}$, with \mathfrak{r} representing the Dehn twist around the puncture.

We will give further details on the modular relations in (3.33) in the rest of this subsection. It is convenient to study the modular relations in (3.33) by acting the operators on the basis vectors in the Hilbert space $\mathcal{H}(\Sigma_{1,1})$. We denote the Hilbert space on a punctured torus as $\mathcal{H}(\Sigma_{1,1}) = \oplus_b V_b^{bz}$, with z representing the anyonic charge at the puncture. Then one has^{10,16}

$$S^{(z)} \begin{array}{c} b \\ \swarrow \\ \mu \\ \uparrow \\ b \end{array} \begin{array}{c} z \\ \nearrow \\ \mu \\ \downarrow \\ a \end{array} := \frac{1}{\mathcal{D}} \sum_a d_a \begin{array}{c} a \\ \swarrow \\ \mu \\ \uparrow \\ a \end{array} \begin{array}{c} z \\ \nearrow \\ \mu \\ \downarrow \\ b \end{array}, \quad (3.34)$$

$$T^{(z)} \begin{array}{c} b \\ \swarrow \\ \mu \\ \uparrow \\ b \end{array} \begin{array}{c} z \\ \nearrow \\ \mu \\ \downarrow \\ b \end{array} := \theta_b \begin{array}{c} b \\ \swarrow \\ \mu \\ \uparrow \\ b \end{array} \begin{array}{c} z \\ \nearrow \\ \mu \\ \downarrow \\ b \end{array}, \quad (3.35)$$

and

$$C^{(z)} \begin{array}{c} b \\ \swarrow \\ \mu \\ \uparrow \\ b \end{array} \begin{array}{c} z \\ \nearrow \\ \mu \\ \downarrow \\ b \end{array} := \theta_b^* \begin{array}{c} \bar{b} \\ \swarrow \\ \mu \\ \uparrow \\ \bar{b} \end{array} \begin{array}{c} z \\ \nearrow \\ \mu \\ \downarrow \\ \bar{b} \end{array}. \quad (3.36)$$

In this basis, $T^{(z)}$ is a diagonal matrix with entries θ_b , which is the topological spin of anyon b that satisfies the fusion rule $b \times \bar{b} = I + N_{b\bar{b}}^z z + \dots$, with $N_{b\bar{b}}^z > 0$. Note that $N_{ij}^k = \dim V_{ij}^k$. Based on the definitions in Eqs.(3.34), (3.35), and (3.36), one can prove the modular relations in Eq.(3.33). For example, the first relation $(S^{(z)})^2 = C^{(z)}$ in Eq.(3.33) can be proved as follows:

$$\begin{aligned} (S^{(z)})^2 \begin{array}{c} b \\ \swarrow \\ \mu \\ \uparrow \\ b \end{array} \begin{array}{c} z \\ \nearrow \\ \mu \\ \downarrow \\ b \end{array} &= \frac{1}{\mathcal{D}^2} \sum_{x,a} d_x d_a \begin{array}{c} x \\ \swarrow \\ \mu \\ \uparrow \\ x \end{array} \begin{array}{c} z \\ \nearrow \\ \mu \\ \downarrow \\ a \end{array} \\ &= \frac{1}{\mathcal{D}^2} \sum_{x,a} d_x d_a \theta_x^* \begin{array}{c} x \\ \swarrow \\ \mu \\ \uparrow \\ x \end{array} \begin{array}{c} z \\ \nearrow \\ \mu \\ \downarrow \\ a \end{array} \\ &= \sum_x \delta_{x,\bar{b}} \theta_x^* \begin{array}{c} x \\ \swarrow \\ \mu \\ \uparrow \\ x \end{array} \begin{array}{c} z \\ \nearrow \\ \mu \\ \downarrow \\ x \end{array} = \theta_b^* \begin{array}{c} \bar{b} \\ \swarrow \\ \mu \\ \uparrow \\ \bar{b} \end{array} \begin{array}{c} z \\ \nearrow \\ \mu \\ \downarrow \\ \bar{b} \end{array}, \end{aligned} \quad (3.37)$$

where we have considered the fact $\theta_b = \theta_{\bar{b}}$ in the last step. By comparing Eq.(3.37) with the definition of $C^{(z)}$ in Eq.(3.36), one can find that $(S^{(z)})^2 = C^{(z)}$. Some further details in (3.37) and the proof of the other two relations in Eq.(3.33) can be found in the appendix B.

Before solving Eqs.(3.33) for $S^{(z)}$, it is helpful to understand the property of matrix elements of $C^{(z)}$, which are expressed as follows:

$$\begin{aligned} C_{a,\mu;b,\nu}^{(z)} &= \delta_{a,\bar{b}} \delta_{\mu,\nu} \frac{\theta_b^*}{\sqrt{d_a d_b d_z}} \begin{array}{c} z \\ \swarrow \\ \mu \\ \uparrow \\ b \end{array} \begin{array}{c} z \\ \nearrow \\ \mu \\ \downarrow \\ b \end{array} \\ &= \delta_{a,\bar{b}} [R_z^{bb}]_{\mu\nu}^{-1} \cdot \theta_b^*, \end{aligned} \quad (3.38)$$

where we have used the definition of R matrix:

$$\begin{array}{c} b \\ \swarrow \\ \mu \\ \uparrow \\ c \end{array} \begin{array}{c} a \\ \nearrow \\ \mu \\ \downarrow \\ c \end{array} = R_{ab} \begin{array}{c} a \\ \swarrow \\ \mu \\ \uparrow \\ c \end{array} \begin{array}{c} b \\ \nearrow \\ \mu \\ \downarrow \\ c \end{array} = \sum_\nu (R_c^{ab})_{\mu\nu} \begin{array}{c} b \\ \swarrow \\ \nu \\ \uparrow \\ c \end{array} \begin{array}{c} a \\ \nearrow \\ \nu \\ \downarrow \\ c \end{array}. \quad (3.39)$$

One can check that for the specific case of $z = 1$, $C_{a,\mu;b,\nu}^{(z)}$ reduces to the conventional charge conjugation:

$$C_{a,b}^{(z=1)} = \delta_{a,\bar{b}} \frac{\theta_b^*}{\sqrt{d_a d_b}} \begin{array}{c} z=1 \\ \swarrow \\ \mu \\ \uparrow \\ b \end{array} \begin{array}{c} z=1 \\ \nearrow \\ \mu \\ \downarrow \\ b \end{array} = \delta_{a,\bar{b}}. \quad (3.40)$$

In addition, from the result in Eq.(3.38), one can prove the relation $(C^{(z)})^2 = \theta_z^*$ in (3.33) straightforwardly as

$$\begin{aligned} [C^{(z)}]_{a,\mu;b,\nu}^2 &= \sum_{c,\lambda} C_{a,\mu;c,\lambda}^{(z)} C_{c,\lambda;b,\nu}^{(z)} \\ &= \sum_{c,\lambda} \delta_{a,\bar{c}} \delta_{c,\bar{b}} (R_z^{c\bar{c}})_{\mu,\lambda}^{-1} \cdot \theta_c^* \cdot (R_z^{b\bar{b}})_{\lambda,\nu}^{-1} \cdot \theta_b^* \\ &= \delta_{a,\bar{b}} \delta_{\mu,\nu} \theta_z^*, \end{aligned} \quad (3.41)$$

where in the last step we have used the ribbon property $\sum_\lambda [R_c^{ab}]_{\mu\lambda} [R_c^{ba}]_{\lambda\nu} = \frac{\theta_c}{\theta_a \theta_b} \delta_{\mu,\nu}$, and the properties of topological spins $\theta_a = \theta_{\bar{a}}$ and $\theta_a^* = \theta_a^{-1}$.

One remark on (3.38):

The term $[R_z^{bb}]_{\mu\nu}^{-1}$ in the expression of $C_{a,\mu;b,\nu}^{(z)}$ in Eq.(3.38) is in general not gauge invariant, even for the multiplicity-free case. As a comparison, R_z^{bb} (and $R_z^{\bar{b}\bar{b}}$) for the multiplicity-free case are gauge invariant quantities, with $R_z^{bb} = \pm \frac{\theta_z^{1/2}}{\theta_b}$, where the sign \pm is determined by the modular data.¹⁵ One can find that R_z^{bb} and $R_z^{\bar{b}\bar{b}}$ (for the multiplicity-free case) are gauge invariant only when $b = \bar{b}$. In MS MTCs, except for the identity anyon I_0 , none of the anyons are self-dual, and R_z^{bb} ($R_z^{\bar{b}\bar{b}}$) are not gauge invariant. We give more discussions on the gauge freedom in $S^{(z)}$ and $C^{(z)}$ in the following subsection.

1. Gauge freedom and patterns in the solutions

The solutions to the modular relation in Eq.(3.33) are not unique, because they have a gauge freedom associated with

each distinct vertex that amounts to the choice of basis vectors. More explicitly, we can consider the basis transformation in the splitting space V_c^{ab} as follows

$$\begin{array}{c} a \quad b \\ \diagdown \quad / \\ \mu \\ \diagup \quad \diagdown \\ c \end{array} = \sum_{\mu'} [u_c^{ab}]_{\mu\mu'} \begin{array}{c} a \quad b \\ \diagdown \quad / \\ \mu' \\ \diagup \quad \diagdown \\ c \end{array} \quad (3.42)$$

or equivalently, $|a, b; c, \mu\rangle = \sum_{\mu'} [u_c^{ab}]_{\mu\mu'} |a, b; c, \mu'\rangle$. If one requires that the F and R matrices in the anyon theory are presented by unitary matrices, the basis transformation above should also be unitary.²⁶ For the multiplicity-free case, such that $u = u'$ denotes the unique fusion channel, then u_c^{ab} in Eq.(3.42) is a $U(1)$ phase.

The gauge freedom in Eq.(3.42) means there are a family of solutions to the modular relations in Eq.(3.33), and also to the more general relations such as Pentagon and Hexagon equations. This can be intuitively seen from the diagrammatic representation of $S_{a,\mu;b,\nu}^{(z)}$ in (3.30) and $C_{a,\mu;b,\nu}^{(z)}$ in (3.38). There are a pair of vertices in both $S_{a,\mu;b,\nu}^{(z)}$ and $C_{a,\mu;b,\nu}^{(z)}$. If we change the gauge choice associated with the vertex structures, then the concrete value of $S_{a,\mu;b,\nu}^{(z)}$ and $C_{a,\mu;b,\nu}^{(z)}$ will change accordingly. More explicitly, with the basis transformation in (3.42), one can find that different quantities transform as:

$$\begin{aligned} [S']_{a,\mu';b,\nu'}^{(z)} &= \sum_{\mu,\nu} (u_b^{bz})_{\nu'\nu}^{-1} \cdot S_{a,\mu;b,\nu}^{(z)} \cdot (u_a^{az})_{\mu\mu'}, \\ [C']_{a,\mu';\bar{a},\nu'}^{(z)} &= \sum_{\mu,\nu} (u_{\bar{a}}^{\bar{a}z})_{\nu'\nu}^{-1} \cdot C_{a,\mu;\bar{a},\nu}^{(z)} \cdot (u_a^{az})_{\mu\mu'}, \\ [T']_{a,\mu';b,\nu'}^{(z)} &= T_{a,\mu';b,\nu'}^{(z)}. \end{aligned} \quad (3.43)$$

where we have considered the expressions of $C^{(z)}$ and $T^{(z)}$ in Eqs.(3.38) and (3.32), respectively. Interestingly, from Eq.(3.43), one can find that

$$\sum_{\mu'} [S']_{a,\mu';a,\mu'}^{(z)} = \sum_{\mu} S_{a,\mu;a,\mu}^{(z)}. \quad (3.44)$$

That is, although $S_{a,\mu;b,\nu}^{(z)}$ is not gauge invariant with respect to the basis transformation in (3.42), $\sum_{\mu} S_{a,\mu;a,\mu}^{(z)}$ is a gauge invariant quantity. The result in Eq.(3.44) is also studied in the diagrammatical representation of anyons in Ref.15.

For simplicity, we will focus on the multiplicity-free case in the following discussions. This is the case we are interested in for the MS MTCs (See, e.g., the fusion rules in (3.12)). Generalization to the case that is not multiplicity-free is straightforward. In the multiplicity-free case, Eq.(3.43) can be simplified as

$$\begin{aligned} [S']_{a,b}^{(z)} &= S_{a,b}^{(z)} \cdot (u_b^{bz})^{-1} \cdot u_a^{az}, \\ [C']_{a,\bar{a}}^{(z)} &= C_{a,\bar{a}}^{(z)} \cdot (u_{\bar{a}}^{\bar{a}z})^{-1} \cdot u_a^{az}, \\ [T']_{a,b}^{(z)} &= T_{a,b}^{(z)}. \end{aligned} \quad (3.45)$$

where u_c^{ab} is simply a phase factor. We give several remarks on Eq.(3.45) as follows:

– One can find that

$$[S']_{a,a}^{(z)} = S_{a,a}^{(z)}, \quad (3.46)$$

which is a simplified version of Eq.(3.44). That is, $S_{a,a}^{(z)}$ is a gauge invariant quantity in the multiplicity-free case. As will be discussed in Sec.(III C), we will use this quantity to distinguish different MS MTCs.

– The punctured S matrix is in general not symmetric, *i.e.*, $S_{a,b}^{(z)} \neq S_{b,a}^{(z)}$. This can be understood based on the first equation in (3.45). One can find that

$$\frac{[S']_{a,b}^{(z)}}{[S']_{b,a}^{(z)}} = \frac{S_{a,b}^{(z)}}{S_{b,a}^{(z)}} \cdot \frac{(u_a^{az})^2}{(u_b^{bz})^2}. \quad (3.47)$$

If $S_{a,b}^{(z)} = S_{b,a}^{(z)}$, then after a basis transformation in (3.42), one can obtain $[S']_{a,b}^{(z)}/[S']_{b,a}^{(z)} = (u_a^{az})^2/(u_b^{bz})^2$, which is in general not equal to 1, and therefore $[S']_{a,b}^{(z)}$ is asymmetric. This is in contrast to the modular S matrix, which is symmetric, *i.e.*, $S_{a,b} = S_{b,a}$.

– $C_{a,\bar{a}}^{(z)}$ is gauge invariant if $\bar{a} = a$, but not gauge invariant if $\bar{a} \neq a$. This is straightforward based on the second equation in (3.45). It is also related to the fact that $R_z^{\bar{b}b}$ in (3.38) is not gauge invariant for $\bar{b} \neq b$. Note that for the counterexamples in MS MTCs, for all anyons but I_0 , we have $\bar{a} \neq a$.

– $T_{a,b}^{(z)}$ is gauge invariant, with the explicit expression in Eq.(3.32).

In the above we have discussed the gauge freedom in $S^{(z)}$, $C^{(z)}$, and $T^{(z)}$ in Eq.(3.33). Now we need to fix a simple gauge choice to solve Eq.(3.33). We will consider the simple currents I_k ($k = 1, 2, 3, 4$) as introduced in Sec.III A 1. The gauge choice we make is

$$\begin{array}{c} B_{i,j'} \quad z \\ \diagdown \quad / \\ \quad \quad \quad \\ \diagup \quad \diagdown \\ B_{i,j'} \end{array} = \begin{array}{c} B_{i,j} \quad z \\ \diagdown \quad / \\ I_k \quad \quad \\ \diagup \quad \diagdown \\ B_{i,j} \end{array} \quad (3.48)$$

where $B_{i,j'} = B_{i,j} \times I_k$. This can be viewed as a generalization of (3.21) to the vertex structure. We emphasize that there is no gauge freedom in (3.21). For (3.48), however, there can be a phase-factor difference on the two sides. For example, under the basis transformation in (3.42), a phase factor $u_{B_{i,j},z}^{B_{i,j',z}}/u_{B_{i,j'},z}^{B_{i,j,z}}$ will be introduced in Eq.(3.48). Here we make the simple gauge choice such that Eq.(3.48) holds. Once we find the solutions to the modular relations in Eq.(3.33), we can obtain a family of gauge-equivalent solutions by considering the basis transformations in (3.42).

With the gauge choice in (3.48), one can find the following patterns in $S^{(z)}$:

$$\begin{array}{c} B_{i,j'} \quad B_{m,n} \\ \diagdown \quad / \\ \quad \quad \quad \\ \diagup \quad \diagdown \\ z \end{array} = \begin{array}{c} B_{i,j} \quad B_{m,n} \\ \diagdown \quad / \\ I_k \quad \quad \\ \diagup \quad \diagdown \\ z \end{array} \quad (3.49)$$

where $B_{i,j'} = B_{i,j} \times I_k$, as seen in Eq.(3.20). By shrinking the I_k anyon, and using the relation in Eq.(3.26), one can obtain the following results:

$$\begin{aligned} S_{(I_k \times B_{i,j}), B_{m,n}}^{(z)} &= \frac{S_{I_k, B_{m,n}}}{S_{I_0, B_{m,n}}} \cdot S_{B_{i,j}, B_{m,n}}^{(z)}, \\ S_{B_{m,n}, (I_k \times B_{i,j})}^{(z)} &= \frac{S_{B_{m,n}, I_k}}{S_{B_{m,n}, I_0}} \cdot S_{B_{m,n}, B_{i,j}}^{(z)}, \end{aligned} \quad (3.50)$$

where the phase factors $\frac{S_{I_k, B_{m,n}}}{S_{I_0, B_{m,n}}}$ and $\frac{S_{B_{m,n}, I_k}}{S_{B_{m,n}, I_0}}$ are expressed in Eq.(3.23). This pattern holds for all the five categories with $u = 0, \dots, 4$ in the simplest counterexamples in MS MTCs with $G = \mathbb{Z}_{11} \rtimes \mathbb{Z}_5$.

The concrete solutions of punctured S matrix for MS MTCs with $G = \mathbb{Z}_{11} \rtimes \mathbb{Z}_5$ can be found in online materials [47]. Recall that in MS MTCs, only type- B anyons contain the information of the 3-cocycle ω^u , with $u = 0, 1, 2, 3, 4$. This indicates the nontrivial $S^{(z)}$ that are candidates to distinguish different MS MTCs are those containing type- B anyons. Based on the fusion rules in Eqs.(3.10), (3.11), and (3.12), the nontrivial $S^{(z)}$ correspond to those with $z = I_5, I_6$, and all type- A anyons.

On the other hand, for $z = I_k$ ($k = 1, 2, 3, 4$), only type- A anyons participate in the fusion $a \times \bar{a} = I_0 + N_{a\bar{a}}^z z + \dots$, i.e., we have $N_{a\bar{a}}^z > 0$ only if a are type- A anyons, as seen from (3.11). In this case, since both I_k and type- A anyons are defined independent of the 3-cocycle ω^u , it is expected that $S^{(z)}$ with $z = I_k$ ($k = 1, 2, 3, 4$) are independent of the 3-cocycle ω^u , and therefore are trivial for our motivations. This is verified in the lattice calculation in Sec.IV. We did not solve for these trivial $S^{(z)}$ which are independent of u .

It is emphasized that the solutions in [47] are not unique, and one can obtain a family of gauge-equivalent solutions by performing the basis transformation in Eq.(3.42). For the multiplicity-free case, this corresponds to the gauge transformation in Eq.(3.45).

C. Distinguish MS MTCs with $S^{(z)}$ and T

As discussed in the previous subsections, in general the punctured S matrix depends on the gauge freedom in the choice of basis vectors in the fusion/splitting space. To distinguish different MS MTCs, we hope to find some topological invariants, which is our main aim in the next subsections. But before that, it is noted that certain matrix elements in the punctured S matrix are topological invariants themselves, such as $\sum_{\mu=1}^{N_{a\bar{a}}^z} S_{a\mu, a\mu}^{(z)}$, as seen from Eq.(3.44).

In this subsection, we show that the simplest counterexamples in MS MTCs can be distinguished based on the diagonal parts of punctured S -matrix together with the modular T matrix. For example, one can find that the permutations of anyons taking $T^{u=1(2)}$ to $T^{u=4(3)}$ cannot take $S_{B,B}^{(z), u=1(2)}$ to $S_{B,B}^{(z), u=4(3)}$ simultaneously, indicating that the punctured S matrix together with T matrix can distinguish the two categories with $u = 1(2)$ and $u = 4(3)$. This method is similar to those used in Ref.15, 24, and 25 in spirit, where one needs to

track whether two sets of topological invariants transform in a consistent way.

More explicitly, let us consider the categories \mathcal{C}_u with $u = 1$ and $u = 4$. From the modular T -matrix in Table II, one can find that, for example, $A_{1,1}$ in $\mathcal{C}_{u=1}$ can only be sent to $A_{1,1}$ or $A_{2,6}$ in $\mathcal{C}_{u=4}$ to keep the topological spin unchanged (Note that $A_{1,1}$ and $A_{2,6}$ are dual anyons in both $\mathcal{C}_{u=1}$ and $\mathcal{C}_{u=4}$ as seen from the fusion rules in (3.11) with $\theta_a = \theta_{\bar{a}}$). Here the meaning of ‘‘sending $A_{1,1}$ in $\mathcal{C}_{u=1}$ to $A_{1,1}$ or $A_{2,6}$ in $\mathcal{C}_{u=1}$ ’’ is the bijection of anyons as introduced in Sec.II B 1. That is, we consider a bijection of anyons between two categories that share the same modular data, such that $T_{p_r(a), p_r(b)}^{(u)} = T_{a,b}^{(u')}$. For the example above, one can find that $T_{A_{1,1}, A_{1,1}}^{(u=4)} = T_{A_{2,6}, A_{2,6}}^{(u=4)} = T_{A_{1,1}, A_{1,1}}^{(u=1)}$.

| a | $u = 1$ | $u = 4$ |
|-----------|---------------------------------------|---------------------------------------|
| $B_{1,0}$ | $\frac{1}{5}e^{-\frac{144}{275}i\pi}$ | $\frac{1}{5}e^{-\frac{274}{275}i\pi}$ |
| $B_{1,1}$ | $\frac{1}{5}e^{-\frac{186}{275}i\pi}$ | $\frac{1}{5}e^{-\frac{54}{275}i\pi}$ |
| $B_{1,2}$ | $\frac{1}{5}e^{-\frac{34}{275}i\pi}$ | $\frac{1}{5}e^{-\frac{166}{275}i\pi}$ |
| $B_{1,3}$ | $\frac{1}{5}e^{-\frac{254}{275}i\pi}$ | $\frac{1}{5}e^{-\frac{164}{275}i\pi}$ |
| $B_{1,4}$ | $\frac{1}{5}e^{-\frac{76}{275}i\pi}$ | $\frac{1}{5}e^{-\frac{56}{275}i\pi}$ |
| $B_{2,0}$ | $\frac{1}{5}e^{-\frac{126}{275}i\pi}$ | $\frac{1}{5}e^{-\frac{104}{275}i\pi}$ |
| $B_{2,1}$ | $\frac{1}{5}e^{-\frac{16}{275}i\pi}$ | $\frac{1}{5}e^{-\frac{6}{275}i\pi}$ |
| $B_{2,2}$ | $\frac{1}{5}e^{-\frac{94}{275}i\pi}$ | $\frac{1}{5}e^{-\frac{116}{275}i\pi}$ |
| $B_{2,3}$ | $\frac{1}{5}e^{-\frac{204}{275}i\pi}$ | $\frac{1}{5}e^{-\frac{226}{275}i\pi}$ |
| $B_{2,4}$ | $\frac{1}{5}e^{-\frac{236}{275}i\pi}$ | $\frac{1}{5}e^{-\frac{214}{275}i\pi}$ |
| $B_{3,0}$ | $\frac{1}{5}e^{-\frac{204}{275}i\pi}$ | $\frac{1}{5}e^{-\frac{116}{275}i\pi}$ |
| $B_{3,1}$ | $\frac{1}{5}e^{-\frac{94}{275}i\pi}$ | $\frac{1}{5}e^{-\frac{6}{275}i\pi}$ |
| $B_{3,2}$ | $\frac{1}{5}e^{-\frac{16}{275}i\pi}$ | $\frac{1}{5}e^{-\frac{104}{275}i\pi}$ |
| $B_{3,3}$ | $\frac{1}{5}e^{-\frac{126}{275}i\pi}$ | $\frac{1}{5}e^{-\frac{214}{275}i\pi}$ |
| $B_{3,4}$ | $\frac{1}{5}e^{-\frac{236}{275}i\pi}$ | $\frac{1}{5}e^{-\frac{226}{275}i\pi}$ |
| $B_{4,0}$ | $\frac{1}{5}e^{-\frac{254}{275}i\pi}$ | $\frac{1}{5}e^{-\frac{166}{275}i\pi}$ |
| $B_{4,1}$ | $\frac{1}{5}e^{-\frac{34}{275}i\pi}$ | $\frac{1}{5}e^{-\frac{54}{275}i\pi}$ |
| $B_{4,2}$ | $\frac{1}{5}e^{-\frac{186}{275}i\pi}$ | $\frac{1}{5}e^{-\frac{274}{275}i\pi}$ |
| $B_{4,3}$ | $\frac{1}{5}e^{-\frac{144}{275}i\pi}$ | $\frac{1}{5}e^{-\frac{56}{275}i\pi}$ |
| $B_{4,4}$ | $\frac{1}{5}e^{-\frac{76}{275}i\pi}$ | $\frac{1}{5}e^{-\frac{164}{275}i\pi}$ |

TABLE III. The diagonal elements $S_{B_{k,n}B_{k,n}}^{(z)}$ of the punctured S matrix with $z = A_{1,1}$ and $A_{2,6}$ ($A_{1,1}$ and $A_{2,6}$ are dual anyons) for $\mathcal{C}_{u=1}$ and $\mathcal{C}_{u=4}$, respectively. The complete data for $S_{a,\mu;b,\nu}^{(z)}$ can be found in materials online.⁴⁷

After fixing how z are sent from $\mathcal{C}_{u=1}$ to $\mathcal{C}_{u=4}$ to keep the modular T matrix unchanged, now let us consider the anyons $B_{k,n}$ in $S_{B_{k,n}B_{k,n}}^{(z)}$. From Table II, the topological spins for type- B anyons have the form

$$\theta = \exp\left(\frac{i2\pi}{25}s\right), \quad (3.51)$$

with

$$\begin{aligned} u = 1, \quad s \in \{ & 1, 6, 11, 16, 21; \quad 4, 14, 24, 9, 19; \\ & 9, 24, 14, 4, 19; \quad 16, 11, 6, 1, 21\}, \\ u = 4, \quad s \in \{ & 4, 9, 14, 19, 24; \quad 16, 1, 11, 21, 6; \\ & 11, 1, 16, 6, 21; \quad 14, 9, 4, 24, 19\}, \end{aligned} \quad (3.52)$$

where s is listed with the order in Table II. One can find that, for example, $B_{1,0}$ in $\mathcal{C}_{u=1}$ can only be sent to $B_{2,1}$ or $B_{3,1}$ in $\mathcal{C}_{u=4}$ (Note that $B_{2,1}$ and $B_{3,1}$ in $\mathcal{C}_{u=4}$ are dual anyons as seen from (3.17), with $\theta_a = \theta_{\bar{a}}$). Till now, based on the modular T matrix, we just observed how different anyons can be sent/permuted from $\mathcal{C}_{u=1}$ to $\mathcal{C}_{u=4}$ categories. Next, we need to check if $S_{B_{k,n}B_{k,n}}^{(z)}$ is mapped in a consistent way.

In Table III, we show the results for the diagonal elements $S_{B_{k,n},B_{k,n}}^{(z)}$ with $z = A_{1,1}$ and $A_{2,6}$, for both $\mathcal{C}_{u=1}$ and $\mathcal{C}_{u=4}$ categories. One can find that $S_{B_{1,0},B_{1,0}}^{(z=A_{1,1})} = \frac{1}{5}e^{-\frac{144}{275}i\pi}$ in $\mathcal{C}_{u=1}$, but $S_{B_{2,1},B_{2,1}}^{(z=A_{1,1})} = S_{B_{3,1},B_{3,1}}^{(z=A_{1,1})} = S_{B_{2,1},B_{2,1}}^{(z=A_{2,6})} = S_{B_{3,1},B_{3,1}}^{(z=A_{2,6})} = \frac{1}{5}e^{\frac{6}{275}i\pi}$ in $\mathcal{C}_{u=4}$. This means $S_{B_{k,n}B_{k,n}}^{(z)}$ is not mapped in the same way as the modular T matrix by permuting anyons, indicating that $\mathcal{C}_{u=1}$ and $\mathcal{C}_{u=4}$ are different categories.

Then curious readers may ask whether $S_{B_{1,0},B_{1,0}}^{(z=A_{1,1})}$ for $\mathcal{C}_{u=1}$ can be sent to any other quantity? By looking through the data for $S_{B_{k,n},B_{k,n}}^{(z)}$, we found that $S_{B_{1,0},B_{1,0}}^{(z=A_{1,1})}$ in $\mathcal{C}_{u=1}$ is sent to $S_{B_{2,1},B_{2,1}}^{(z=A_{1,9})} = S_{B_{2,1},B_{2,1}}^{(z=A_{2,10})} = S_{B_{3,1},B_{3,1}}^{(z=A_{1,9})} = S_{B_{3,1},B_{3,1}}^{(z=A_{2,10})}$ in $\mathcal{C}_{u=4}$, as seen from Table IV. That is, to fix $S_{B_{k,n},B_{k,n}}^{(z)}$, we need to send $A_{1,1}$ in $\mathcal{C}_{u=1}$ to $A_{1,9}$ or $A_{2,10}$ in $\mathcal{C}_{u=4}$. Apparently, $A_{1,1}$ and $A_{1,9}$ ($A_{2,10}$) have different topological spins and the corresponding T matrix elements cannot be mapped consistently from $\mathcal{C}_{u=1}$ to $\mathcal{C}_{u=4}$.

A summary of how $S_{B_{i,j},B_{i,j}}^{(z)}$ in $\mathcal{C}_{u=1}$ are mapped to $S_{B_{i',j'},B_{i',j'}}^{(z')}$ in $\mathcal{C}_{u=4}$ can be found in appendix B 1 a.

| a | $u = 1$ | $u = 4$ |
|-----------|---------------------------------------|---------------------------------------|
| $B_{1,0}$ | $\frac{1}{5}e^{\frac{156}{275}i\pi}$ | $\frac{1}{5}e^{\frac{24}{275}i\pi}$ |
| $B_{1,1}$ | $\frac{1}{5}e^{-\frac{64}{275}i\pi}$ | $\frac{1}{5}e^{-\frac{196}{275}i\pi}$ |
| $B_{1,2}$ | $\frac{1}{5}e^{\frac{266}{275}i\pi}$ | $\frac{1}{5}e^{\frac{134}{275}i\pi}$ |
| $B_{1,3}$ | $\frac{1}{5}e^{\frac{46}{275}i\pi}$ | $\frac{1}{5}e^{-\frac{86}{275}i\pi}$ |
| $B_{1,4}$ | $\frac{1}{5}e^{-\frac{174}{275}i\pi}$ | $\frac{1}{5}e^{\frac{244}{275}i\pi}$ |
| $B_{2,0}$ | $\frac{1}{5}e^{\frac{274}{275}i\pi}$ | $\frac{1}{5}e^{-\frac{254}{275}i\pi}$ |
| $B_{2,1}$ | $\frac{1}{5}e^{-\frac{166}{275}i\pi}$ | $\frac{1}{5}e^{-\frac{144}{275}i\pi}$ |
| $B_{2,2}$ | $\frac{1}{5}e^{-\frac{56}{275}i\pi}$ | $\frac{1}{5}e^{-\frac{34}{275}i\pi}$ |
| $B_{2,3}$ | $\frac{1}{5}e^{\frac{54}{275}i\pi}$ | $\frac{1}{5}e^{\frac{76}{275}i\pi}$ |
| $B_{2,4}$ | $\frac{1}{5}e^{\frac{164}{275}i\pi}$ | $\frac{1}{5}e^{\frac{186}{275}i\pi}$ |
| $B_{3,0}$ | $\frac{1}{5}e^{\frac{54}{275}i\pi}$ | $\frac{1}{5}e^{-\frac{34}{275}i\pi}$ |
| $B_{3,1}$ | $\frac{1}{5}e^{-\frac{56}{275}i\pi}$ | $\frac{1}{5}e^{-\frac{144}{275}i\pi}$ |
| $B_{3,2}$ | $\frac{1}{5}e^{-\frac{166}{275}i\pi}$ | $\frac{1}{5}e^{-\frac{254}{275}i\pi}$ |
| $B_{3,3}$ | $\frac{1}{5}e^{\frac{274}{275}i\pi}$ | $\frac{1}{5}e^{\frac{186}{275}i\pi}$ |
| $B_{3,4}$ | $\frac{1}{5}e^{\frac{164}{275}i\pi}$ | $\frac{1}{5}e^{\frac{76}{275}i\pi}$ |
| $B_{4,0}$ | $\frac{1}{5}e^{\frac{46}{275}i\pi}$ | $\frac{1}{5}e^{\frac{134}{275}i\pi}$ |
| $B_{4,1}$ | $\frac{1}{5}e^{\frac{266}{275}i\pi}$ | $\frac{1}{5}e^{-\frac{196}{275}i\pi}$ |
| $B_{4,2}$ | $\frac{1}{5}e^{-\frac{64}{275}i\pi}$ | $\frac{1}{5}e^{\frac{24}{275}i\pi}$ |
| $B_{4,3}$ | $\frac{1}{5}e^{\frac{156}{275}i\pi}$ | $\frac{1}{5}e^{\frac{244}{275}i\pi}$ |
| $B_{4,4}$ | $\frac{1}{5}e^{-\frac{174}{275}i\pi}$ | $\frac{1}{5}e^{-\frac{86}{275}i\pi}$ |

TABLE IV. The diagonal elements $S_{B_{k,n}B_{k,n}}^{(z)}$ of the punctured S matrix with $z = A_{1,9}$ and $A_{2,10}$ ($A_{1,9}$ and $A_{2,10}$ are dual anyons) for $u = 1$ and $u = 4$, respectively. The complete data for $S_{a,\mu;b,\nu}^{(z)}$ can be found in materials online.

In short, by permuting anyons, the topological invariants $S_{B_{k,n}B_{k,n}}^{(z)}$ and T matrix are mapped from $\mathcal{C}_{u=1}$ to $\mathcal{C}_{u=4}$ categories in different ways. Therefore, we conclude that the punctured S matrix together with the modular T matrix can distinguish $\mathcal{C}_{u=1}$ and $\mathcal{C}_{u=4}$ categories. One can check that $\mathcal{C}_{u=2}$ and $\mathcal{C}_{u=3}$ categories can be distinguished in the same way.

Several remarks before we leave this subsection:

– Not all the punctured S matrices can be used to distinguish different categories. This is true even if z are type- A anyons. For example, when $z = A_{1,0}$ or $A_{2,0}$, which has trivial topological spin, the punctured S matrix $S^{(z)}$ together with T matrix cannot distinguish different categories. This is explicitly shown in Appendix B 1 a. We observed that only for $z = A_{1,i}$ and $A_{2,i}$ with $i = 1, \dots, 10$, which have nontrivial topological spins, *i.e.*, $\theta_z \neq 1$, the corresponding punctured S matrix $S^{(z)}$ together with T can distinguish different categories.

– As discussed in Sec.II B, because of Galois symmetry in the modular data, it is well understood about the transformation property of modular S and T matrices by permuting anyons in the same category as well as among different categories. It is interesting to study how the punctured S matrix transforms under the permutation of anyons.

– Although the method above can be used to distinguish MS MTCs, but the procedure is complicate. We need to track how the bijections/permutations of anyons map the data of T and $S_{a,a}^{(z)}$ between two different categories. It will be nice if we can distinguish the MS MTCs with a single number. In addition, if we work on a lattice gauge theory (see Sec.IV), since it is not clear to us how to write down the quasi-particle basis, it is difficult to do anyon permutation as what we have done in this subsection. For these reasons, it is desired to define topological invariants which are independent of anyon types, as studied in the following subsection.

– In Ref.15, the link invariant of Whitehead link was proposed to distinguish the most simplest counterexamples in MS MTCs. It is proved that the Whitehead link invariant is determined by the diagonal elements of punctured S matrix together with the modular data. Here we obtain the punctured S matrix with both the diagonal and off-diagonal elements, which provide more information than the Whitehead link invariant.

D. Topological invariants: Trace of words and link invariants

Based on the punctured S and T matrices obtained in the previous subsections, we can construct topological invariants on a punctured torus or a genus-two closed manifold. More precisely, we calculate these topological invariants in the Hilbert space $\mathcal{H}(\Sigma_{1,1})$ or $\mathcal{H}(\Sigma_{2,0})$.

The merit of topological invariants constructed in this subsection is that *we only need a single number to distinguish those different MS MTCs.*

We illustrate this idea in the cases of (i) a punctured torus and (ii) a genus-two manifold, respectively.

1. Punctured torus

With the punctured S and T matrices, we can construct an arbitrary ‘word’ of the following form:

$$w^{(z)} := (S^{(z)})^{n_1} (T^{(z)})^{n_2} (S^{(z)})^{n_3} (T^{(z)})^{n_4} \dots \quad (3.53)$$

where n_i are arbitrary integers. The topological invariant can be expressed as a trace of words as

$$W_{\Sigma_{1,1}}^{(z)} = \text{Tr}(w^{(z)}), \quad (3.54)$$

where the trace is over the Hilbert space $\mathcal{H}(\Sigma_{1,1}; z)$ with a fixed anyon charge z (see the basis of $\mathcal{H}(\Sigma_{1,1}; z)$ in the left plot of (3.3)).

There are infinite number of nontrivial words which may be used to distinguish the MS MTCs. Here we list a few of them:

$$\begin{cases} w_1^{(z)} = (\theta^{(z)})^2 \cdot (T^{(z)})^7 S^{(z)}, \\ w_2^{(z)} = (\theta^{(z)})^3 \cdot [(T^{(z)})^3 S^{(z)}]^2, \\ w_3^{(z)} = (\theta^{(z)})^2 \cdot [(T^{(z)})^4 S^{(z)}]^3, \\ w_4^{(z)} = [(T^{(z)})^5 S^{(z)}]^4, \\ w_5^{(z)} = (\theta^{(z)})^3 \cdot [(T^{(z)})^3 S^{(z)}]^2 \cdot [(T^{(z)})^2 S^{(z)}]^5, \\ w_6^{(z)} = (\theta^{(z)})^5 \cdot [(T^{(z)})^3 S^{(z)}]^4, \\ w_7^{(z)} = (\theta^{(z)})^8 \cdot [(T^{(z)})^3 S^{(z)}]^2, \end{cases} \quad (3.55)$$

where we have $\theta^{(z)} = (S^{(z)})^{-4}$.

The reason why the trace of words in Eqs.(3.54) are topological invariants is that they are related to the link invariants. In the following, we give two examples on $\text{Tr}(w_1^{(z)})$ and $\text{Tr}(w_2^{(z)})$, and then give some general remarks.

Let us present some preliminaries first, by looking at the expression of $\text{Tr}(T^{(z)})$ and $\text{Tr}(S^{(z)})$. For $\text{Tr}(T^{(z)})$, it is straightforward to check that $\text{Tr}(T^{(z)}) = \sum_a N_{a\bar{a}}^z \theta_a$. For $\text{Tr}(S^{(z)})$, we have

$$\text{Tr}[S^{(z)}] = \sum_{a,\mu} S_{a\mu,a\mu}^{(z)} = \sum_{a,\mu} \frac{1}{\mathcal{D}} \cdot \frac{1}{\sqrt{d_z}} \cdot \text{Diagram} \quad (3.56)$$

By using the following relation (see also Eq.(B16) in the appendix):

$$\sum_x S_{0z} S_{zx}^* \text{Diagram} = \sum_\mu \sqrt{\frac{d_z}{d_a d_b}} \text{Diagram} \quad (3.57)$$

Eq.(3.56) can be rewritten as

$$\text{Tr}[S^{(z)}] = \frac{1}{\mathcal{D}} \sum_{a,x} \frac{d_a}{d_z} \cdot S_{0\bar{z}} \cdot S_{\bar{z}x}^* \text{Diagram} \quad (3.58)$$

which is related to the whitehead link as studied in Ref.15. Then for $\text{Tr}(w_1^{(z)})$, since both $\theta^{(z)}$ and $T^{(z)}$ are diagonal matrices, it is straightforward to check that

$$\text{Tr}(w_1^{(z)}) = \frac{1}{\mathcal{D}} \sum_{a,x} \theta_z^2 \cdot \theta_a^7 \cdot \frac{d_a}{d_z} \cdot S_{0\bar{z}} \cdot S_{\bar{z}x}^* \text{Diagram} \quad (3.59)$$

As the second example, now let us check $W_{\Sigma_{1,1}}^{(z)} := \text{Tr}(w_2^{(z)})$. First, let us look at how $\omega_2^{(z)}$ acts on the basis as follows:

$$\begin{aligned} & (\theta^{(z)})^3 (T^{(z)})^3 S^{(z)} (T^{(z)})^3 S^{(z)} \text{Diagram} \\ &= (\theta^{(z)})^3 (T^{(z)})^3 S^{(z)} \frac{1}{\mathcal{D}} \sum_a d_a (\theta_a)^3 \text{Diagram} \\ &= \frac{1}{\mathcal{D}^2} \sum_{a,x} d_a d_x (\theta_x)^3 (\theta_a)^3 (\theta_a)^3 \text{Diagram} \end{aligned} \quad (3.60)$$

Including the normalization of basis vectors, one can obtain

$$\text{Tr}(w_2^{(z)}) = \frac{1}{\mathcal{D}^2} \sum_{a,b} \frac{d_a}{\sqrt{d_z}} (\theta_z)^3 (\theta_a)^3 (\theta_b)^3 \sum_\mu \text{Diagram} \quad (3.61)$$

which, based on Eq.(3.57), can be further simplified as

$$\begin{aligned} \text{Tr}(w_2^{(z)}) &= \frac{1}{\mathcal{D}^2} \sum_{a,b} \frac{d_a d_b}{d_z} (\theta_z)^3 (\theta_a)^3 (\theta_b)^3 \\ &\times \sum_x S_{0\bar{z}} \cdot S_{\bar{z}x}^* \text{Diagram} \end{aligned} \quad (3.62)$$

Apparently, $W_{\Sigma_{1,1}}^{(z)} := \text{Tr}(w_2^{(z)})$ can be expressed in terms of link invariants, and therefore it is a topological invariant. Similarly, one can check that the trace of other words are all topological invariants. One basic reason is that the only possible gauge-dependent term comes from the tri-junction structure in (3.4). By performing trace over the words with the rule in Eq.(3.57), it is found that this tri-junction structure is removed.

In the following, we present results of trace of the words for those in Eq.(3.55), as listed in tables (V) ~ (XI).

| $W_{\Sigma_{1,1}}^{(z)}$ | $W_{\Sigma_{1,1}}^{I_0}$ | $\sum_{i=1}^4 W_{\Sigma_{1,1}}^{I_i}$ | $W_{\Sigma_{1,1}}^{I_5, I_6}$ | $W_{\Sigma_{1,1}}^{A_1, A_2}$ |
|--------------------------|-----------------------------|---------------------------------------|-------------------------------|----------------------------------|
| $u=0$ | 9 | -4 | 4 | 22 |
| $u=1$ | $4 \cos \frac{2\pi}{5} + 5$ | -4 | $4 \cos \frac{2\pi}{5}$ | $22e^{\frac{2i\pi}{5} \times 1}$ |
| $u=2$ | $4 \cos \frac{4\pi}{5} + 5$ | -4 | $4 \cos \frac{4\pi}{5}$ | $22e^{\frac{2i\pi}{5} \times 2}$ |
| $u=3$ | $4 \cos \frac{4\pi}{5} + 5$ | -4 | $4 \cos \frac{4\pi}{5}$ | $22e^{\frac{2i\pi}{5} \times 3}$ |
| $u=4$ | $4 \cos \frac{2\pi}{5} + 5$ | -4 | $4 \cos \frac{2\pi}{5}$ | $22e^{\frac{2i\pi}{5} \times 4}$ |

TABLE V. $W_{\Sigma_{1,1}}^{(z)}$ with $w_1^{(z)}$ in (3.55).

| $W_{\Sigma_{1,1}}^{(z)}$ | $W_{\Sigma_{1,1}}^{I_0}$ | $\sum_{i=1}^4 W_{\Sigma_{1,1}}^{I_i}$ | $W_{\Sigma_{1,1}}^{I_5, I_6}$ | $W_{\Sigma_{1,1}}^{A_1, A_2}$ |
|--------------------------|-----------------------------|---------------------------------------|-------------------------------|----------------------------------|
| $u=0$ | 9 | -4 | 4 | 22 |
| $u=1$ | $4 \cos \frac{4\pi}{5} + 5$ | -4 | $4 \cos \frac{4\pi}{5}$ | $22e^{\frac{2i\pi}{5} \times 3}$ |
| $u=2$ | $4 \cos \frac{2\pi}{5} + 5$ | -4 | $4 \cos \frac{2\pi}{5}$ | $22e^{\frac{2i\pi}{5} \times 1}$ |
| $u=3$ | $4 \cos \frac{2\pi}{5} + 5$ | -4 | $4 \cos \frac{2\pi}{5}$ | $22e^{\frac{2i\pi}{5} \times 4}$ |
| $u=4$ | $4 \cos \frac{4\pi}{5} + 5$ | -4 | $4 \cos \frac{4\pi}{5}$ | $22e^{\frac{2i\pi}{5} \times 2}$ |

TABLE VI. $W_{\Sigma_{1,1}}^{(z)}$ with $w_2^{(z)}$ in (3.55).

| $W_{\Sigma_{1,1}}^{(z)}$ | $W_{\Sigma_{1,1}}^{I_0}$ | $\sum_{i=1}^4 W_{\Sigma_{1,1}}^{I_i}$ | $W_{\Sigma_{1,1}}^{I_5, I_6}$ | $W_{\Sigma_{1,1}}^{A_1, A_2}$ |
|--------------------------|--------------------------|---------------------------------------|-------------------------------|----------------------------------|
| $u=0$ | 25 | 0 | 24 | 66 |
| $u=1$ | -5 | 0 | -6 | $66e^{\frac{2i\pi}{5} \times 2}$ |
| $u=2$ | -5 | 0 | -6 | $66e^{\frac{2i\pi}{5} \times 4}$ |
| $u=3$ | -5 | 0 | -6 | $66e^{\frac{2i\pi}{5} \times 1}$ |
| $u=4$ | -5 | 0 | -6 | $66e^{\frac{2i\pi}{5} \times 3}$ |

TABLE VII. $W_{\Sigma_{1,1}}^{(z)}$ with $w_3^{(z)}$ in (3.55).

| $W_{\Sigma_{1,1}}^{(z)}$ | $W_{\Sigma_{1,1}}^{I_0}$ | $\sum_{i=1}^4 W_{\Sigma_{1,1}}^{I_i}$ | $W_{\Sigma_{1,1}}^{I_5, I_6}$ | $W_{\Sigma_{1,1}}^{A_1, A_2}$ |
|--------------------------|--------------------------|---------------------------------------|-------------------------------|----------------------------------|
| $u=0$ | 25 | 0 | 24 | 44 |
| $u=1$ | 5 | 0 | 4 | $44e^{\frac{2i\pi}{5} \times 3}$ |
| $u=2$ | 5 | 0 | 4 | $44e^{\frac{2i\pi}{5} \times 1}$ |
| $u=3$ | 5 | 0 | 4 | $44e^{\frac{2i\pi}{5} \times 4}$ |
| $u=4$ | 5 | 0 | 4 | $44e^{\frac{2i\pi}{5} \times 2}$ |

TABLE VIII. $W_{\Sigma_{1,1}}^{(z)}$ with $w_4^{(z)}$ in (3.55).

| $W_{\Sigma_{1,1}}^{(z)}$ | $W_{\Sigma_{1,1}}^{I_0}$ | $\sum_{i=1}^4 W_{\Sigma_{1,1}}^{I_i}$ | $W_{\Sigma_{1,1}}^{I_5, I_6}$ | $W_{\Sigma_{1,1}}^{A_1, A_2}$ |
|--------------------------|-----------------------------|---------------------------------------|-------------------------------|----------------------------------|
| $u=0$ | 5 | 0 | 4 | 22 |
| $u=1$ | $4 \cos \frac{4\pi}{5} + 1$ | 0 | $4 \cos \frac{4\pi}{5}$ | $22e^{\frac{2i\pi}{5} \times 2}$ |
| $u=2$ | $4 \cos \frac{2\pi}{5} + 1$ | 0 | $4 \cos \frac{2\pi}{5}$ | $22e^{\frac{2i\pi}{5} \times 4}$ |
| $u=3$ | $4 \cos \frac{2\pi}{5} + 1$ | 0 | $4 \cos \frac{2\pi}{5}$ | $22e^{\frac{2i\pi}{5} \times 1}$ |
| $u=4$ | $4 \cos \frac{4\pi}{5} + 1$ | 0 | $4 \cos \frac{4\pi}{5}$ | $22e^{\frac{2i\pi}{5} \times 3}$ |

TABLE IX. $W_{\Sigma_{1,1}}^{(z)}$ with $w_5^{(z)}$ in (3.55).

| $W_{\Sigma_{1,1}}^{(z)}$ | $W_{\Sigma_{1,1}}^{I_0}$ | $\sum_{i=1}^4 W_{\Sigma_{1,1}}^{I_i}$ | $W_{\Sigma_{1,1}}^{I_5, I_6}$ | $W_{\Sigma_{1,1}}^{A_1, A_2}$ |
|--------------------------|-----------------------------|---------------------------------------|-------------------------------|----------------------------------|
| $u=0$ | 9 | -4 | 4 | 22 |
| $u=1$ | $4 \cos \frac{2\pi}{5} + 5$ | -4 | $4 \cos \frac{2\pi}{5}$ | $22e^{\frac{2i\pi}{5} \times 4}$ |
| $u=2$ | $4 \cos \frac{4\pi}{5} + 5$ | -4 | $4 \cos \frac{4\pi}{5}$ | $22e^{\frac{2i\pi}{5} \times 3}$ |
| $u=3$ | $4 \cos \frac{4\pi}{5} + 5$ | -4 | $4 \cos \frac{4\pi}{5}$ | $22e^{\frac{2i\pi}{5} \times 2}$ |
| $u=4$ | $4 \cos \frac{2\pi}{5} + 5$ | -4 | $4 \cos \frac{2\pi}{5}$ | $22e^{\frac{2i\pi}{5} \times 1}$ |

TABLE X. $W_{\Sigma_{1,1}}^{(z)}$ with $w_6^{(z)}$ in (3.55).

| $W_{\Sigma_{1,1}}^{(z)}$ | $W_{\Sigma_{1,1}}^{I_0}$ | $\sum_{i=1}^4 W_{\Sigma_{1,1}}^{I_i}$ | $W_{\Sigma_{1,1}}^{I_5, I_6}$ | $W_{\Sigma_{1,1}}^{A_1, A_2}$ |
|--------------------------|-----------------------------|---------------------------------------|-------------------------------|----------------------------------|
| $u=0$ | 9 | -4 | 4 | 22 |
| $u=1$ | $4 \cos \frac{4\pi}{5} + 5$ | -4 | $4 \cos \frac{4\pi}{5}$ | $22e^{\frac{2i\pi}{5} \times 2}$ |
| $u=2$ | $4 \cos \frac{2\pi}{5} + 5$ | -4 | $4 \cos \frac{2\pi}{5}$ | $22e^{\frac{2i\pi}{5} \times 4}$ |
| $u=3$ | $4 \cos \frac{2\pi}{5} + 5$ | -4 | $4 \cos \frac{2\pi}{5}$ | $22e^{\frac{2i\pi}{5} \times 1}$ |
| $u=4$ | $4 \cos \frac{4\pi}{5} + 5$ | -4 | $4 \cos \frac{4\pi}{5}$ | $22e^{\frac{2i\pi}{5} \times 3}$ |

TABLE XI. $W_{\Sigma_{1,1}}^{(z)}$ with $w_7^{(z)}$ in (3.55).

Let us explain the meaning of data in Table V. Taking $u=1$ for example, $W_{\Sigma_{1,1}}^{(z)}$ is defined in Eq.(3.54). Then we have $W_{\Sigma_{1,1}}^{I_0} = 4 \cos \frac{2\pi}{5} + 5$, $\sum_{i=1}^4 W_{\Sigma_{1,1}}^{I_i} = W_{\Sigma_{1,1}}^{I_1} + W_{\Sigma_{1,1}}^{I_2} + W_{\Sigma_{1,1}}^{I_3} + W_{\Sigma_{1,1}}^{I_4} = -4$, $W_{\Sigma_{1,1}}^{I_5} = W_{\Sigma_{1,1}}^{I_6} = 4 \cos \frac{2\pi}{5}$, $W_{\Sigma_{1,1}}^{A_1} = \sum_{i=0}^{10} W_{\Sigma_{1,1}}^{A_1, i} = 22e^{\frac{2i\pi}{5} \times 1}$, and $W_{\Sigma_{1,1}}^{A_2} = \sum_{i=0}^{10} W_{\Sigma_{1,1}}^{A_2, i} = 22e^{\frac{2i\pi}{5} \times 1}$. The same definition is used in the other tables in this subsection.

The data in gray indicate they are not obtained in the quasi-particle basis calculation, but are obtained by comparing with the lattice theory calculation in Sec.IV. One can find that they are independent of u . The reason is that for $z = I_1, I_2, I_3, I_4$, only type- I and type- A anyons participate in the definition of punctured S matrix, and therefore the results are independent of the 3-cocycles ω^u and u . (Recall that only type- B anyons carry the information of the 3-cocycle ω . See also the discussion at the end of Sec.III B). For this reason, we did not solve for S^z with $z = I_1, I_2, I_3, I_4$ explicitly in the quasiparticle basis. Nevertheless, they are calculated in the lattice gauge theory approach in Sec.IV.

From the results in tables (V) ~ (XI), one can find that for each choice of word, there are at most three sets of $W_{\Sigma_{1,1}}^{I_0}$ for (i) $\mathcal{C}_{u=0}$, (ii) $\mathcal{C}_{u=1}$ and $\mathcal{C}_{u=4}$, and (iii) $\mathcal{C}_{u=2}$ and $\mathcal{C}_{u=3}$, respectively. Recall that $W_{\Sigma_{1,1}}^{I_0}$ are actually obtained from the modular S and T matrices, this agrees with the conclusion that there are only three sets of modular data.

The pieces that can distinguish those five different categories are $W_{\Sigma_{1,1}}^{A_1}$ and $W_{\Sigma_{1,1}}^{A_2}$. Remarkably, the difference for the five inequivalent categories lies simply in the phase factor $e^{\frac{2i\pi}{5}n}$, with $n = 0, 1, 2, 3, 4$.

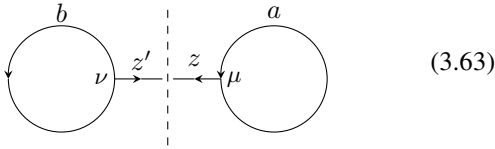
There are some detailed feature on the phase factor $e^{\frac{2i\pi}{5}n}$ for different categories. For $u=0$ where the 3-cocycle is trivial, *i.e.*, $\omega = 1$, the phase factor is always 1. The phase factor for $u=1$ ($u=2$) are always conjugate to that for $u=4$ ($u=3$). An interesting observation is that by replacing $e^{\frac{2i\pi}{5}n}$ with $\cos \frac{2n\pi}{5}$, the information becomes degenerate.

There are 3 distinct data instead of 5. Note that $\cos \frac{2n\pi}{5}$ appear in $W_{\Sigma_{1,1}}^{I_0}$, which is contributed by the modular data. From this point of view, the reason why the modular data cannot distinguish different categories can be intuitively understood as the degeneracy of information.

A detailed comparison of the topological invariants with the lattice gauge theory approach can be found in Appendix C 1.

2. Genus two

Now we study the topological invariants defined in the Hilbert space $\mathcal{H}(\Sigma_{2,0})$ of degenerate ground states on genus-2 surface. A genus-2 manifold can be obtained by gluing two punctured tori along their punctures, and so does the genus-2 groundstate basis. As shown in the following, we glue two punctured-torus basis vectors by identifying the anyon charge at the puncture, *i.e.*, $z' = \bar{z}$ (Note that for an anyon z , there is a unique z' such that $z' = \bar{z}$):



Then we obtain the genus-2 basis in (3.1). Now we define the words

$$w_{\Sigma_{2,0}}^{(z)} := I_L^{(\bar{z})} \otimes w_R^{(z)}, \quad (3.64)$$

where $I_L^{(\bar{z})}$ is the identity matrix acting on the basis of the *left* punctured torus in (3.63) with fixed $z' = \bar{z}$, and $w_R^{(z)}$ has the same expression as (3.53) and acts on the basis of the *right* punctured torus. Then we define the following topological invariants

$$W_{\Sigma_{2,0}} = \text{Tr} \left(\bigoplus_z w_{\Sigma_{2,0}}^{(z)} \right) = \text{Tr} \left[\bigoplus_z (I_L^{(\bar{z})} \otimes W_R^{(z)}) \right], \quad (3.65)$$

where the ‘Tr’ is over the Hilbert space of the degenerate ground states, *i.e.*, $\mathcal{H}(\Sigma_{2,0})$. Eq.(3.65) can be further rewritten as

$$W_{\Sigma_{2,0}} = \sum_z \dim \mathcal{H}(\Sigma_{1,1}, \bar{z}) \times W_{\Sigma_{1,1}}^{(z)}, \quad (3.66)$$

where $W_{\Sigma_{1,1}}^{(z)}$ is the same as that in Eq.(3.54), and $\dim \mathcal{H}(\Sigma_{1,1}, \bar{z})$ is the dimension of Hilbert space for a punctured torus with an anyon charge \bar{z} at the puncture. Based on Eq.(1.12), we have

$$\dim \mathcal{H}(\Sigma_{1,1}, \bar{z}) = \sum_p \frac{S_{\bar{z}p}}{S_{0p}} = \sum_p N_{p\bar{p}}^z. \quad (3.67)$$

For the simplest counterexamples with $G = \mathbb{Z}_{11} \times \mathbb{Z}_5$ in MS MTCs, it is found that $\dim \mathcal{H}(\Sigma_{1,1}, \bar{z})$ is 49 for $z = I_0$, and 24 for $z = I_i$ with $i = 1 \sim 6$ and all type-*A* anyons. To track the

fine structures in $W_{\Sigma_{2,0}}$, it is helpful to split $W_{\Sigma_{2,0}}$ into three pieces as follows

$$W_{\Sigma_{2,0}} = W_{\Sigma_{2,0}}^I + W_{\Sigma_{2,0}}^{A_1} + W_{\Sigma_{2,0}}^{A_2}, \quad (3.68)$$

where the upper indices *I*, *A*₁, and *A*₂ indicate that the summation over z in Eq.(3.66) is performed within type-*I*, -*A*₁, and -*A*₂ anyons.

The results are summarized in tables (XII)~(XVIII). The data in gray are again contributed by $W_{\Sigma_{2,0}}^{I_i}$, with $i = 1, \dots, 4$. They are obtained not by the quasi-particle basis calculation, but by comparing with the lattice gauge theory calculation in Sec.(IV). One can find they are independent of u . The reason is the same as that for a punctured torus, *i.e.*, for $z = I_i$ with $i = 1, \dots, 4$, only type-*I* and type-*A* anyons contribute to the punctures *S* matrix, and the information of 3-cocycle ω^u will not come in.

There are at most three different sets of $W_{\Sigma_{2,0}}^I$ for each $W_{\Sigma_{2,0}}$, and cannot distinguish different categories. The pieces of data that can distinguish the five inequivalent categories are $W_{\Sigma_{2,0}}^{A_1}$ and $W_{\Sigma_{2,0}}^{A_2}$, with the difference in the phase factor $e^{\frac{2i\pi}{5}n}$, where $n = 0, 1, 2, 3, 4$. Similar to the case of $W_{\Sigma_{1,1}}^{(z)}$, the phase factor for $u = 1$ ($u = 2$) is conjugate to that for $u = 4$ ($u = 3$).

A comparison of the topological invariants with the lattice gauge theory approach can be found in Sec.IV C.

| $W_{\Sigma_{2,0}}$ | $W_{\Sigma_{2,0}}^I$ | $W_{\Sigma_{2,0}}^{A_1}$ | $W_{\Sigma_{2,0}}^{A_2}$ |
|--------------------|---|--|--|
| $u = 0$ | $633 - 24 \times 4$ | 528 | 528 |
| $u = 1$ | $245 - 24 \times 4 + 388 \cdot \cos \frac{2\pi}{5}$ | $528 \cdot e^{\frac{2i\pi}{5} \times 1}$ | $528 \cdot e^{\frac{2i\pi}{5} \times 1}$ |
| $u = 2$ | $245 - 24 \times 4 + 388 \cdot \cos \frac{4\pi}{5}$ | $528 \cdot e^{\frac{2i\pi}{5} \times 2}$ | $528 \cdot e^{\frac{2i\pi}{5} \times 2}$ |
| $u = 3$ | $245 - 24 \times 4 + 388 \cdot \cos \frac{4\pi}{5}$ | $528 \cdot e^{\frac{2i\pi}{5} \times 3}$ | $528 \cdot e^{\frac{2i\pi}{5} \times 3}$ |
| $u = 4$ | $245 - 24 \times 4 + 388 \cdot \cos \frac{2\pi}{5}$ | $528 \cdot e^{\frac{2i\pi}{5} \times 4}$ | $528 \cdot e^{\frac{2i\pi}{5} \times 4}$ |

TABLE XII. $W_{\Sigma_{2,0}}$, with $w_R^{(z)} = w_1^{(z)}$ in Eq.(3.55).

| $W_{\Sigma_{2,0}}$ | $W_{\Sigma_{2,0}}^I$ | $W_{\Sigma_{2,0}}^{A_1}$ | $W_{\Sigma_{2,0}}^{A_2}$ |
|--------------------|---|--|--|
| $u = 0$ | $633 - 24 \times 4$ | 528 | 528 |
| $u = 1$ | $245 - 24 \times 4 + 388 \cdot \cos \frac{4\pi}{5}$ | $528 \cdot e^{\frac{2i\pi}{5} \times 3}$ | $528 \cdot e^{\frac{2i\pi}{5} \times 3}$ |
| $u = 2$ | $245 - 24 \times 4 + 388 \cdot \cos \frac{2\pi}{5}$ | $528 \cdot e^{\frac{2i\pi}{5} \times 1}$ | $528 \cdot e^{\frac{2i\pi}{5} \times 1}$ |
| $u = 3$ | $245 - 24 \times 4 + 388 \cdot \cos \frac{2\pi}{5}$ | $528 \cdot e^{\frac{2i\pi}{5} \times 4}$ | $528 \cdot e^{\frac{2i\pi}{5} \times 4}$ |
| $u = 4$ | $245 - 24 \times 4 + 388 \cdot \cos \frac{4\pi}{5}$ | $528 \cdot e^{\frac{2i\pi}{5} \times 2}$ | $528 \cdot e^{\frac{2i\pi}{5} \times 2}$ |

TABLE XIII. $W_{\Sigma_{2,0}}$, with $w_R^{(z)} = w_2^{(z)}$ in Eq.(3.55).

| $W_{\Sigma_{2,0}}$ | $W_{\Sigma_{2,0}}^I$ | $W_{\Sigma_{2,0}}^{A_1}$ | $W_{\Sigma_{2,0}}^{A_2}$ |
|--------------------|----------------------|---|---|
| $u = 0$ | $2377 + 0$ | 1584 | 1584 |
| $u = 1$ | $-533 + 0$ | $1584 \cdot e^{\frac{2i\pi}{5} \times 2}$ | $1584 \cdot e^{\frac{2i\pi}{5} \times 2}$ |
| $u = 2$ | $-533 + 0$ | $1584 \cdot e^{\frac{2i\pi}{5} \times 4}$ | $1584 \cdot e^{\frac{2i\pi}{5} \times 4}$ |
| $u = 3$ | $-533 + 0$ | $1584 \cdot e^{\frac{2i\pi}{5} \times 1}$ | $1584 \cdot e^{\frac{2i\pi}{5} \times 1}$ |
| $u = 4$ | $-533 + 0$ | $1584 \cdot e^{\frac{2i\pi}{5} \times 3}$ | $1584 \cdot e^{\frac{2i\pi}{5} \times 3}$ |

TABLE XIV. $W_{\Sigma_{2,0}}$, with $w_R^{(z)} = w_3^{(z)}$ in Eq.(3.55).

| $W_{\Sigma_{2,0}}$ | $W_{\Sigma_{2,0}}^I$ | $W_{\Sigma_{2,0}}^{A_1}$ | $W_{\Sigma_{2,0}}^{A_2}$ |
|--------------------|----------------------|---|---|
| $u = 0$ | $2377 + 0$ | 1056 | 1056 |
| $u = 1$ | $437 + 0$ | $1056 \cdot e^{\frac{21\pi}{5} \times 3}$ | $1056 \cdot e^{\frac{21\pi}{5} \times 3}$ |
| $u = 2$ | $437 + 0$ | $1056 \cdot e^{\frac{21\pi}{5} \times 1}$ | $1056 \cdot e^{\frac{21\pi}{5} \times 1}$ |
| $u = 3$ | $437 + 0$ | $1056 \cdot e^{\frac{21\pi}{5} \times 4}$ | $1056 \cdot e^{\frac{21\pi}{5} \times 4}$ |
| $u = 4$ | $437 + 0$ | $1056 \cdot e^{\frac{21\pi}{5} \times 2}$ | $1056 \cdot e^{\frac{21\pi}{5} \times 2}$ |

TABLE XV. $W_{\Sigma_{2,0}}$, with $w_R^{(z)} = w_4^{(z)}$ in Eq.(3.55).

| $W_{\Sigma_{2,0}}$ | $W_{\Sigma_{2,0}}^I$ | $W_{\Sigma_{2,0}}^{A_1}$ | $W_{\Sigma_{2,0}}^{A_2}$ |
|--------------------|--|--|--|
| $u = 0$ | $437 + 0$ | 528 | 528 |
| $u = 1$ | $49 + 0 + 388 \cdot \cos \frac{4\pi}{5}$ | $528 \cdot e^{\frac{21\pi}{5} \times 2}$ | $528 \cdot e^{\frac{21\pi}{5} \times 2}$ |
| $u = 2$ | $49 + 0 + 388 \cdot \cos \frac{2\pi}{5}$ | $528 \cdot e^{\frac{21\pi}{5} \times 4}$ | $528 \cdot e^{\frac{21\pi}{5} \times 4}$ |
| $u = 3$ | $49 + 0 + 388 \cdot \cos \frac{2\pi}{5}$ | $528 \cdot e^{\frac{21\pi}{5} \times 1}$ | $528 \cdot e^{\frac{21\pi}{5} \times 1}$ |
| $u = 4$ | $49 + 0 + 388 \cdot \cos \frac{4\pi}{5}$ | $528 \cdot e^{\frac{21\pi}{5} \times 3}$ | $528 \cdot e^{\frac{21\pi}{5} \times 3}$ |

TABLE XVI. $W_{\Sigma_{2,0}}$, with $w_R^{(z)} = w_5^{(z)}$ in Eq.(3.55).

| $W_{\Sigma_{2,0}}$ | $W_{\Sigma_{2,0}}^I$ | $W_{\Sigma_{2,0}}^{A_1}$ | $W_{\Sigma_{2,0}}^{A_2}$ |
|--------------------|---|--|--|
| $u = 0$ | $633 - 24 \times 4$ | 528 | 528 |
| $u = 1$ | $245 - 24 \times 4 + 388 \cdot \cos \frac{2\pi}{5}$ | $528 \cdot e^{\frac{21\pi}{5} \times 4}$ | $528 \cdot e^{\frac{21\pi}{5} \times 4}$ |
| $u = 2$ | $245 - 24 \times 4 + 388 \cdot \cos \frac{4\pi}{5}$ | $528 \cdot e^{\frac{21\pi}{5} \times 3}$ | $528 \cdot e^{\frac{21\pi}{5} \times 3}$ |
| $u = 3$ | $245 - 24 \times 4 + 388 \cdot \cos \frac{4\pi}{5}$ | $528 \cdot e^{\frac{21\pi}{5} \times 2}$ | $528 \cdot e^{\frac{21\pi}{5} \times 2}$ |
| $u = 4$ | $245 - 24 \times 4 + 388 \cdot \cos \frac{2\pi}{5}$ | $528 \cdot e^{\frac{21\pi}{5} \times 1}$ | $528 \cdot e^{\frac{21\pi}{5} \times 1}$ |

TABLE XVII. $W_{\Sigma_{2,0}}$, with $w_R^{(z)} = w_6^{(z)}$ in Eq.(3.55).

| $W_{\Sigma_{2,0}}$ | $W_{\Sigma_{2,0}}^I$ | $W_{\Sigma_{2,0}}^{A_1}$ | $W_{\Sigma_{2,0}}^{A_2}$ |
|--------------------|---|--|--|
| $u = 0$ | $633 - 24 \times 4$ | 528 | 528 |
| $u = 1$ | $245 - 24 \times 4 + 388 \cdot \cos \frac{4\pi}{5}$ | $528 \cdot e^{\frac{21\pi}{5} \times 2}$ | $528 \cdot e^{\frac{21\pi}{5} \times 2}$ |
| $u = 2$ | $245 - 24 \times 4 + 388 \cdot \cos \frac{2\pi}{5}$ | $528 \cdot e^{\frac{21\pi}{5} \times 4}$ | $528 \cdot e^{\frac{21\pi}{5} \times 4}$ |
| $u = 3$ | $245 - 24 \times 4 + 388 \cdot \cos \frac{2\pi}{5}$ | $528 \cdot e^{\frac{21\pi}{5} \times 1}$ | $528 \cdot e^{\frac{21\pi}{5} \times 1}$ |
| $u = 4$ | $245 - 24 \times 4 + 388 \cdot \cos \frac{4\pi}{5}$ | $528 \cdot e^{\frac{21\pi}{5} \times 3}$ | $528 \cdot e^{\frac{21\pi}{5} \times 3}$ |

TABLE XVIII. $W_{\Sigma_{2,0}}$, with $w_R^{(z)} = w_7^{(z)}$ in Eq.(3.55).

IV. TOPOLOGICAL LATTICE GAUGE THEORY

In this section, we will use the lattice gauge theory approach to study the representations of $MCG(\Sigma_{g,0})$ or $MCG(\Sigma_{g,n})$ for an arbitrary twisted quantum double of finite groups G with 3-cocycle $\omega \in H^3(G, U(1))$, which is also called Dijkgraaf-Witten (DW) theory.⁴⁸ Compared to the method in Sec.III, the lattice gauge theory approach is a bottom-up approach by simply inputting the data of G and ω .

In general, one may consider the string-net model, which is a generalization of the quantum double model for unitary tensor categories,⁴⁹ and provides us with a general approach to translate mathematical objects to physical concepts and vice versa. Here, for our interest of distinguishing the MS MTCs,

which are twisted quantum double of finite groups, we will focus on the DW theory.

The general idea is as follows. DW theory in (2+1)-d is defined on a triangulation of the spacetime 3-manifold together with a G -coloring, *i.e.*, we assign group elements in G to every 1-simplex of the triangulation, and a 3-cocycle ω to each tetrahedron. Within this approach, there is no need to solve the modular equations in Eqs.(3.33) which are nonlinear. We simply need to choose the bases of the degenerate ground states, and do modular transformations. The representations of MCG can be obtained by studying the overlap between the bases before and after the transformations. The MCG representations will look different from those obtained in the quasiparticle basis, since we are now using a different set of bases. But the topological invariants, which are basis independent, constructed from these MCG representations will be the same.

For the introduction of the group cohomology on a lattice theory, one can refer to, *e.g.*, Refs.50 and 51 for further details.

A. Exactly solvable model

We may work either in the path-integral version or in the hamiltonian version of Dijkgraaf-Witten theory.⁵¹⁻⁵⁴ Here we will consider the hamiltonian version. Previous works on the mapping class group of T^2 and T^3 for a DW theory can be found, *e.g.*, in Refs.51, 53-56. Now we generalize the method to the mapping class group of higher-genus manifolds. In particular, we will focus on the genus-2 manifold.

Our convention on the group-element action in the lattice gauge theory is that *elements of a group are applied from right to left*. For example, $g \cdot h$ means g acts on h .

The hamiltonian version of Dijkgraaf-Witten theory is an exactly solvable lattice model with the following hamiltonian^{51,53,55}

$$H = - \sum_v A_v - \sum_f B_f, \quad (4.1)$$

where $A_v = \frac{1}{|G|} \sum_{t \in G} A_v^t$ is the vertex operator defined on each vertex, and it plays the role of implementing gauge transformation on the group elements living on the links that meet at the vertex v . B_f is the face operator defined on each triangulated face f , and its effect is to impose zero flux (or flat connection constrain) through the face f . The reason we impose flat connection is that we are interested in a TQFT, which has no local observables. Then with flat connection one can find that the holonomy along a closed curve only depends on its homotopy group.

Next, let us consider the Hilbert space of the (possibly) degenerate ground states. First, the moduli space of G bundles on a closed oriented surface $\Sigma_{g,0}$ of genus g can be identified with $\mathcal{V}_g := \text{Hom}(\pi_1(\Sigma_{g,0}, x), G)/G$, where $x \in \Sigma_{g,0}$ is a basepoint, π_1 denotes the fundamental group of the surface, and G acts by conjugation. A representation of the fundamental group of $\Sigma_{g,0}$ consists of elements (g_i, h_i) ($i = 1, \dots, g$)

that satisfy:

$$\prod_{i=1}^g [g_i, h_i] = 1. \quad (4.2)$$

where the commutation is defined as

$$[g, h] := h^{-1} g^{-1} h g. \quad (4.3)$$

Then the gauge equivalent classes of G bundles are determined by this representation up to conjugation. If the 3-cocycle ω is trivial, one can find that the dimension of Hilbert space of degenerate ground states is $\dim \mathcal{H}(\Sigma_{g,0}) = |\mathcal{V}_g|$. For a general ω , one has $\dim \mathcal{H}(\Sigma_{g,0}) \leq |\mathcal{V}_g|$. This is because a generic 3-cocycle ω will introduce phase factors in the basis vectors, and therefore some basis vectors may be canceled and ‘disappear’ in the Hilbert space^{48,53}.

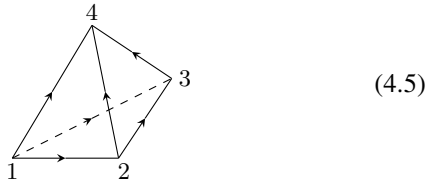
Now if we consider a manifold with punctures, the case becomes more subtle. First, the representation of the fundamental group of $\Sigma_{g,n}$ now reads⁵⁷

$$\prod_{i=1}^g [g_i, h_i] \prod_{s=1}^n c_s = 1 \quad (4.4)$$

where c_s denote the homotopy class of the non-contractable loops around the punctures. In terms of G -bundle, c_s correspond to the holonomy around the punctures. Furthermore, in contrast to the closed manifold where the equivalent classes of gauge bundles are determined by the holonomy up to conjugacy, now we have to rigid the holonomy at the puncture without conjugacy, which will affect the dimension of the Hilbert space.^{58,59}

Since we are considering a $(2+1)$ -d theory, we will focus on the two-dimensional (spatial) triangulated lattice, and assign a group element g_{ij} to each oriented link $i \rightarrow j$. An arbitrary quantum state in the Hilbert space \mathcal{H} is then labeled by $|\{g_{ij}\}\rangle$. By performing a modular transformation, we evolve the wavefunction along the ‘time’ direction. Then the path integral associated to the modular transformation is defined on a three dimensional ‘spacetime’ manifold. It is known that tetrahedra can be viewed as the building block of a 3-manifold. To evaluate the path integral over a generic 3-manifold, let us start by assigning a complex number to a tetrahedra, given a three-cocycle $\omega(g, h, k) \in H^3(G, U(1))$.

There are mainly two steps: ordering and coloring. For a tetrahedron depicted as follows,



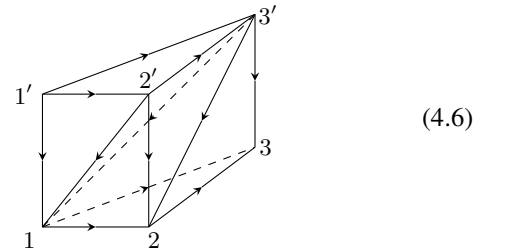
we label the four vertices by 1, 2, 3, and 4 with a chosen ordering, say, $1 < 2 < 3 < 4$. For each link, the direction of the link points from i to j with $i < j$. That is, we use the convention that lower vertex labels point towards the higher vertex labels. Then we color the tetrahedron by assigning a group

element $g_{ij} \in G$ to each link pointing from i to j , and automatically we have $g_{ji} = g_{ij}^{-1}$. These group elements are subjected to the flat-connection constraints. For a triangle with link variables $[ij]$, $[jk]$, and $[ki]$, we have $g_{ij} \cdot g_{jk} \cdot g_{ki} = 1$, where 1 is the identity group element of G . This ensures that the holonomy along a curve only depends on the homotopy class of this curve. With the ordering and coloring introduced above, now we can assign a $U(1)$ phase $\omega^\epsilon(g_{ij}, g_{jk}, g_{kl})$ to each tetrahedron, with $\epsilon = \pm 1$. The sign ϵ is determined by the ‘chirality’. For example, for the tetrahedron in (4.5), looking from the lowest labeled vertex 1, a (counter-) clockwise $2 \rightarrow 3 \rightarrow 4$ loop means $\epsilon = -1 (+1)$. Then one can find the phase assigned to the tetrahedron in (4.5) is $\omega(g_{12}, g_{23}, g_{34})$. For convenience, we may use the definition $[ij] := g_{ij}$ interchangeably.

As a remark, in the topological lattice gauge theory, the 3-cocycle condition in (2.1) has a intuitive geometric meaning. For example, for the tetrahedron in (4.5), one can add one more vertex inside the tetrahedron. Then the original tetrahedron can be triangulated into four pieces of smaller tetrahedra, each of which is associated with a 3-cocycle. Then one can find that the product of the four new phases is the same as the original $U(1)$ phase.⁵¹ This process will result in the 3-cocycle condition in (2.1).

The action of A_v^t on vertex v can be considered as creating a new vertex v' , with $[vv'] = t$ and $t \in G$. We use the convention of ordering such that $v' < v$, and $v' > v_i$ for arbitrary $v_i < v$.⁵³ For those vertex v_i that are linked to v , now we generate new links between v_i and v' , with the group element $[v_i v']$ satisfying $[v_i v'] \cdot [v' v] \cdot [v v_i] = 1$. These new generated vertex and links will introduce extra tetrahedra, and result in certain $U(1)$ phases, as will be discussed in the following examples on manifold of genus $g = 1$ and $g = 2$.

For later convenience, we also introduce a useful manifold $Y \times I$, where Y represents a 2-sphere with three punctures and I is an interval, as follows:



where we take the ordering $1' < 2' < 3' < 1 < 2 < 3$. One can find the weight associated to this triangular prism can be obtained by dividing it into three tetrahedra. Then one has $\omega([3'1], [12], [23]) \cdot \omega([2'3'], [3'1], [12]) \cdot \omega([1'2'], [2'3'], [3'1]) =: Y_{[123], [1'2'3']}$, which is a $U(1)$ phase. Hereafter, for brevity we will use $Y_{[abc], [a'b'c']}$ in certain cases to represent the $U(1)$ phase associated to the triangular prism. It is reminded that the concrete expression of $Y_{[abc], [a'b'c']}$ may depend on the ordering of vertices as well as how we triangulate the prism, but the topological invariants constructed from these building blocks are independent of such choices.^{51,53}

B. Modular transformation

Before we study the modular transformation on a genus-2 manifold, it is helpful to briefly review how to perform the modular transformation for the case of a genus-1 torus.⁵³ Then one can generalize the procedure to a punctured torus, and then study the genus-2 case by gluing two punctured tori by identifying the punctures.

1. Genus one

Let us first check the Hilbert space of ground state on the torus $\Sigma_{1,0}$. The simplest triangulation of a torus is as follows

$$(4.7)$$

where we identify the edges [13] with [24], and [12] with [34]. We take the ordering $1 < 2 < 3 < 4$, and the coloring [13] = [24] = g_x and [12] = [34] = g_y . One can find that there is essentially only one vertex in this triangulation. The flat connection (imposed by the term B_f in the Hamiltonian) on a torus satisfies the constraint $[g_x, g_y] = 1$, where the commutation is defined in Eq.(4.3). The flat connection on a torus simply means that $g_x g_y = g_y g_x$. Denoting the basis in (4.7) as $|g_x, g_y\rangle$ with $g_x, g_y \in G$, then the action of A^t in (4.1) on $|g_x, g_y\rangle$ can be written as (here we simplify A_v^t as A^t since there is only one vertex now):

$$A^t |g_x, g_y\rangle = \eta^t(g_x, g_y) |tg_x t^{-1}, tg_y t^{-1}\rangle, \quad (4.8)$$

where the $U(1)$ phase is associated with the path integral defined on the following 3-manifold:

$$\eta^t(g_x, g_y) : \quad (4.9)$$

The group elements on the links along the ‘time’ direction are $[11'] = [22'] = [33'] = [44'] = t$. The new basis $|h_x, h_y\rangle := |[1'3'], [3'4']\rangle$ are given by $h_x = tg_x t^{-1}$ and $h_y = tg_y t^{-1}$ due to the flat connection constraint. Then one can evaluate $\eta^t(g_x, g_y)$ explicitly by dividing the cube into two triangular prisms, with each prism containing three tetrahedra as shown in (4.6). From the convention of defining A^t in the previous section, we have the ordering $1' < 1 < 2' < 2 < 3' < 3 < 4' < 4$ in the triangulation in (4.9). The $U(1)$ phase $\eta^t(g_x, g_y)$

is then expressed as:

$$\begin{aligned} & Y_{[124],[1'2'4']} \cdot Y_{[134],[1'3'4']}, \\ & = [\omega([12], [24'], [4'4])^{-1} \cdot \omega([12'], [2'2], [24']) \\ & \quad \cdot \omega([1'1], [12'], [2'4'])^{-1}] \cdot [\omega([13], [34'], [4'4]) \\ & \quad \cdot \omega([13'], [3'3], [34'])^{-1} \cdot \omega([1'1], [13'], [3'4'])] \\ & = [\omega(g_y, tg_x, t^{-1})^{-1} \cdot \omega(tg_y, t, tg_x) \\ & \quad \cdot \omega(t^{-1}, tg_y, tg_x t^{-1})^{-1}] \cdot [\omega(g_x, tg_y, t^{-1}) \\ & \quad \cdot \omega(tg_x, t^{-1}, tg_y)^{-1} \cdot \omega(t^{-1}, tg_x, tg_y t^{-1})] =: \eta^t(g_x, g_y). \end{aligned} \quad (4.10)$$

One can check that $A^t A^{t'} = A^{t \cdot t'}$ by using the 3-cocycle condition in Eq.(2.1). Based on Eq.(4.8), the ground states are spanned by the vectors

$$\left\{ \frac{1}{|G|} \sum_{x \in G} \eta^t(g_x, g_y) |tg_x t^{-1}, tg_y t^{-1}\rangle \mid [g_x, g_y] = 1 \right\}. \quad (4.11)$$

Now let us consider the mapping class group for the torus $\Sigma_{1,0}$. There are two generators for $\text{MCG}(\Sigma_{1,0})$, which can be chosen as the two Dehn twists t_x and t_y along x and y directions, or alternatively their combination such as \mathfrak{s} and \mathfrak{t} transformations (See introduction). They are related by

$$\mathfrak{t} := t_x, \quad \mathfrak{s} := t_y \cdot t_x^{-1} \cdot t_y. \quad (4.12)$$

One can check that the modular relation $t_y \cdot t_x^{-1} \cdot t_y = t_x^{-1} \cdot t_y \cdot t_x^{-1}$ is equivalent to $(\mathfrak{st})^3 = \mathfrak{s}^2$. For a lattice gauge theory, it is more convenient to perform Dehn twists directly, based on which we can get the representations T_x and T_y for t_x and t_y , respectively. Then S and T matrices can be defined as

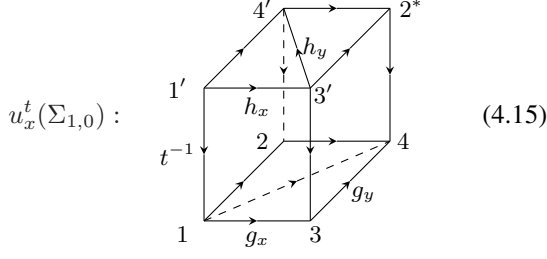
$$T := T_x, \quad S := T_y \cdot T_x^{-1} \cdot T_y. \quad (4.13)$$

In the following, let us check how the representations of Dehn twists T_x and T_y act on the basis $|g_x, g_y\rangle$ in (4.7). For the effect of T_x on the basis vector $|g_x, g_y\rangle$, we have⁵³

$$(4.14)$$

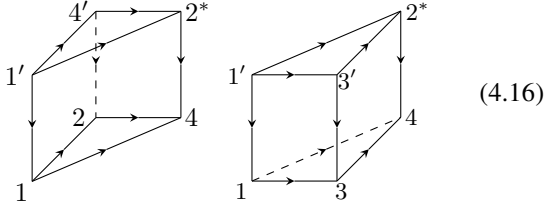
The basis $|g_x, g_y\rangle$ is transformed to $|h_x, h_y\rangle := |[1'3'], [3'4']\rangle = |tg_x t^{-1}, t(g_x^{-1} \cdot g_y)t^{-1}\rangle$, where $t \in G$, up to a $U(1)$ phase $u_x^t(\Sigma_{1,0})$. By restricting to the unit squares spanned by $1, 2, 3, 4$ and $1', 3', 4', 2^*$, one can find that the $U(1)$ phase $u_x^t(\Sigma_{1,0})$ is associated with the path

integral as follows:

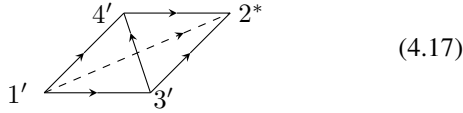


with the ordering: $1' < 3' < 4' < 2^* < 1 < 2 < 3 < 4$. The group elements on the links along the ‘time’ direction are $[11'] = [33'] = [24'] = [42^*] = t$, with $t \in G$. With the flat connection condition, $h_x = t g_x t^{-1}$ and $h_y = t(g_x^{-1} \cdot g_y) t^{-1}$ is automatically satisfied.

The phase in (4.15) can be decomposed into the product of three pieces. The first two pieces correspond to the two triangular prisms as follows



with each prism containing three tetrahedra and expressed in terms of the product of three 3-cocycles. The third piece is



which contributes a single 3-cocycle $\omega([1'3'], [3'4'], [4'2^*])$. Combining all the contributions above, the phase in (4.15) is the product of seven 3-cocycles as follows

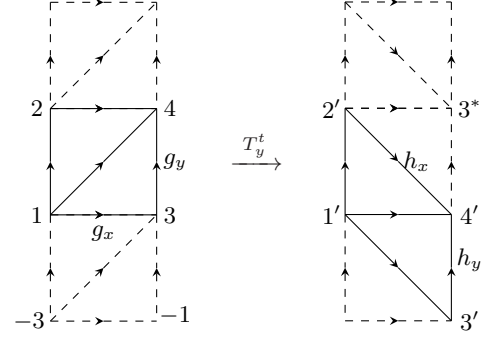
$$\begin{aligned}
& Y_{[124],[1'4'2^*]} \cdot Y_{[134],[1'3'2^*]} \cdot \omega([1'3'], [3'4'], [4'2^*]) \\
&= [\omega^{-1}([2^*1], [12], [24]) \cdot \omega^{-1}([4'2^*], [2^*1], [12]) \\
&\quad \cdot \omega^{-1}([1'4'], [4'2^*], [2^*1])] \cdot [\omega([2^*1], [13], [34]) \\
&\quad \cdot \omega([3'2^*], [2^*1], [13]) \cdot \omega([1'3'], [3'2^*], [2^*1])] \\
&\quad \cdot \omega([1'3'], [3'4'], [4'2^*]) \\
&= \omega^{-1}(g_x^{-1} g_y^{-1} t^{-1}, g_y, g_x) \cdot \omega^{-1}(t g_x t^{-1}, g_x^{-1} g_y^{-1} t^{-1}, g_y) \\
&\quad \cdot \omega^{-1}(t g_y t^{-1}, t g_x t^{-1}, g_x^{-1} g_y^{-1} t^{-1}) \cdot \omega(g_x^{-1} g_y^{-1} t^{-1}, g_x, g_y) \\
&\quad \cdot \omega(t g_y t^{-1}, g_x^{-1} g_y^{-1} t^{-1}, g_x) \cdot \omega(t g_x t^{-1}, t g_y t^{-1}, g_x^{-1} g_y^{-1} t^{-1}) \\
&\quad \cdot \omega(t g_x t^{-1}, t g_x^{-1} g_y t^{-1}, t g_x t^{-1}) =: u_x^t(\Sigma_{1,0}).
\end{aligned} \tag{4.18}$$

Then the effect of T_x^t on the basis $|g_x, g_y\rangle$ is

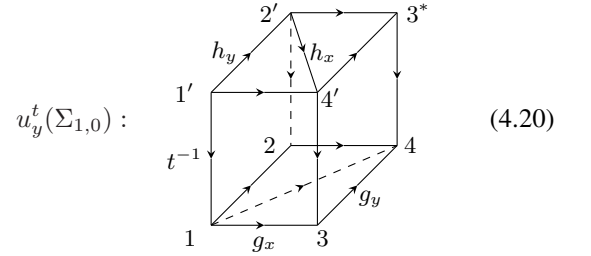
$$T_x^t |g_x, g_y\rangle = u_x^t(\Sigma_{1,0}) |t g_x t^{-1}, t(g_x^{-1} \cdot g_y) t^{-1}\rangle, \tag{4.19}$$

with the phase $u_x^t(\Sigma_{1,0})$ expressed in Eq.(4.18).

Next we consider the effect of T_y on the basis $|g_x, g_y\rangle$ as follows:



Similar to the T_x transformation, here the basis vector $|g_x, g_y\rangle$ is transformed to $|h_x, h_y\rangle := |[1'3'], [3'4']\rangle = |t(g_y^{-1} g_x) t^{-1}, t g_y t^{-1}\rangle$ up to a $U(1)$ phase $u_y^t(\Sigma_{1,0})$. By restricting to the unit squares spanned by $1, 2, 3, 4$ and $1', 2', 4', 3^*$, one can find that $u_y^t(\Sigma_{1,0})$ is associated with the path integral defined on the following 3-manifold:



with the ordering: $1' < 2' < 4' < 3^* < 1 < 2 < 3 < 4$. Again, the group elements on the links in the ‘time’ direction are $[11'] = [22'] = [34'] = [43^*] = t$. With the flat connection condition one can find $h_x = t(g_y^{-1} g_x) t^{-1}$ and $h_y = t g_y t^{-1}$. Similar to (4.15), the phase $u_y^t(\Sigma_{1,0})$ corresponding to (4.20) is the product of seven 3-cocycles as

$$\begin{aligned}
& Y_{[124],[1'2'3^*]} \cdot Y_{[134],[1'4'3^*]} \cdot \omega^{-1}([1'2'], [2'4'], [4'3^*]) \\
&= [\omega^{-1}([3^*1], [12], [24]) \cdot \omega^{-1}([2'3^*], [3^*1], [12]) \\
&\quad \cdot \omega^{-1}([1'2'], [2'3^*], [3^*1])] \cdot [\omega([3^*1], [13], [34]) \\
&\quad \cdot \omega([4'3^*], [3^*1], [13]) \cdot \omega([1'4'], [4'3^*], [3^*1])] \\
&\quad \cdot \omega^{-1}([1'2'], [2'4'], [4'3^*]) \\
&= \omega^{-1}(g_x^{-1} g_y^{-1} t^{-1}, g_y, g_x) \cdot \omega^{-1}(t g_x t^{-1}, g_x^{-1} g_y^{-1} t^{-1}, g_y) \\
&\quad \cdot \omega^{-1}(t g_y t^{-1}, t g_x t^{-1}, g_x^{-1} g_y^{-1} t^{-1}) \cdot \omega(g_x^{-1} g_y^{-1} t^{-1}, g_x, g_y) \\
&\quad \cdot \omega(t g_y t^{-1}, g_x^{-1} g_y^{-1} t^{-1}, g_x) \cdot \omega(t g_x t^{-1}, t g_y t^{-1}, g_x^{-1} g_y^{-1} t^{-1}) \\
&\quad \cdot \omega^{-1}(t g_y t^{-1}, t g_y^{-1} g_x t^{-1}, t g_y t^{-1}) =: u_y^t(\Sigma_{1,0}).
\end{aligned} \tag{4.21}$$

Then the effect of T_y^t on the basis $|g_x, g_y\rangle$ is

$$T_y^t |g_x, g_y\rangle = u_y^t(\Sigma_{1,0}) |t(g_y^{-1} g_x) t^{-1}, t g_y t^{-1}\rangle. \tag{4.22}$$

Having known how $T_{x,y}^t$ act on the basis $|g_x, g_y\rangle$, now we can define $T_{x,y} := \frac{1}{|G|} \sum_{t \in G} T_{x,y}^t$. It can be checked that $T_{x,y}^t \cdot A^t = A^t \cdot T_{x,y}^{t'} = T_{x,y}^{t \cdot t'}$. The modular S and T matrices

are defined as

$$S := \frac{1}{|G|} \sum_{t \in G} S^t, \quad T := \frac{1}{|G|} \sum_{t \in G} T^t, \quad (4.23)$$

where $T^t = T_x^t$, and $S^t = T_y^{t'=1} \cdot (T_x^{t'=1})^{-1} \cdot T_y^{t'=1} \cdot A^t = A^t \cdot T_y^{t'=1} \cdot (T_x^{t'=1})^{-1} \cdot T_y^{t'=1}$. Then one can calculate the modular S and T matrices with the groundstate bases in (4.11).⁵³

Before we end this part, we remark that for the genus-1 torus $\Sigma_{1,0}$, one can construct the quasi-particle basis $|g, \chi\rangle$ corresponding to (2.6) in terms of the group-element basis $|g_x, g_y\rangle$, so that the T matrix is diagonal with the diagonal elements being topological spins of anyons (see appendix C3 for an illustration). With the quasi-particle basis $|g, \chi\rangle$, one can obtain the modular S and T matrices exactly of the form in Eqs.(2.13) and (2.21).⁵³

2. Punctured torus

Now we generalize the previous procedure to the punctured torus $\Sigma_{1,1}$. Here we are interested in $\Sigma_{1,1}$ because the genus-2 manifold $\Sigma_{2,0}$ can be obtained by gluing two copies of $\Sigma_{1,1}$ by identifying their punctures.

The simplest configuration for a punctured torus is as follows:

$$(4.24)$$

where the left and right configurations are equivalent to each other. For the configuration on the right, we identify the edges $[13]$ with $[24]$, $[\bar{1}2]$ with $[34]$, and therefore there is essentially only one vertex. The triangulation of the punctured torus is:

$$(4.25)$$

where we take the ordering: $\bar{1} < 1 < 2 < 3 < 4$, and the coloring $[13] = [24] = g_x$, $[\bar{1}2] = [34] = g_y$, and $[\bar{1}1] = k$. The flat connection condition is [see Eq.(4.4)]

$$k \cdot [g_x, g_y] = 1, \quad (4.26)$$

i.e., $k \cdot g_y^{-1} g_x^{-1} g_y g_x = 1$, where 1 is the identity group element. Here the holonomy k measures the ‘flux’ of anyon z in the single-puncture torus basis in (3.27).

Denoting the punctured-torus basis in (4.25) as $[[13], [34]; [\bar{1}1]] = |g_x, g_y; k\rangle$, we will study how modular transformations act on this basis vector. It is known that $\text{MCG}(\Sigma_{1,1})$ is generated by the same \mathfrak{s} and \mathfrak{t} (or equivalently the two Dehn twists \mathfrak{t}_x and \mathfrak{t}_y) as those for $\text{MCG}(\Sigma_{1,0})$. The

difference is that for a punctured torus one has $\mathfrak{s}^4 = \mathfrak{t}^{-1}$, where \mathfrak{t} represents the Dehn twist along the closed curve that encloses the puncture, and for the torus without puncture one simply has $\mathfrak{s}^4 = 1$. Following the procedure in the previous section, we denote $T_{x,y} := \frac{1}{|G|} \sum_{t \in G} T_{x,y}^t$ as the representation of Dehn twists $\mathfrak{t}_{x,y}$. Then one can find the effect of T_x^t on $|g_x, g_y; k\rangle$ as

$$T_x^t |g_x, g_y; k\rangle = u_x^t(\Sigma_{1,1}) |t g_x t^{-1}, t(g_x^{-1} \cdot g_y) t^{-1}; t k t^{-1}\rangle, \quad (4.27)$$

where the $U(1)$ phase $u_x^t(\Sigma_{1,1})$ is associated to the path integral on the following 3-manifold: (It is helpful to compare this with the phase $u_x^t(\Sigma_{1,0})$ in (4.15).)

$$u_x^t(\Sigma_{1,1}) : \quad (4.28)$$

The ordering is taken as: $\bar{1}' < \bar{1} < 1' < 3' < 4' < 2^* < 1 < 2 < 3 < 4$. The group elements living on the vertical links are $[\bar{1}\bar{1}'] = [11'] = [24'] = [33'] = [42^*] = t$. With the flat connection condition, one can find that $[h_x, h_y; k'] := [[1'3'], [3'4']; [\bar{1}'1']] = |t g_x t^{-1}, t(g_x^{-1} g_y) t^{-1}; t k t^{-1}\rangle$. The phase $u_x^t(\Sigma_{1,1})$ in (4.28) is composed of $3 \times 3 + 2 = 11$ 3-cocycles as follows:

$$u_x^t(\Sigma_{1,1}) = Y_{[\bar{1}24], [\bar{1}'4'2^*]} \cdot Y_{[\bar{1}14], [\bar{1}'1'2^*]} \cdot Y_{[134], [1'3'2^*]} \cdot \omega([\bar{1}'1'], [1'4'], [4'2^*]) \cdot \omega([1'3'], [3'4'], [4'2^*]), \quad (4.29)$$

where each $Y_{[abc], [a'b'c']}$ is composed of three 3-cocycles, corresponding to the triangular prism spanned by $[abc]$ and $[a'b'c']$. The explicit expression of $u_x^t(\Sigma_{1,1})$ can be found in Eqs.(C17)-(C20) in Appendix C4. The last two 3-cocycles in Eq.(4.29) correspond to the following two tetrahedra:

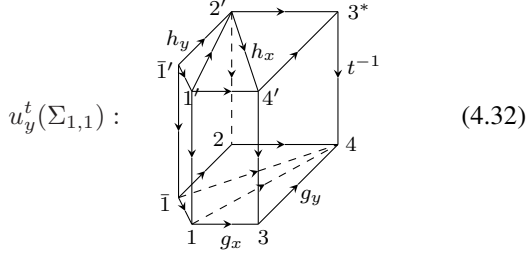
$$(4.30)$$

Similarly, the Dehn twist along y direction acts on the basis $|g_x, g_y; k\rangle$ in the following way

$$T_y^t |g_x, g_y; k\rangle = u_y^t(\Sigma_{1,1}) |t g_y^{-1} g_x t^{-1}, t g_y t^{-1}; t k t^{-1}\rangle. \quad (4.31)$$

The $U(1)$ phase $u_y^t(\Sigma_{1,1})$ is associated to the 3-manifold (It is

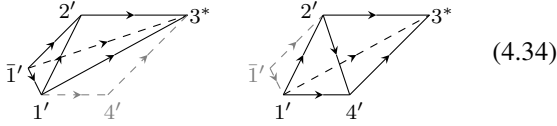
helpful to compare this with the phase $u_y^t(\Sigma_{1,0})$ in (4.20).)



The ordering is taken as: $\bar{1}' < \bar{1} < 1' < 2' < 4' < 3^* < 1 < 2 < 3 < 4$. Again, the group elements living on the vertical links are $[\bar{1}\bar{1}'] = [11'] = [22'] = [34'] = [43^*] = t$. With the flat connection condition, one can find the old basis is transformed to $|h_x, h_y; k'\rangle := |[2'4'], [\bar{1}'2']; [\bar{1}'1']\rangle = |t(g_y^{-1}g_x)t^{-1}, tg_y t^{-1}; tkt^{-1}\rangle$. The phase $u_y^t(\Sigma_{1,1})$ in (4.32) is composed of $3 \times 3 + 2 = 11$ three-cocycles:

$$u_y^t(\Sigma_{1,1}) = Y_{[\bar{1}24], [\bar{1}'2'3^*]} \cdot Y_{[\bar{1}14], [\bar{1}'1'3^*]} \cdot Y_{[134], [1'4'3^*]} \cdot \omega([\bar{1}'1'], [1'2'], [2'3^*]) \cdot \omega([1'2'], [2'4'], [4'3^*])^{-1}, \quad (4.33)$$

where each $Y_{[abc], [a'b'c']}$ corresponding to a triangular prism is the product of three 3-cocycles. An explicit expression of $u_y^t(\Sigma_{1,1})$ can be found in Eqs.(C21)-(C24) in Appendix C4. The last two terms in Eq.(4.33) are contributed by the following two tetrahedra:

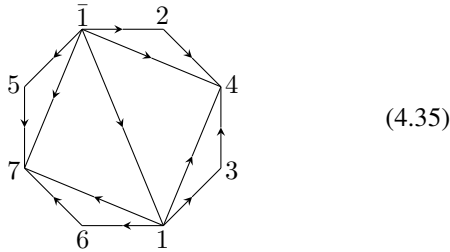


and the concrete expression can be found in Eq.(C24).

Till now, we have studied how to perform Denh twists on the basis $|g_x, g_y; k\rangle$ in (4.24) for a punctured torus. In the next section, we will use these basic operations to study the modular transformations of the degenerate ground states on a genus-2 manifold.

3. Genus two

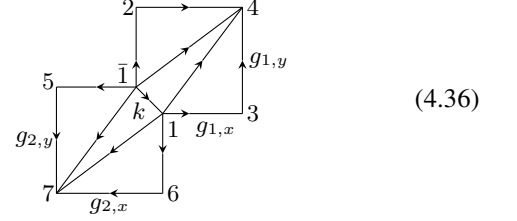
The simplest triangulation of a genus-2 manifold is an octagon as follows:



where we identify the edges $[13]$ with $[24]$, $[34]$ with $[\bar{1}2]$, $[16]$ with $[57]$, and $[67]$ with $[\bar{1}5]$, and take the ordering $\bar{1} < 1 <$

$2 < 3 < 4 < 5 < 6 < 7$. This triangulation has six triangle faces and only one vertex.

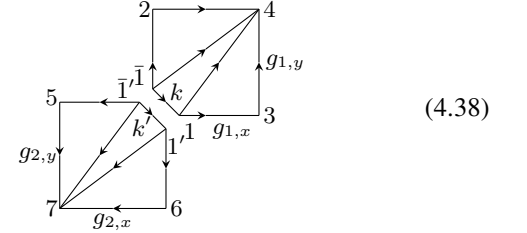
To compare with the configuration of a punctured torus, it is convenient to replot the octagon in (4.35) in the following way:



where we have colored the triangulation with $[13] = [24] = g_{1,x}$, $[\bar{1}2] = [34] = g_{1,y}$, $[\bar{1}5] = [67] = g_{2,x}$, $[16] = [57] = g_{2,y}$, and $[\bar{1}1] = k$, with $g_{i,x}, g_{i,y}, k \in G$. We denote the basis vector corresponding to the configuration in (4.36) as

$$|g_{1,x}, g_{1,y}; g_{2,x}, g_{2,y}\rangle. \quad (4.37)$$

By comparing with the punctured-torus basis in (4.25), one can find that the genus-2 basis in (4.36) can be obtained by gluing two copies of punctured-torus bases along the puncture as follows:



with the holonomy around the puncture identified, *i.e.*, $k = k'$.

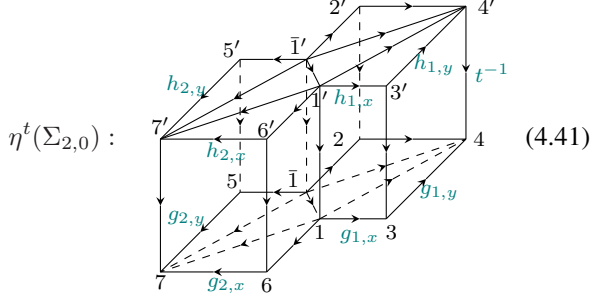
For the ground state of the Hamiltonian in Eq.(4.1), the terms B_f enforce the flat connection condition for each face (triangle), and then we have

$$[g_{2,x}, g_{2,y}] \cdot [g_{1,x}, g_{1,y}] = 1, \quad (4.39)$$

where the commutation relation $[g, h]$ is defined in Eq.(4.3). The holonomy k is determined by $k \cdot [g_{1,x}, g_{1,y}] = k^{-1} \cdot [g_{2,x}, g_{2,y}] = 1$. For the basis $|g_{1,x}, g_{1,y}; g_{2,x}, g_{2,y}\rangle$ in (4.36), one can find that A^t in Eq.(4.1) acts on it as

$$A^t |g_{1,x}, g_{1,y}; g_{2,x}, g_{2,y}\rangle = \eta^t(g_{1,x}, g_{1,y}; g_{2,x}, g_{2,y}) |tg_{1,x}t^{-1}, tg_{1,y}t^{-1}; tg_{2,x}t^{-1}, tg_{2,y}t^{-1}\rangle \quad (4.40)$$

The $U(1)$ phase $\eta^t(g_{1,x}, g_{1,y}; g_{2,x}, g_{2,y})$, also written as $\eta^t(\Sigma_{2,0})$ for brevity, corresponds to the path integral over the following 3-manifold:



with the ordering $i' < i < (i+1)'$, and $\bar{1} < 1$. The group elements on all the vertical links are $[ii'] = t$. The new basis $|h_{1,x}, h_{1,y}; h_{2,x}, h_{2,y}\rangle := |[1'3'], [3'4']; [1'6'], [\bar{1}'5']\rangle = |tg_{1,x}t^{-1}, tg_{1,y}t^{-1}; tg_{2,x}t^{-1}, tg_{2,y}t^{-1}\rangle$ automatically satisfies the flat connection condition. One can find that $\eta^t(\Sigma_{2,0})$ in (4.41) is the product of $6 \times 3 = 18$ three-cocyles:

$$\begin{aligned} \eta^t(\Sigma_{2,0}) = & Y_{[167],[1'6'7']} \cdot Y_{[\bar{1}17],[\bar{1}'1'7']} \cdot Y_{[\bar{1}57],[\bar{1}'5'7']} \\ & \cdot Y_{[134],[1'3'4']} \cdot Y_{[\bar{1}14],[\bar{1}'1'4']} \cdot Y_{[\bar{1}24],[\bar{1}'2'4']} \end{aligned} \quad (4.42)$$

where each $Y_{[abc],[a'b'c']}$ corresponding to a triangular prism is the product of three 3-cocyles. The explicit expression of $\eta^t(\Sigma_{2,0})$ can be found in Eqs.(C25)-(C27) in the appendix. Similar to the case of $\Sigma_{1,0}$, one can check that $A^t \cdot A^{t'} = A^{t \cdot t'}$ by using the 3-cocyle condition in Eq.(2.1).

It follows from Eq.(4.40) that the degenerate ground states on $\Sigma_{2,0}$ are spanned by the vectors:

$$\left\{ \frac{1}{|G|} \sum_{t \in G} \eta^t(\Sigma_{2,0}) |tg_{1,x}t^{-1}, tg_{1,y}t^{-1}, tg_{2,x}t^{-1}, tg_{2,y}t^{-1}\rangle \right\}, \quad (4.43)$$

where $g_{1,x}, g_{1,y}, g_{2,x}$, and $g_{2,y}$ satisfy the flat connection constraint in Eq.(4.39).

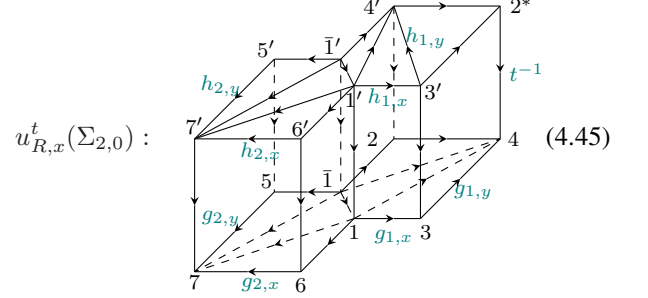
One remark here: The expression in (4.43) may suggest that the ground state degeneracy (GSD) on $\Sigma_{2,0}$ is counted by $\text{Hom}(\pi_1(\Sigma_{2,0}), G)/G$, where G acts by conjugation. As emphasized in Ref.48, this is true for the case with trivial three-cocyle $\omega = 1$. For general $\omega \in H^3(G, U(1))$, we have $\text{GSD} \leq |\text{Hom}(\pi_1(\Sigma_{2,0}), G)/G|$. This is because for certain $g_{i,x}$ and $g_{i,y}$, the summation in (4.43) may vanish because of the phase factor $\eta^t(\Sigma_{2,0})$.⁵³ Therefore, one may overcount the states with $\text{Hom}(\pi_1(\Sigma_{2,0}), G)/G$. For the MS MTCs as studied in this work, it is found that $\text{GSD} = |\text{Hom}(\pi_1(\Sigma_{2,0}), G)/G|$.

Now let us look at how the modular transformations act on the basis $|g_{1,x}, g_{1,y}; g_{2,x}, g_{2,y}\rangle$. In particular, we will focus on the Dehn twists along the closed curves a_1, b_1, a_2 , and b_2 in (1.1). Considering that the genus-2 manifold is obtained by gluing two punctured tori along the punctures, we can act the Dehn twists on the two punctured tori separately, and then the results on the punctured torus in the previous section can be applied here. Let us denote the punctured torus spanned by $[1\bar{1}567]$ in (4.36) as the left punctured torus, and that spanned by $[1\bar{1}234]$ as the right punctured torus. Now we consider how the Dehn twists act on, without loss of generality, the right punctured torus of the basis in (4.36). That is, we will

consider the operation $I_L^t \otimes T_{R,\alpha}^t$, where I means no modular transformation, and $\alpha = x, y$. For $\alpha = x$, we have

$$\begin{aligned} & I_L^t \otimes T_{R,x}^t |g_{1,x}, g_{1,y}; g_{2,x}, g_{2,y}\rangle \\ & = u_{R,x}^t(\Sigma_{2,0}) |tg_{1,x}t^{-1}, t(g_{1,x}^{-1} \cdot g_{1,y})t^{-1}; tg_{2,x}t^{-1}, tg_{2,y}t^{-1}\rangle \end{aligned} \quad (4.44)$$

Here the $U(1)$ phase $u_{R,x}^t(\Sigma_{2,0})$ is associated with the path integral defined on the following 3-manifold:



The ordering is taken as $\bar{1}' < 1' < 3' < 4' < 2^* < 5' < 6' < 7' < \bar{1} < 1 < 2 < 3 < 4 < 5 < 6 < 7$. All the group elements assigned on the directed vertical links are t^{-1} . The new basis after Dehn twist is $|h_{1,x}, h_{1,y}; h_{2,x}, h_{2,y}\rangle := |[1'3'], [3'4']; [6'7'], [1'6']\rangle = |tg_{1,x}t^{-1}, t(g_{1,x}^{-1} \cdot g_{1,y})t^{-1}; tg_{2,x}t^{-1}, tg_{2,y}t^{-1}\rangle$ which satisfies the flat connection condition. The $U(1)$ phase $u_{R,x}^t(\Sigma_{2,0})$ in (4.45) can be expressed as

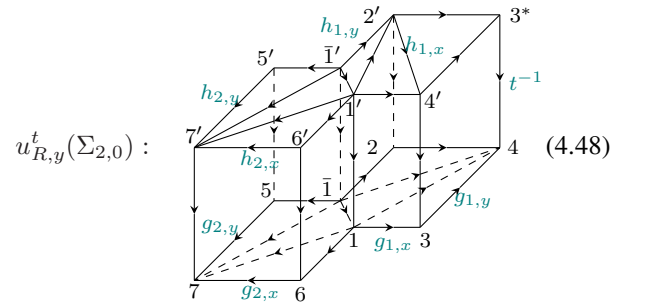
$$u_{R,x}^t(\Sigma_{2,0}) = I_L^t(\Sigma_{1,1}) \cdot u_x^t(\Sigma_{1,1}) \quad (4.46)$$

where the second term, which is the same as that in (4.29), is contributed by the Dehn twist on the right punctured torus. The first term $I_L^t(\Sigma_{1,1})$ is contributed by the left punctured torus, with the expression given in Eq.(C28).

For the Dehn twist $T_{R,y}$ acting on the right punctured torus, we have

$$\begin{aligned} & I_L^t \otimes T_{R,y}^t |g_{1,x}, g_{1,y}; g_{2,x}, g_{2,y}\rangle \\ & = u_{R,y}^t(\Sigma_{2,0}) |t(g_{1,y}^{-1} \cdot g_{1,x})t^{-1}, tg_{1,y}t^{-1}; tg_{2,x}t^{-1}, tg_{2,y}t^{-1}\rangle \end{aligned} \quad (4.47)$$

where the $U(1)$ phase $u_{R,y}^t(\Sigma_{2,0})$ is associated with the path integral defined on the following 3-manifold:



with the ordering $\bar{1}' < 1' < 2' < 4' < 3^* < 5' < 6' < 7' < \bar{1} < 1 < 2 < 3 < 4 < 5 < 6 < 7$. Again the

group elements on the directed vertical links are t^{-1} . The new basis $|h_{1,x}, h_{1,y}; h_{2,x}, h_{2,y}\rangle := |[2'4'], [1'2']; [6'7'], [1'6']\rangle = |t(g_{1,y}^{-1} \cdot g_{1,x})t^{-1}, tg_{1,y}t^{-1}; tg_{2,x}t^{-1}, tg_{2,y}t^{-1}\rangle$ satisfies the flat connection condition. The $U(1)$ phase $u_{R,y}^t(\Sigma_{2,0})$ in (4.48) can be written as:

$$u_{R,y}^t(\Sigma_{2,0}) = I_L^t(\Sigma_{1,1}) \cdot u_y^t(\Sigma_{1,1}) \quad (4.49)$$

where the first term $I_L^t(\Sigma_{1,1})$ is the same as that in Eq.(4.46), with the expression given in Eq.(C28). The second term $u_y^t(\Sigma_{1,1})$, which is the same as (4.32), is contributed by the Denh twist acting on the right punctured torus.

Similar to the case of $\Sigma_{1,0}$, it can be checked that $(I_L^t \otimes T_{R,x(y)}^t) \cdot A^t = A^t \cdot (I_L^t \otimes T_{R,x(y)}^t) = I_L^{t \cdot t'} \otimes T_{R,x(y)}^{t \cdot t'}$, with A^t defined in Eq.(4.40). We can define the following quantities

$$T_R := \frac{1}{|G|} \sum_{t \in G} I^t \otimes T_{R,x}^t, \quad S_R := \frac{1}{|G|} \sum_{t \in G} I^t \otimes S_R^t, \quad (4.50)$$

where $I^t \otimes S_R^t = (I^{t'=1} \otimes T_{R,y}^{t'=1}) \cdot (I^{t'=1} \otimes (T_{R,x}^{t'=1})^{-1}) \cdot (I^{t'=1} \otimes T_{R,y}^{t'=1}) \cdot A^t = A^t \cdot (I^{t'=1} \otimes T_{R,y}^{t'=1}) \cdot (I^{t'=1} \otimes (T_{R,x}^{t'=1})^{-1}) \cdot (I^{t'=1} \otimes T_{R,y}^{t'=1})$. It is noted that here we act the modular transformations only on the right punctured torus in the basis (4.36). One can certainly consider the same procedure by performing modular transformations on the left punctured torus.

Given T_R and S_R in Eq.(4.50), we can calculate the matrix representations $(T_R)_{ij} = \langle \Phi_i | T_R | \Phi_j \rangle$ and $(S_R)_{ij} = \langle \Phi_i | S_R | \Phi_j \rangle$, with the ground state bases $|\Phi_i\rangle$ in (4.43).

C. Topological invariants

The lattice gauge theory approach discussed in the previous subsections work for general Dijkgraaf-Witten theories, and here we apply it to the MS MTCs. In particular, we focus on the simplest counterexamples in MS MTCs with $G = \mathbb{Z}_{11} \rtimes \mathbb{Z}_5$, twisted by 3-cocycles $\omega \in H^3(G, U(1)) \cong \mathbb{Z}_5$. One can find that even for these simplest examples the GSD on a genus-2 manifold is 18529.

As introduced in Sec.III, we construct the topological invariants based on the ‘words’ composed of S_R and T_R in Eq.(4.50) as:

$$W_{\Sigma_{2,0}} := \text{Tr} \left[(S_R)^{n_1} (T_R)^{n_2} (S_R)^{n_3} (T_R)^{n_4} \dots \right], \quad (4.51)$$

where the trace is over the Hilbert space of degenerate ground states on a genus-2 manifold in Eq.(4.43).

To compare with the results in Sec.III in more details, let us first point out some fine structures in the degenerate ground states in Eq.(4.43). For each ground state $\frac{1}{|G|} \sum_{t \in G} \eta^t(\Sigma_{2,0}) |tg_{1,x}t^{-1}, tg_{1,y}t^{-1}, tg_{2,x}t^{-1}, tg_{2,y}t^{-1}\rangle$, one can find that the conjugacy class of ‘ k ’ in (4.36) is well defined, with $k = t \cdot [g_{1,x}, g_{1,y}]^{-1} \cdot t^{-1} = t \cdot [g_{2,x}, g_{2,y}] \cdot t^{-1}$, where $t \in G$. For the MS MTCs we consider here, it is found that the conjugacy class $[k]$ can only be $[1]$, $[a^1]$, and $[a^2]$ (see Table I). Considering that $[k]$ measures the ‘magnetic flux’

of anyon z in (3.1), this means the anyon type for z can only be type- I or type- A , which agrees with the fusion rules as studied in Sec.III.

According to the conjugacy class of k , now we divide the ground states in Eq.(4.43) into three groups with $[k] = [1]$, $[a^1]$, and $[a^2]$, respectively. One can find that the number of degenerate ground states is 5857 for $[k] = [1]$, 6336 for $[k] = [a^1]$, and 6336 for $[k] = [a^2]$ (This agrees with the fact that the GSD on a genus-2 surface is 18529). Then the topological invariant defined in Eq.(4.51) can be written as

$$\begin{aligned} W_{\Sigma_{2,0}} &= W_{\Sigma_{2,0}}^{[1]} + W_{\Sigma_{2,0}}^{[a^1]} + W_{\Sigma_{2,0}}^{[a^2]} \\ &=: W_{\Sigma_{2,0}}^I + W_{\Sigma_{2,0}}^{A_1} + W_{\Sigma_{2,0}}^{A_2}, \end{aligned} \quad (4.52)$$

where $W_{\Sigma_{2,0}}^{[k]}$ is defined in (4.51), except that now the trace is taken over the degenerate ground states with a fixed $[k]$.

In the following, we study the trace of word samples in (3.55). More explicitly, the word $w_1^{(z)} = (\theta^{(z)})^2 \cdot (T^{(z)})^7 S^{(z)} = (S^{(z)})^{-7} (T^{(z)})^7 S^{(z)}$ in Eq.(3.55) corresponds to $w_1 = S_R^{-8} \cdot T_R^7 \cdot S_R$ in the lattice gauge theory approach here, and similarly for other words. The results for the trace over different words are summarized in Tables XIX - XXV.

For convenience, we compare the results of quasi-particle basis calculation and the lattice gauge theory calculation for the trace of word $w_1^{(z)}$ (see Eq.3.55) in Table XIX. The comparisons for other words are similar and straightforward. It is remarkable that although we work with two independent methods and the ground state bases are chosen in different ways, the topological invariants we obtained are the same.

It is reminded that for the quasi-particle basis result in Table XIX, the data in gray are contributed by $W_{\Sigma_{2,0}}^{I_i}$, with $i = 1, \dots, 4$. As explained in Sec.III D, for $z = I_i$ with $i = 1, \dots, 4$, only type- I and type- A anyons appear in the punctured S matrix, and therefore the information of 3-cocycle ω^u will not come in (Recall that only type- B anyons carry the information of 3-cocycles). This is more transparent by considering the lattice gauge theory approach: For the basis vector in (4.36), $z = I_i$ ($i = 1, \dots, 4$) correspond to the case that the group element $k = 1$, where 1 denotes the identity group element. Then with the fusion rules in Sec.III A, one can find for $a \times \bar{a} = \sum_z N_{a\bar{a}}^z z$ where $z = I_i$ ($i = 1, \dots, 4$), $N_{a\bar{a}}^z$ is nonzero only when a are type- I or type- A anyons. This indicates that the group elements $g_{1,x}$ and $g_{1,y}$ in (4.36) can only be of the form (a^l, b^0) with $l = 0, \dots, 10$. By performing modular transformation on the right half torus in (4.36), one can find that the 3-cocycles ω involved in this process are always trivial with $\omega = 1$. This explains why $W_{\Sigma_{2,0}}^{I_i}$ ($i = 1, \dots, 4$) are independent of the three-cocycle ω^u and u .

The invariants that can distinguish different categories are $W_{\Sigma_{2,0}}^{A_1}$ and $W_{\Sigma_{2,0}}^{A_2}$, with the difference in the phase factor $e^{\frac{2i\pi}{5}n}$, where $n = 0, 1, 2, 3, 4$. In addition, the phase factor for $u = 1$ ($u = 2$) is conjugate to that for $u = 4$ ($u = 3$).

It is emphasized that the topological invariants $W_{\Sigma_{2,0}}$ we defined is independent of the permutation of anyons. This is different from the method we used in Sec.III C, where we need

to track how the topological invariants (diagonal elements of $S^{(z)}$ and T matrix) transform with the bijection of anyons between two categories. Here, a single number is enough to distinguish different categories.

One remark here: As mentioned in Sec.III D, corresponding to the five different phase factors $e^{\frac{2i\pi}{5}n}$ with $n = 0, 1, 2, 3, 4$, if we consider $\cos\left(\frac{2\pi}{5}n\right)$, there are only three different values left. The distinct information becomes degenerate now. In fact, as seen from Sec.III D, the invariants that contain $\cos\left(\frac{2\pi}{5}n\right)$ are contributed by the modular data with $z = I_0$. This agrees with the fact that there are only three distinct sets of modular data in MS MTCs. From this point of view, the reason that the modular data is not enough to distinguish different categories is because the information becomes degenerate. With the MCG representations of higher genus manifold, we can split this information degeneracy and distinguish different categories.

| Quasi-particle basis result | | | |
|-----------------------------|---|--|--|
| $W_{\Sigma_{2,0}}$ | $W_{\Sigma_{2,0}}^I$ | $W_{\Sigma_{2,0}}^{A_1}$ | $W_{\Sigma_{2,0}}^{A_2}$ |
| $u = 0$ | $633 - 24 \times 4$ | 528 | 528 |
| $u = 1$ | $245 - 24 \times 4 + 388 \cdot \cos \frac{2\pi}{5}$ | $528 \cdot e^{\frac{2i\pi}{5} \times 1}$ | $528 \cdot e^{\frac{2i\pi}{5} \times 1}$ |
| $u = 2$ | $245 - 24 \times 4 + 388 \cdot \cos \frac{4\pi}{5}$ | $528 \cdot e^{\frac{2i\pi}{5} \times 2}$ | $528 \cdot e^{\frac{2i\pi}{5} \times 2}$ |
| $u = 3$ | $245 - 24 \times 4 + 388 \cdot \cos \frac{4\pi}{5}$ | $528 \cdot e^{\frac{2i\pi}{5} \times 3}$ | $528 \cdot e^{\frac{2i\pi}{5} \times 3}$ |
| $u = 4$ | $245 - 24 \times 4 + 388 \cdot \cos \frac{2\pi}{5}$ | $528 \cdot e^{\frac{2i\pi}{5} \times 4}$ | $528 \cdot e^{\frac{2i\pi}{5} \times 4}$ |

| Lattice gauge theory result | | | |
|-----------------------------|---------------------------------------|--|--|
| $W_{\Sigma_{2,0}}$ | $W_{\Sigma_{2,0}}^I$ | $W_{\Sigma_{2,0}}^{A_1}$ | $W_{\Sigma_{2,0}}^{A_2}$ |
| $u = 0$ | 537 | 528 | 528 |
| $u = 1$ | $149 + 388 \cdot \cos \frac{2\pi}{5}$ | $528 \cdot e^{\frac{2i\pi}{5} \times 1}$ | $528 \cdot e^{\frac{2i\pi}{5} \times 1}$ |
| $u = 2$ | $149 + 388 \cdot \cos \frac{4\pi}{5}$ | $528 \cdot e^{\frac{2i\pi}{5} \times 2}$ | $528 \cdot e^{\frac{2i\pi}{5} \times 2}$ |
| $u = 3$ | $149 + 388 \cdot \cos \frac{4\pi}{5}$ | $528 \cdot e^{\frac{2i\pi}{5} \times 3}$ | $528 \cdot e^{\frac{2i\pi}{5} \times 3}$ |
| $u = 4$ | $149 + 388 \cdot \cos \frac{2\pi}{5}$ | $528 \cdot e^{\frac{2i\pi}{5} \times 4}$ | $528 \cdot e^{\frac{2i\pi}{5} \times 4}$ |

TABLE XIX. Comparison of the quasi-particle basis results in Table (XII) and the lattice gauge theory results, for $W_{\Sigma_{2,0}}$ with the word $w_1^{(z)}$ in Eq.(3.55).

| $W_{\Sigma_{2,0}}$ | $W_{\Sigma_{2,0}}^I$ | $W_{\Sigma_{2,0}}^{A_1}$ | $W_{\Sigma_{2,0}}^{A_2}$ |
|--------------------|---------------------------------------|--|--|
| $u = 0$ | 537 | 528 | 528 |
| $u = 1$ | $149 + 388 \cdot \cos \frac{4\pi}{5}$ | $528 \cdot e^{\frac{2i\pi}{5} \times 3}$ | $528 \cdot e^{\frac{2i\pi}{5} \times 3}$ |
| $u = 2$ | $149 + 388 \cdot \cos \frac{2\pi}{5}$ | $528 \cdot e^{\frac{2i\pi}{5} \times 1}$ | $528 \cdot e^{\frac{2i\pi}{5} \times 1}$ |
| $u = 3$ | $149 + 388 \cdot \cos \frac{2\pi}{5}$ | $528 \cdot e^{\frac{2i\pi}{5} \times 4}$ | $528 \cdot e^{\frac{2i\pi}{5} \times 4}$ |
| $u = 4$ | $149 + 388 \cdot \cos \frac{4\pi}{5}$ | $528 \cdot e^{\frac{2i\pi}{5} \times 2}$ | $528 \cdot e^{\frac{2i\pi}{5} \times 2}$ |

TABLE XX. $W_{\Sigma_{2,0}}$ with the word $w_2^{(z)}$ in Eq.(3.55), based on the lattice gauge theory calculation.

| $W_{\Sigma_{2,0}}$ | $W_{\Sigma_{2,0}}^I$ | $W_{\Sigma_{2,0}}^{A_1}$ | $W_{\Sigma_{2,0}}^{A_2}$ |
|--------------------|----------------------|---|---|
| $u = 0$ | 2377 | 1584 | 1584 |
| $u = 1$ | -533 | $1584 \cdot e^{\frac{2i\pi}{5} \times 2}$ | $1584 \cdot e^{\frac{2i\pi}{5} \times 2}$ |
| $u = 2$ | -533 | $1584 \cdot e^{\frac{2i\pi}{5} \times 4}$ | $1584 \cdot e^{\frac{2i\pi}{5} \times 4}$ |
| $u = 3$ | -533 | $1584 \cdot e^{\frac{2i\pi}{5} \times 1}$ | $1584 \cdot e^{\frac{2i\pi}{5} \times 1}$ |
| $u = 4$ | -533 | $1584 \cdot e^{\frac{2i\pi}{5} \times 3}$ | $1584 \cdot e^{\frac{2i\pi}{5} \times 3}$ |

TABLE XXI. $W_{\Sigma_{2,0}}$ with the word $w_3^{(z)}$ in Eq.(3.55), based on the lattice gauge theory calculation.

| $W_{\Sigma_{2,0}}$ | $W_{\Sigma_{2,0}}^I$ | $W_{\Sigma_{2,0}}^{A_1}$ | $W_{\Sigma_{2,0}}^{A_2}$ |
|--------------------|----------------------|---|---|
| $u = 0$ | 2377 | 1056 | 1056 |
| $u = 1$ | 437 | $1056 \cdot e^{\frac{2i\pi}{5} \times 3}$ | $1056 \cdot e^{\frac{2i\pi}{5} \times 3}$ |
| $u = 2$ | 437 | $1056 \cdot e^{\frac{2i\pi}{5} \times 1}$ | $1056 \cdot e^{\frac{2i\pi}{5} \times 1}$ |
| $u = 3$ | 437 | $1056 \cdot e^{\frac{2i\pi}{5} \times 4}$ | $1056 \cdot e^{\frac{2i\pi}{5} \times 4}$ |
| $u = 4$ | 437 | $1056 \cdot e^{\frac{2i\pi}{5} \times 2}$ | $1056 \cdot e^{\frac{2i\pi}{5} \times 2}$ |

TABLE XXII. $W_{\Sigma_{2,0}}$ with the word $w_4^{(z)}$ in Eq.(3.55), based on the lattice gauge theory calculation.

| $W_{\Sigma_{2,0}}$ | $W_{\Sigma_{2,0}}^I$ | $W_{\Sigma_{2,0}}^{A_1}$ | $W_{\Sigma_{2,0}}^{A_2}$ |
|--------------------|--------------------------------------|--|--|
| $u = 0$ | 437 | 528 | 528 |
| $u = 1$ | $49 + 388 \cdot \cos \frac{4\pi}{5}$ | $528 \cdot e^{\frac{2i\pi}{5} \times 2}$ | $528 \cdot e^{\frac{2i\pi}{5} \times 2}$ |
| $u = 2$ | $49 + 388 \cdot \cos \frac{2\pi}{5}$ | $528 \cdot e^{\frac{2i\pi}{5} \times 4}$ | $528 \cdot e^{\frac{2i\pi}{5} \times 4}$ |
| $u = 3$ | $49 + 388 \cdot \cos \frac{2\pi}{5}$ | $528 \cdot e^{\frac{2i\pi}{5} \times 1}$ | $528 \cdot e^{\frac{2i\pi}{5} \times 1}$ |
| $u = 4$ | $49 + 388 \cdot \cos \frac{4\pi}{5}$ | $528 \cdot e^{\frac{2i\pi}{5} \times 3}$ | $528 \cdot e^{\frac{2i\pi}{5} \times 3}$ |

TABLE XXIII. $W_{\Sigma_{2,0}}$ with the word $w_5^{(z)}$ in Eq.(3.55), based on the lattice gauge theory calculation.

| $W_{\Sigma_{2,0}}$ | $W_{\Sigma_{2,0}}^I$ | $W_{\Sigma_{2,0}}^{A_1}$ | $W_{\Sigma_{2,0}}^{A_2}$ |
|--------------------|---------------------------------------|--|--|
| $u = 0$ | 537 | 528 | 528 |
| $u = 1$ | $149 + 388 \cdot \cos \frac{2\pi}{5}$ | $528 \cdot e^{\frac{2i\pi}{5} \times 4}$ | $528 \cdot e^{\frac{2i\pi}{5} \times 4}$ |
| $u = 2$ | $149 + 388 \cdot \cos \frac{4\pi}{5}$ | $528 \cdot e^{\frac{2i\pi}{5} \times 3}$ | $528 \cdot e^{\frac{2i\pi}{5} \times 3}$ |
| $u = 3$ | $149 + 388 \cdot \cos \frac{4\pi}{5}$ | $528 \cdot e^{\frac{2i\pi}{5} \times 2}$ | $528 \cdot e^{\frac{2i\pi}{5} \times 2}$ |
| $u = 4$ | $149 + 388 \cdot \cos \frac{2\pi}{5}$ | $528 \cdot e^{\frac{2i\pi}{5} \times 1}$ | $528 \cdot e^{\frac{2i\pi}{5} \times 1}$ |

TABLE XXIV. $W_{\Sigma_{2,0}}$ with the word $w_6^{(z)}$ in Eq.(3.55), based on the lattice gauge theory calculation.

| $W_{\Sigma_{2,0}}$ | $W_{\Sigma_{2,0}}^I$ | $W_{\Sigma_{2,0}}^{A_1}$ | $W_{\Sigma_{2,0}}^{A_2}$ |
|--------------------|---------------------------------------|--|--|
| $u = 0$ | 537 | 528 | 528 |
| $u = 1$ | $149 + 388 \cdot \cos \frac{4\pi}{5}$ | $528 \cdot e^{\frac{2i\pi}{5} \times 2}$ | $528 \cdot e^{\frac{2i\pi}{5} \times 2}$ |
| $u = 2$ | $149 + 388 \cdot \cos \frac{2\pi}{5}$ | $528 \cdot e^{\frac{2i\pi}{5} \times 4}$ | $528 \cdot e^{\frac{2i\pi}{5} \times 4}$ |
| $u = 3$ | $149 + 388 \cdot \cos \frac{2\pi}{5}$ | $528 \cdot e^{\frac{2i\pi}{5} \times 1}$ | $528 \cdot e^{\frac{2i\pi}{5} \times 1}$ |
| $u = 4$ | $149 + 388 \cdot \cos \frac{4\pi}{5}$ | $528 \cdot e^{\frac{2i\pi}{5} \times 3}$ | $528 \cdot e^{\frac{2i\pi}{5} \times 3}$ |

TABLE XXV. $W_{\Sigma_{2,0}}$ with the word $w_7^{(z)}$ in Eq.(3.55), based on the lattice gauge theory calculation.

V. DISCUSSION AND CONCLUSION

In this work, we study in detail the representations of mapping class group of a closed genus-2 manifold $\Sigma_{2,0}$ and a punctured torus $\Sigma_{1,1}$. These data provide more information than the modular data obtained on a torus $\Sigma_{1,0}$. We use these data to construct topological invariants, which are used to distinguish the simplest counterexamples in MS MTCs that are indistinguishable by the modular data.

The mapping class group representation itself can be used to distinguish the counterexamples as well. For example, for the punctured S matrix, although containing gauge redundancy in the entries, the diagonal elements $\sum_{\mu} (S_{a,\mu;a,\mu}^{(z)})$ are gauge invariant. It is found that the diagonal elements of $S^{(z)}$ together with the modular T matrix can be used to distinguish different categories, in the sense that $\sum_{\mu} (S_{a,\mu;a,\mu}^{(z)})$ and T matrix do not transform in a consistent way as we consider the bijection of anyons between two different categories.

Furthermore, we propose a more convenient and efficient way to distinguish different MS MTCs by constructing topological invariants. These topological invariants are obtained by tracing over the ‘words’ where the ‘letters’ are representations of $MCG(\Sigma_{2,0})$ or $MCG(\Sigma_{1,1})$. With these topological invariants, there is no need to permute anyons among different categories. That is, a single number is enough to distinguish different MS MTCs.

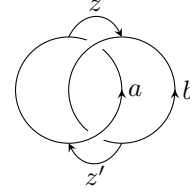
In addition, we use the lattice gauge theory approach to study the mapping class group representations of $\Sigma_{2,0}$ and $\Sigma_{1,1}$ for a general Dijkgraaf-Witten theory. This approach is practical since one only needs to input the group data and the 3-cocycle ω . This approach can in principle be used to study any counterexamples in the MS MTCs with $G = \mathbb{Z}_q \rtimes \mathbb{Z}_p$, and the only constraint is the large size of Hilbert space for large q and p . In this work, we apply this approach to the simplest counterexamples in MS MTCs with $q = 11$ and $p = 5$. The topological invariants obtained from the lattice gauge theory approach agree with those obtained from the quasi-particle basis calculation.

Comparing the two different approaches, the MCG representations may look totally different, since two different sets of basis vectors are considered, one with quasi-particle basis colored by anyons, and the other with group-element basis. However, the topological invariants (which are basis independent) constructed from these MCG representations are the same.

There are some open questions to be studied in the future. We mention a few as follows.

- There are five generators for the representations of $MCG(\Sigma_{2,0})$ in (1.1), and we only study four of them, *i.e.*, S_i and T_i ($i = 1, 2$). The fifth generator T_c corresponds to the Dehn twist along the closed curve c in (1.1). By choosing the basis vectors in (1.2), it can be found that to obtain T_c one

needs to evaluate the twice-punctured S matrix as:



(5.1)

It is straightforward to check the twice-punctured S matrix is different from the punctured S matrix in (3.30) by two F transformations. From this point of view, the twice-punctured S matrix $S^{(z,z')}$ may contain more information than the punctured S matrix $S^{(z)}$. Practically, once the fifth generator T_c is introduced, the modular relations for the five generators of $MCG(\Sigma_{2,0})$ become quite complicate.^{16,29} Solving the modular relations in the quasi-particle basis would become challenging. Nevertheless, it is still possible to calculate T_c with the lattice gauge theory approach as introduced in Sec.IV.

- We only focus on the simplest counterexamples in MS MTCs with $G = \mathbb{Z}_{11} \rtimes \mathbb{Z}_5$. It is noted there are a family of counterexamples with $G = \mathbb{Z}_q \rtimes \mathbb{Z}_p$ (p and q are primes with $p|(q - 1)$) that are indistinguishable by the modular data.¹³ It is interesting to check those counterexamples with our methods. In particular, the application of the lattice gauge theory approach to other counterexamples is straightforward, at least for the next few examples with small p and q .

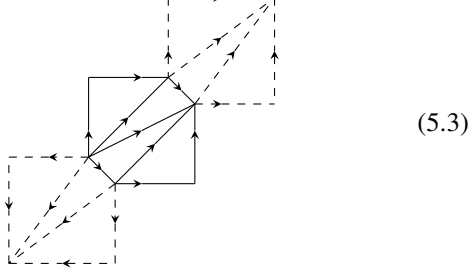
Moreover, one possible way to show that the representations of $MCG(\Sigma_{g,0})$ may distinguish *all* the MS MTCs can be considered as follows. In Ref.25, it is found that the link invariant of a Borromean ring together with T matrix are enough to distinguish all the counterexamples in MS-MTCs. If we can express the Borromean ring in terms of MCG representations of $\Sigma_{g,0}$, this will indicate that the representations of $MCG(\Sigma_{g,0})$ can distinguish all the counterexamples in MS MTCs. A nice illustration of this method for $MCG(\Sigma_{2,0})$ can be found in Ref.60, as also briefly introduced in appendix. B 3 It is found that the invariant of a figure-eight knot can be obtained by evaluating the expectation value of combinations of $MCG(\Sigma_{2,0})$ representations within a certain ground state on $\Sigma_{2,0}$.⁶⁰ On the other hand, based on a computer search, it is found that the figure-eight knot invariant together with the modular T matrix can be used to distinguish the simplest counterexamples in MS MTCs. Therefore, based on the connection of the figure-eight knot and $MCG(\Sigma_{2,0})$, one can immediately conclude that the representations of $MCG(\Sigma_{2,0})$ can be used to distinguish the simplest counterexamples in MS MTCs. Now, to distinguish *all* the MS MTCs, it is interesting to generalize this construction to the Borromean ring.

- We mainly focus on the representations of $MCG(\Sigma_{g,0})$ with $g = 2$ in this work. It is interesting to ask if there is more information contained in the representations of $MCG(\Sigma_{g,0})$ with $g > 2$. By choosing the canonical basis in the quantum Hilbert space $\mathcal{H}(\Sigma_{g,0})$ in (1.9), one can find that as g grows, there is no new structure beyond the following building block:



(5.2)

Considering the generators of $\text{MCG}(\Sigma_{g,0})$ in (3), this indicates that there will be no more information beyond the representations of $\text{MCG}(\Sigma_{3,0})$. As a remark, it is noted that the representations of $\text{MCG}(\Sigma_{g,0})$ has been studied in terms of F and R symbols in Ref.35. One can check explicitly there is no more new information for the cases of $g > 3$. In the lattice gauge theory approach, the structure in (5.2) can be studied by considering the following triangulation (with appropriate ordering of vertices)



where we take a genus-3 manifold for example. The action of Dehn twists on this basis vectors can be performed straightforwardly following the procedure in Sec.IV B, as briefly described in appendix C 2. It will be interesting to work out the details of the $\text{MCG}(\Sigma_{g,0})$ representations for MS MTCs.

– For a (twisted) quantum double of a finite group G with $\omega \in H^3(G, U(1))$, the modular S and T matrices can be constructed in terms of the group data and 3-cocycle ω (see Eqs.(2.21) and (2.13)).³⁹ It is interesting to find an explicit expression for the punctured S matrix in terms of the group data and ω , at least for the diagonal elements $\sum_{\mu} (S_{a,\mu}^{(z)}; a,\mu)$ which are gauge invariant. This question is also related to how to make a direct connection of the quasi-particle basis approach in Sec.III and the lattice gauge theory approach in Sec.IV. More explicitly, in the lattice gauge theory, it is known how to express the quasi-particle basis of the ground state on a torus $\Sigma_{1,0}$ in terms of the group-element basis.⁵³ Then one can obtain the modular S and T matrices in terms of group data and 3-cocycle ω . For the punctured torus $\Sigma_{1,1}$ or a genus-2 manifold $\Sigma_{2,0}$, it is open to us how to write the quasi-particle basis (see, e.g., 1.2) in terms of the group-element basis (see 4.36). Understanding this correspondence will help to express the $\text{MCG}(\Sigma_{g,n})$ representations in terms of the group data and 3-cocycle ω for a general twisted quantum double of a finite group G .

ACKNOWLEDGEMENT

We thank for helpful conversations and communications with Xie Chen, Liang Kong, Tian Lan, Shinsei Ryu, Peter Schauenburg, and Chenjie Wang. This research is partially supported by the Gordon and Betty Moore Foundations EPiQS initiative through Grant No. GBMF4303 at MIT (X.W.), NSF Grant No. DMR-1506475 and DMS-1664412 (X.-G.W.).

Appendix A: More on twisted quantum double of $G = \mathbb{Z}_q \rtimes_n \mathbb{Z}_p$

1. Basic property of $G = \mathbb{Z}_q \rtimes_n \mathbb{Z}_p$

In this subsection, we introduce the basic property of $G = \mathbb{Z}_q \rtimes_n \mathbb{Z}_p$, including the conjugacy class and the centralizer subgroup. Elements of G are denoted as (a^l, b^m) , with $a^q = b^p = 1, l \in \{0, 1, \dots, q-1\}, m \in \{0, 1, \dots, p-1\}$, and the multiplication is

$$(a^l, b^m) \cdot (a^{l'}, b^{m'}) = (a^l (b^m a^{l'} b^{-m}), b^{m+m'}) \\ = (a^{l+n^m l'}, b^{m+m'}), \quad (\text{A1})$$

where we have used $bab^{-1} = a^n$. The inverse of (a^l, b^m) is

$$(a^l, b^m)^{-1} = (b^{-m} a^{-l} b^m, b^{-m}) \\ = (b^{p-m} a^{q-l} b^{-(p-m)}, b^{p-m}) \quad (\text{A2}) \\ = (a^{(q-l) \cdot n^{p-m}}, b^{p-m}).$$

Then one can find the conjugate of (a^{l_0}, b^{m_0}) by (a^l, b^m) as:

$$(a^l, b^m) \cdot (a^{l_0}, b^{m_0}) \cdot (a^l, b^m)^{-1} \\ = (a^x, b^{m_0}), \quad (\text{A3})$$

where $x := l + (q-l) \cdot n^{p+m_0} + l_0 \cdot n^m$.

For the simplest case of $l_0 = m_0 = 0$, one has $x = 0 \bmod q$. That is, the conjugacy class of $1 := (a^0, b^0)$ is 1 itself.

Now let us look at the case of $l_0 \neq 0$ and $m_0 = 0$, which correspond to the conjugacy classes for type-A anyons in the main text. One has

$$(a^l, b^m) \cdot (a^{l_0}, b^0) \cdot (a^l, b^m)^{-1} = (a^x, b^0), \quad (\text{A4})$$

where $x = l + (q-l) \cdot n^p + l_0 \cdot n^m$. Since $n^p = 1 \bmod q$, then x can be simplified as

$$x = l_0 \cdot n^m \bmod q. \quad (\text{A5})$$

Then it is convenient to choose (a^l, b^0) as the representative in the corresponding conjugacy class, with $l \in \mathbb{Z}_q^{\times} / \langle n \rangle$, which is Eq.(2.9). Then the conjugacy class $[(a^l, b^0)]$ is (a^x, b^0) with $x = l \cdot n^m$, where $m = 0, 1, \dots, p-1$. Apparently, the size of conjugacy class $[(a^l, b^0)]$ is p , and the number of conjugacy classes of this type are $\frac{q-1}{p}$.

Then let us look at the case of $m_0 \neq 0$, i.e., $m \in \{1, 2, \dots, p-1\}$ in Eq.(A3). This corresponds to the conjugacy class for the type-B anyon. Let us check $l_0 = 0$ for simplicity. Then x in Eq.(A3) can be further simplified as $x := l(1 - n^{m_0}) \bmod q$. It is found that by choosing all possible l with $l \in \{0, 1, \dots, q-1\}$, x can be any value in $\{0, 1, \dots, q-1\}$. That is, the conjugacy class $[(a^l, b^m)] = \{(a^0, b^m), (a^1, b^m), \dots, (a^{q-1}, b^m)\}$. The size of conjugacy class $[(a^l, b^m)]$ is q , and the number of conjugacy classes $[(a^l, b^m)]$ with $m \neq 0$ is $p-1$, corresponding to $m = 1, 2, \dots, p-1$.

Next, let us check the centralizer subgroup of (a^{l_0}, b^{m_0}) . First, it is straightforward to see that for $l_0 = m_0 = 0$, the

corresponding centralizer subgroup is G . Then for $l_0 \neq 0$ and $m_0 = 0$, the group elements in the centralizer subgroup $\{(a^l, b^m)\}$ of (a^{l_0}, b^0) should satisfy Eq.(A4) with $x = l_0$. That is, $l_0 = l + (q-l) \cdot n^p + l_0 \cdot n^m \pmod q$. Note that $n^p = 1 \pmod q$, then one has $l_0 = l_0 \cdot n^m \pmod q$ for arbitrary l . Here m can only be chosen as $m = 0$. Therefore, the centralizer subgroup of (a^{l_0}, b^0) is $\mathbb{Z}_q = \{(a^l, b^0) | l = 0, 1, \dots, q-1\}$.

Then let us check the centralizer subgroup of (a^{l_0}, b^{m_0}) with $m_0 \neq 0$. The group elements (a^l, b^m) in the centralizer subgroup satisfy Eq.(A3) with $x = l_0$, i.e., $l_0 = l + (q-l) \cdot n^{p+m_0} + l_0 \cdot n^m \pmod q$. This can be further simplified as $l_0(1-n^m) = l(1-n^{m_0})$. Note that for the case of $l_0 = 0$, one has $l = 0$. That is, the centralizer of (a^0, b^{m_0}) is $\mathbb{Z}_p = \{(a^0, b^m) | m = 0, 1, \dots, p-1\}$. For general $l_0 \neq 0$, the centralizer of (a^{l_0}, b^{m_0}) is also an abelian group $\mathbb{Z}_p = \{(a^l, b^m) | l_0(1-n^m) = l(1-n^{m_0}), m = 0, 1, 2, \dots, p-1\}$. For arbitrary two elements (a^l, b^m) and $(a^{l'}, b^{m'})$ in the centralizer, one can check that $l(1-n^{m'}) = l'(1-n^m)$, and thus the two group elements commute with each other.

2. More on modular S matrix

In this part, we discuss more properties of the modular S -matrix. We show that for MS MTCs with $G = \mathbb{Z}_q \times \mathbb{Z}_p$, only $S_{B_{k,n}, B_{k',n}}$ depend on the 3-cocycle $\omega \in H^3(G, U(1))$. In addition, we give explicit expressions for the modular S matrix of MS MTCs with $G = \mathbb{Z}_{11} \times \mathbb{Z}_5$.

In Sec.II A, we show there are three types of anyons in MS MTCs, i.e., type- I anyons $(1, \chi_i)$, type- A anyons (a^l, χ_m) , and type- B anyons $(b^k, \tilde{\chi}_n)$. Only the characters $\tilde{\chi}$ in type- B anyons are . For the modular S matrix in Eq.(2.21), it is expressed as a combination of different characters corresponding to the types of anyons. One can find that if we require S_{ab} depends on the 3-cocycle $\omega \in H^3(G, U(1))$, at least one of a and b should be type- B anyons. With this observation, now let us check the following three cases: (1) $a = I_i$ and $b = B_{k,n}$, or $a = B_{k,n}$ and $b = I_i$; (2) $a = A_{l,m}$ and $b = B_{k,n}$, or $a = B_{k,n}$ and $b = A_{l,m}$; (3) $a = B_{k,m}$ and $b = B_{k',n}$.

For case (1), since $S_{ab} = S_{ba}$, we just need to consider $a = I_i$ and $b = B_{k,n}$. Based on Eq.(2.21), one can find that

$$S_{(1, \chi_i), (b^k, \tilde{\chi}_n)} = \frac{1}{|G|} \sum_{h \in [b^k]} (\chi_i(h))^* \cdot (\tilde{\chi}_n^h(1))^*. \quad (\text{A6})$$

From Eq.(2.18), the irreducible representation is related to the linear one as $\tilde{\chi}_n^h(x) = \chi_n(x) \cdot \epsilon_g(x)$. Here χ_n is the linear representation of \mathbb{Z}_p , and $\epsilon_g(x)$ is expressed in Eq.(2.17). One can find that $\tilde{\chi}_n^h(1) = 1$ for arbitrary $h \in [b^k]$. Therefore, we have $S_{(1, \chi_i), (b^k, \tilde{\chi}_n)} = \frac{1}{|G|} \sum_{h \in [b^k]} (\chi_i(h))^*$, which is independent of the 3-cocycle ω .

Similarly, for case (2), let us consider $a = A_{l,m}$ and $b = B_{k,n}$. One can check that for arbitrary $g \in [a^l]$ and $h \in [b^k]$, g and h will not commute with each other. This can be straightforwardly seen as follows. For $h = (a^r, b^k) \in [b^k]$, from the analysis in the previous section, if $g = (a^{l'}, b^0) \in [a^l]$ commutes with h , then one has $r(1-n^0) = l'(1-n^k)$. Since $n^k \neq 1 \pmod q$, and $l' \neq 0 \pmod q$, the above equation

cannot hold. Therefore, g and h cannot commute with each other. Then from Eq.(2.21), one can find that $S_{A_{l,m}, B_{k,n}} = 0$.

For case (3), when both indexes a and b belong to type- B anyons, S_{ab} has a very concise expression. We denote the two anyons as $(b^k, \tilde{\chi}_m)$ and $(b^{k'}, \tilde{\chi}_n)$. Recall that the conjugacy class of b^k is $[b^k] = \{(a^0, b^k), (a^1, b^k), \dots, (a^{p-1}, b^k)\}$, then for $g \in [b^k]$, there is a unique $h \in [b^{k'}]$ so that $[g, h] = 1$. Denoting $g = (a^l, b^k)$, then $h = (a^{l'}, b^{k'})$ is uniquely determined by $l(1-n^{k'}) = l'(1-n^k)$. One can find that

$$\tilde{\chi}_m^g(h) = e^{\frac{2\pi i}{p} \cdot mk'} \cdot e^{\frac{2\pi i}{p^2} kk' u}, \quad (\text{A7})$$

and

$$\tilde{\chi}_n^h(g) = e^{\frac{2\pi i}{p} \cdot nk} \cdot e^{\frac{2\pi i}{p^2} kk' u}. \quad (\text{A8})$$

Then, the modular S matrix in Eq.(2.21) can be expressed as

$$S_{(b^k, \tilde{\chi}_m), (b^{k'}, \tilde{\chi}_n)}^{(u)} = \frac{1}{|G|} \cdot q \cdot \exp\left(-\frac{2\pi i}{p^2} [2ukk' + p(kn + k'm)]\right), \\ = \frac{1}{p} \exp\left(-\frac{2\pi i}{p^2} [2ukk' + p(kn + k'm)]\right), \quad (\text{A9})$$

where we have considered $|G| = pq$. Then we obtain Eq.(2.22) in the main text.

In the following, we will focus on the simplest examples of MS MTCs with $G = \mathbb{Z}_{11} \times \mathbb{Z}_5$, and give the expression of S matrix explicitly. The simple objects are labeled as [see Eq.(3.5)]: $I_i := (1, \chi_i)$, $A_{l,m} = (a^l, \omega_{11}^m)$, and $B_{k,n} = (b^k, \tilde{\omega}_5^n)$. Here χ_i , ω_{11}^m , and $\tilde{\omega}_5^n$ represent the () irreducible representations of G , \mathbb{Z}_{11} , and \mathbb{Z}_5 , respectively. We will check S_{ab} for different cases explicitly:

- (1) $a, b \in \{I_i\}$.
- (2) $a, b \in \{A_{l,m}\}$.
- (3) $a, b \in \{B_{k,n}\}$.
- (4) $a \in \{I_i\}$ and $b \in \{A_{l,m}\}$, or $a \in \{A_{l,m}\}$ and $b \in \{I_i\}$.
- (5) $a \in \{I_i\}$ and $b \in \{B_{k,n}\}$, or $a \in \{B_{k,n}\}$ and $b \in \{I_i\}$.
- (6) $a \in \{A_{l,m}\}$ and $b \in \{B_{k,n}\}$, or $a \in \{B_{k,n}\}$ and $b \in \{A_{l,m}\}$.

The details are as follows.

(1) $a, b \in \{I_i\}$. That is, we check S_{I_i, I_j} first. Based on Eq.(2.21), one can obtain

$$S_{I_i, I_j} = \frac{1}{|G|} \chi_i^*(1) \chi_j^*(1), \quad (\text{A10})$$

where 1 is the identity group element in G . For $G = \mathbb{Z}_{11} \times \mathbb{Z}_5$, the characters are shown in Eq.(3.6). One can find that for $I_i, I_j \in \{I_1, \dots, I_5\}$, $S_{I_i, I_j} = \frac{1}{55}$; for $I_i, I_j \in \{I_6, I_7\}$, then $S_{I_i, I_j} = \frac{5 \times 5}{55} = \frac{5}{11}$. If I_i, I_j belong to $\{I_1, \dots, I_5\}$ and I_6, I_7 separately, then one has $S_{I_i, I_j} = \frac{1 \times 5}{55} = \frac{1}{11}$.

(2) $a, b \in \{A_{l,m}\}$. Now we check $S_{A_{l_1, m_1}, A_{l_2, m_2}}$, with $l_1, l_2 = 1, 2$, and $m_1, m_2 = 0, 1, \dots, 10$. The conjugacy class of $a^l := (a^l, b^0)$ is shown in Table I, and the centralizer of a^l is $\mathbb{Z}_{11} = \{a^0, a^1, \dots, a^{10}\}$. Then, based on Eq.(2.21), we have

$$S_{A_{l_1, m_1}, A_{l_2, m_2}} = \frac{1}{|G|} \sum_{\substack{a^{l'_1} \in [a^{l_1}], \\ a^{l'_2} \in [a^{l_2}]}} (\omega_{11}^{m_1}(a^{l'_1}))^* \cdot (\omega_{11}^{m_2}(a^{l'_2}))^* \quad (\text{A11})$$

where $\omega_{11}^m(a^l) = e^{\frac{2\pi i}{11}ml}$. Then $S_{A_{l_1, m_1}, A_{l_2, m_2}}$ can be further written as

$$S_{A_{l_1, m_1}, A_{l_2, m_2}} = \frac{1}{|G|} \sum_{a^{l'_1} \in [a^{l_1}], a^{l'_2} \in [a^{l_2}]} e^{-\frac{2\pi i}{11}(m_1 \cdot l'_2 + m_2 \cdot l'_1)} \quad (\text{A12})$$

There are in total 25 terms in the summation. This can be simplified in certain cases. In particular, for $m_1 = m_2 = 0$, the above formula can be simplified as $S_{A_{l_1, 0}, A_{l_2, 0}} = \frac{25}{55} = \frac{5}{11}$. If one of m_1 and m_2 is zero, say $m_1 = 0$, then one has $S_{A_{l_1, 0}, A_{l_2, m_2}} = \frac{|[a^{l'_2}]|}{|G|} \sum_{a^{l'_2} \in [a^{l_2}]} (\omega_{11}^{m_2}(a^{l'_2}))^*$.

(3) $a, b \in \{B_{k, n}\}$. The results are obtained in Eq.(A9). For $G = \mathbb{Z}_{11} \rtimes \mathbb{Z}_5$, one has

$$S_{(b^k, \bar{x}_m), (b^{k'}, \bar{x}_n)} = \frac{1}{5} \exp\left(-\frac{2\pi i}{25}[2ukk' + 5(kn + k'm)]\right), \quad (\text{A13})$$

where $u = 0, 1, 2, 3, 4$.

(4) $a \in \{I_i\}$ and $b \in \{A_{l, m}\}$, or $a \in \{A_{l, m}\}$ and $b \in \{I_i\}$.

We consider the case of $a \in \{I_i\}$ and $b \in \{A_{l, m}\}$, and the later case can be obtained based on the symmetric property of modular S matrix, *i.e.*, $S_{ab} = S_{ba}$. One can find

$$S_{(1, \chi_i), (a^l, \omega_{11}^m)} = \frac{1}{|G|} \sum_{h \in [a^l]} \chi_i^*(h), \quad (\text{A14})$$

where we have considered $\omega_{11}^m(1) = 1$. If $I_i = I_0, I_1, I_2, I_3$ or I_4 , then $\chi_i([a^l]) = 1$, and the S matrix can be simplified as $S_{I_i, A_{l, m}} = \frac{1}{11}$. If $I_i = I_5, I_6$, then from the character table in Eq.(3.6), one can obtain $S_{I_5, A_{l, m}} = S_{I_6, A_{l, m}} = \frac{1}{11}\sigma^*$, and $S_{I_5, A_{2, m}} = S_{I_6, A_{1, m}} = \frac{1}{11}\sigma$, where $\sigma = e^{\frac{2\pi i}{11}3} + e^{\frac{2\pi i}{11}4} + e^{\frac{2\pi i}{11}5} + e^{\frac{2\pi i}{11}9}$.

(5) $a \in \{I_i\}$ and $b \in \{B_{k, n}\}$, or $a \in \{B_{k, n}\}$ and $b \in \{I_i\}$. Let us consider $a \in \{I_i\}$ and $b \in \{B_{k, n}\}$. Then based on Eq.(2.21), one can find that

$$S_{(1, \chi_i), (b^k, \tilde{\omega}_5^n)} = \frac{1}{|G|} \sum_{h \in [b^k]} \chi_i(h) \cdot \tilde{\omega}_5^n(1) = \frac{1}{|G|} \sum_{h \in [b^k]} \chi_i(h), \quad (\text{A15})$$

where we have considered the fact that $\tilde{\omega}_5(1) = 1$. In particular, for $I_i = I_5, I_6$, from the character table in Eq.(3.6), one can find that $\chi_i([b^k]) = 0$, and then $S_{I_i, B_{k, n}} = 0$. For $I_i = I_0$, one has $\chi_0([b^k]) = 1$, and then $S_{I_0, B_{k, n}} = \frac{1}{5}$. For $I_j = I_1, I_2, I_3, I_4$, one has $\chi_j([b^k]) = e^{\frac{2\pi i}{5} \cdot j \cdot k}$. Then the S matrix has the form $S_{I_j, B_{k, n}} = S_{B_{k, n}, I_j} = \frac{1}{5} e^{-\frac{2\pi i}{5} \cdot j \cdot k}$.

(6) $a \in \{A_{l, m}\}$ and $b \in \{B_{k, n}\}$, or $a \in \{B_{k, n}\}$ and $b \in \{A_{l, m}\}$. Let us consider the case of $a \in \{A_{l, m}\}$ and $b \in \{B_{k, n}\}$. One can find that for arbitrary $g \in [a^l]$ and $h \in [b^k]$ in Eq.(2.21), they do not communicate with each other. Then we have $S_{A_{l, m}, B_{k, n}} = 0$. In fact, this result applies to an arbitrary $G = \mathbb{Z}_q \rtimes \mathbb{Z}_p$ in MS MTCs.

As a short summary, only $S_{(b^k, \bar{x}_m), (b^{k'}, \bar{x}_n)}$ depend on the equivalent cohomology class u . Other components of the modular S matrix are determined by the finite group G itself.

Appendix B: On algebraic theory of anyons and others

In this appendix, we introduce some notions and conventions on algebraic theory of anyons that are necessary for studying the punctured S and T matrices, as well as the topological invariants in the main text. A more complete description of the algebraic theory of anyons can be found, *e.g.*, in Refs.10, 16, and 26. We also introduce other choices of quasi-particle basis in $\mathcal{H}(\Sigma_{g,0})$, and express the representation of $\text{MCG}(\Sigma_{g,0})$ in terms of F and R matrices.

We assign a fusion vector space V_{ab}^c to each fusion product of two anyons $a \times b = \sum_c N_{ab}^c c$. The dual space, also called ‘splitting space’, is denoted as V_c^{ab} . The numbers $N_{ab}^c = \dim(V_{ab}^c) = \dim(V_c^{ab})$ are called fusion multiplicities. If N_{ab}^c are equal to 0 or 1, we will call such fusion rules multiplicity free. The orthonormal basis vectors $|a, b, c, \mu\rangle \in V_c^{ab}$ and $\langle a, b, c, \mu| \in V_{ab}^c$ can be diagrammatically expressed as

$$\begin{aligned} (d_c/d_a d_b)^{1/4} \begin{array}{c} a \quad b \\ \diagdown \quad \diagup \\ \mu \\ \uparrow \\ c \end{array} &= |a, b, c, \mu\rangle \in V_c^{ab}, \\ (d_c/d_a d_b)^{1/4} \begin{array}{c} c \\ \uparrow \\ \mu \\ \diagdown \quad \diagup \\ a \quad b \end{array} &= \langle a, b, c, \mu| \in V_{ab}^c, \end{aligned} \quad (\text{B1})$$

where the normalization factor $(d_c/d_a d_b)^{1/4}$ is introduced so that diagrams are in the isotopy invariant convention.^{10,26}

In Eq.(3.38) in the main text, we use the operation of R move, which describes the braiding of two anyons. The braiding operations of pairs of anyons can be expressed as^{10,16,26}

$$R_{ab} = \begin{array}{c} \diagdown \quad \diagup \\ a \quad b \end{array}, \quad R_{ab}^{-1} = R_{ab}^\dagger = \begin{array}{c} \diagup \quad \diagdown \\ b \quad a \end{array}. \quad (\text{B2})$$

By acting on the basis vectors in Eq.(B1), we have

$$\begin{aligned} R_{ab}|a, b, c, \mu\rangle &= \sum_\nu [R_c^{ab}]_{\mu\nu} |b, a, c, \nu\rangle, \\ R_{ab}^{-1}|b, a, c, \mu\rangle &= \sum_\nu [R_c^{ab}]_{\mu\nu}^{-1} |a, b, c, \nu\rangle, \end{aligned} \quad (\text{B3})$$

which are represented diagrammatically as

$$\begin{array}{c} b \quad a \\ \diagdown \quad \diagup \\ \mu \\ \uparrow \\ c \end{array} = R_{ab} \begin{array}{c} a \quad b \\ \diagdown \quad \diagup \\ \mu \\ \uparrow \\ c \end{array} = \sum_\nu (R_c^{ab})_{\mu\nu} \begin{array}{c} b \quad a \\ \diagdown \quad \diagup \\ \nu \\ \uparrow \\ c \end{array}, \quad (\text{B4})$$

and

$$\begin{array}{c} a \quad b \\ \diagdown \quad \diagup \\ \mu \\ \uparrow \\ c \end{array} = R_{ab}^{-1} \begin{array}{c} b \quad a \\ \diagdown \quad \diagup \\ \mu \\ \uparrow \\ c \end{array} = \sum_\nu (R_c^{ab})_{\mu\nu}^{-1} \begin{array}{c} a \quad b \\ \diagdown \quad \diagup \\ \nu \\ \uparrow \\ c \end{array}. \quad (\text{B5})$$

The R matrices satisfy the so-called ribbon property:

$$\sum_\lambda [R_c^{ab}]_{\mu\lambda} [R_c^{ba}]_{\lambda, \nu} = \frac{\theta_c}{\theta_a \theta_b} \delta_{\mu, \nu}. \quad (\text{B6})$$

Another useful quantity is the so-called F matrix, or F -symbol, defined as

$$\begin{array}{c} a & b & c \\ & \nearrow & \nearrow \\ & \alpha & e \\ & \searrow & \searrow \\ & \beta & d \end{array} = \sum_{f,\mu,\nu} [F_d^{abc}]_{(e,\alpha,\beta),(f,\mu,\nu)} \begin{array}{c} a & b & c \\ & \nearrow & \nearrow \\ & f & \mu \\ & \searrow & \searrow \\ & \nu & d \end{array} \quad (\text{B7})$$

where α, β, μ and ν denote the fusion channels. As will be seen later, F -symbol will be used in expressing the representation for MCG($\Sigma_{g,0}$) in Sec.B2. We may use F, R symbols and F, R matrices interchangeably. The F and R symbols satisfy consistency conditions called Pentagon and Hexagon equations.¹⁰ In certain cases, it is useful to consider the following F transformation:

$$\begin{array}{c} a & b \\ & \nearrow & \nearrow \\ & e & \\ & \searrow & \searrow \\ c & & d \end{array} = \sum_{f,\mu,\nu} [F_{cd}^{ab}]_{(e,\alpha,\beta),(f,\mu,\nu)} \begin{array}{c} a & b \\ & \nearrow & \nearrow \\ & f & \mu \\ & \searrow & \searrow \\ c & & d \end{array} \quad (\text{B8})$$

where

$$[F_{cd}^{ab}]_{(e,\alpha,\beta),(f,\mu,\nu)} = \sqrt{\frac{d_e d_f}{d_a d_d}} [F_f^{ceb}]_{(a,\alpha,\mu),(d,\beta,\nu)}^* \quad (\text{B9})$$

In the following are some relations we will use in Sec.III in the main text.

$$\begin{array}{c} a & b \\ & \nearrow & \nearrow \\ & & \\ & \searrow & \searrow \\ a & & b \end{array} = \sum_{c,\mu} \sqrt{\frac{d_c}{d_a d_b}} \begin{array}{c} a & b \\ & \nearrow & \nearrow \\ & c & \mu \\ & \searrow & \searrow \\ a & & b \end{array} \quad (\text{B10})$$

Based on Eqs.(B10) and (B4), one may express R_{ab} in Eq.(B2) as

$$R_{ab} = \sum_{c,\mu,\nu} \sqrt{\frac{d_c}{d_a d_b}} [R_c^{ab}]_{\mu\nu} \begin{array}{c} b & \\ & \nearrow & \nearrow \\ & \nu & \\ & \searrow & \searrow \\ a & & \mu & \\ & & & \searrow \\ & & & b \end{array} \quad (\text{B11})$$

In addition, we have

$$\begin{array}{c} c' \\ & \nearrow & \nearrow \\ a & & b \\ & \searrow & \searrow \\ & \mu' & \\ & & c \end{array} = \delta_{c,c'} \delta_{\mu,\mu'} \sqrt{\frac{d_a d_b}{d_c}} \begin{array}{c} c \\ & \nearrow & \nearrow \\ & & \\ & \searrow & \searrow \\ & & c \end{array} \quad (\text{B12})$$

$$\frac{1}{\mathcal{D}^2} \sum_a d_a \begin{array}{c} x & y \\ & \nearrow & \nearrow \\ & & \\ & \searrow & \searrow \\ x & & y \end{array} a = \frac{1}{d_x} \delta_{x,\bar{y}} \begin{array}{c} x & y \\ & \nearrow & \nearrow \\ & 1 & \\ & \searrow & \searrow \\ x & & y \end{array} \quad (\text{B13})$$

where the dashed line indicates the world line of the identity anyon 1. One may not be confused with the simple currents I_k in Eq.(3.21) in the main text.

It is also useful to introduce the ω loop, which is defined as⁶¹

$$\omega_z = \omega_{\bar{z}} = \sum_x S_{0z} S_{zx}^* \begin{array}{c} \circlearrowleft \\ x \end{array} \quad (\text{B14})$$

For a modular tensor category, in which the modular S matrix is unitary, one can find that the ω loop acts as a projector on the total charge of anyons that go through the ω loop. For example, we have

$$\begin{array}{c} a \\ & \nearrow \\ & \omega_z \\ & \searrow \\ a \end{array} = \sum_x S_{0z} S_{zx}^* \begin{array}{c} a \\ & \nearrow \\ & x \\ & \searrow \\ a \end{array} = \delta_{za} \begin{array}{c} a \\ | \\ a \end{array} \quad (\text{B15})$$

where in the last step we have used Eq.(3.26) and the unitarity property of modular S matrix. Similarly, one can find that

$$\begin{array}{c} a & b \\ & \nearrow & \nearrow \\ & & \\ & \searrow & \searrow \\ a & & b \end{array} \omega_z = \sum_x S_{0z} S_{zx}^* \begin{array}{c} a & b \\ & \nearrow & \nearrow \\ & & \\ & \searrow & \searrow \\ a & & b \end{array} x = \sum_\mu \sqrt{\frac{d_z}{d_a d_b}} \begin{array}{c} a & b \\ & \nearrow & \nearrow \\ & z & \mu \\ & \searrow & \searrow \\ a & & b \end{array} \quad (\text{B16})$$

where we have used Eqs.(B10) and (B15). Eq.(B16) will be used to remove the vertex structures in $\sum_\mu S_{a,\mu;a,\mu}^{(z)}$ and the words introduced in Eq.(3.55).

One useful formula in proving the modular relations is $\sum_a d_a \theta_a S_{a\bar{x}} = \frac{1}{\mathcal{D}} \sum_{a,y} d_a \theta_a N_{ax}^y \frac{\theta_y}{\theta_a \theta_x} d_y = \frac{1}{\mathcal{D}} \sum_y d_y^2 \theta_y \cdot d_x \theta_x^* = \Theta d_x \theta_x^*$, where we used the fact that $S_{ab} = \frac{1}{\mathcal{D}} \sum_c N_{ab}^c \frac{\theta_c}{\theta_a \theta_b} d_c$, and $\Theta := \mathcal{D}^{-1} \sum_a d_a^2 \theta_a$ is a phase factor. For the MS MTCs we are interested in here, one can check that $\Theta = 1$. Nevertheless, we will keep the phase factor Θ in the following discussion. Diagrammatically, one has

$$\frac{1}{\mathcal{D}} \sum_a d_a \theta_a \begin{array}{c} x \\ & \nearrow \\ & a \\ & \searrow \\ x \end{array} = \Theta \begin{array}{c} x \\ | \\ x \end{array} \quad (\text{B17})$$

It can be generalized to the following case:

$$\frac{1}{\mathcal{D}} \sum_a d_a \theta_a \begin{array}{c} x & y \\ & \nearrow & \nearrow \\ & & \\ & \searrow & \searrow \\ x & & y \end{array} a = \Theta \begin{array}{c} x & y \\ & \nearrow & \nearrow \\ & & \\ & \searrow & \searrow \\ x & & y \end{array} = \Theta \cdot \theta_x^* \theta_y^* \begin{array}{c} x & y \\ & \nearrow & \nearrow \\ & & \\ & \searrow & \searrow \\ x & & y \end{array} \quad (\text{B18})$$

1. Properties of punctured S matrix

Based on the fusion and braiding of anyons introduced above, now we are ready to discuss the properties of punctured S matrix. The punctured S matrix is defined through

the following action:

$$S^{(z)} \begin{array}{c} b \\ \swarrow \\ \mu \\ \uparrow \\ b \end{array} \begin{array}{c} z \\ \nearrow \\ \mu \\ \downarrow \\ a \end{array} := \frac{1}{\mathcal{D}} \sum_a d_a \begin{array}{c} a \\ \uparrow \\ \mu \\ \downarrow \\ a \end{array} \begin{array}{c} z \\ \nearrow \\ \mu \\ \downarrow \\ b \end{array}. \quad (\text{B19})$$

Similarly, for $(S^{(z)})^\dagger$, we have

$$(S^{(z)})^\dagger \begin{array}{c} b \\ \swarrow \\ \mu \\ \uparrow \\ b \end{array} \begin{array}{c} z \\ \nearrow \\ \mu \\ \downarrow \\ a \end{array} := \frac{1}{\mathcal{D}} \sum_a d_a \begin{array}{c} a \\ \uparrow \\ \mu \\ \downarrow \\ a \end{array} \begin{array}{c} z \\ \nearrow \\ \mu \\ \downarrow \\ b \end{array}. \quad (\text{B20})$$

Then the the unitarity property of $S^{(z)}$ can be shown as follows.

$$\begin{aligned} (S^{(z)})^\dagger S^{(z)} \begin{array}{c} b \\ \swarrow \\ \mu \\ \uparrow \\ b \end{array} \begin{array}{c} z \\ \nearrow \\ \mu \\ \downarrow \\ a \end{array} &= \frac{1}{\mathcal{D}^2} \sum_{x,a} d_x d_a \begin{array}{c} x \\ \uparrow \\ \mu \\ \downarrow \\ x \end{array} \begin{array}{c} z \\ \nearrow \\ \mu \\ \downarrow \\ a \end{array} \\ &= \sum_x \delta_{xb} \begin{array}{c} x \\ \swarrow \\ \mu \\ \uparrow \\ x \end{array} \begin{array}{c} z \\ \nearrow \\ \mu \\ \downarrow \\ b \end{array}, \end{aligned} \quad (\text{B21})$$

where we used Eq.(B13) in the last second step. Similarly, for $S^{(z)}(S^{(z)})^\dagger$, we have

$$\begin{aligned} S^{(z)}(S^{(z)})^\dagger \begin{array}{c} b \\ \swarrow \\ \mu \\ \uparrow \\ b \end{array} \begin{array}{c} z \\ \nearrow \\ \mu \\ \downarrow \\ a \end{array} &= \frac{1}{\mathcal{D}^2} \sum_{x,a} d_x d_a \begin{array}{c} x \\ \uparrow \\ \mu \\ \downarrow \\ x \end{array} \begin{array}{c} z \\ \nearrow \\ \mu \\ \downarrow \\ a \end{array} \\ &= \sum_x \delta_{xb} \begin{array}{c} x \\ \swarrow \\ \mu \\ \uparrow \\ x \end{array} \begin{array}{c} z \\ \nearrow \\ \mu \\ \downarrow \\ b \end{array}. \end{aligned} \quad (\text{B22})$$

Therefore, we have $(S^{(z)})^\dagger S^{(z)} = S^{(z)}(S^{(z)})^\dagger = 1$.

Next, we prove the modular relations in Eq.(3.33). Let us prove $(S^{(z)})^2 = C^{(z)}$ first. By acting $(S^{(z)})^2$ on the basis vector, one has

$$\begin{aligned} (S^{(z)})^2 \begin{array}{c} b \\ \swarrow \\ \mu \\ \uparrow \\ b \end{array} \begin{array}{c} z \\ \nearrow \\ \mu \\ \downarrow \\ a \end{array} &= \frac{1}{\mathcal{D}^2} \sum_{x,a} d_x d_a \begin{array}{c} x \\ \uparrow \\ \mu \\ \downarrow \\ x \end{array} \begin{array}{c} z \\ \nearrow \\ \mu \\ \downarrow \\ a \end{array} \\ &= \frac{1}{\mathcal{D}^2} \sum_{x,a} d_x d_a \theta_x^* \begin{array}{c} x \\ \swarrow \\ \mu \\ \uparrow \\ x \end{array} \begin{array}{c} z \\ \nearrow \\ \mu \\ \downarrow \\ a \end{array} \\ &= \sum_x \delta_{x,\bar{b}} \theta_x^* \begin{array}{c} x \\ \swarrow \\ \mu \\ \uparrow \\ x \end{array} \begin{array}{c} z \\ \nearrow \\ \mu \\ \downarrow \\ \bar{b} \end{array} = \theta_{\bar{b}}^* \begin{array}{c} \bar{b} \\ \swarrow \\ \mu \\ \uparrow \\ \bar{b} \end{array} \begin{array}{c} z \\ \nearrow \\ \mu \\ \downarrow \\ \bar{b} \end{array}, \end{aligned} \quad (\text{B23})$$

where we have considered the fact $\theta_b = \theta_{\bar{b}}$. Comparing (B23) with the definition of $C^{(z)}$ in Eq.(3.36), one can find that $(S^{(z)})^2 = C^{(z)}$.

Then, to prove $(S^{(z)})^4 = (C^{(z)})^2 = \theta_z^*$, since we have already proved that $(S^{(z)})^2 = C^{(z)}$, we only need to show $(C^{(z)})^2 = \theta_z^*$. Based on the definition of $C^{(z)}$ in Eq.(3.36), one can find that

$$(C^{(z)})^2 \begin{array}{c} b \\ \swarrow \\ \mu \\ \uparrow \\ b \end{array} \begin{array}{c} z \\ \nearrow \\ \mu \\ \downarrow \\ a \end{array} = (\theta_b^*)^2 \begin{array}{c} b \\ \swarrow \\ \mu \\ \uparrow \\ b \end{array} \begin{array}{c} z \\ \nearrow \\ \mu \\ \downarrow \\ a \end{array} = \theta_z^* \begin{array}{c} b \\ \swarrow \\ \mu \\ \uparrow \\ b \end{array} \begin{array}{c} z \\ \nearrow \\ \mu \\ \downarrow \\ a \end{array} \quad (\text{B24})$$

where in the last step we have used the ribbon property in Eq.(B6).

Next, we give the proof of $(S^{(z)}T^{(z)})^3 = \Theta(S^{(z)})^2$ in Eq.(3.33):

$$\begin{aligned} (S^{(z)}T^{(z)})^3 \begin{array}{c} b \\ \swarrow \\ \mu \\ \uparrow \\ b \end{array} \begin{array}{c} z \\ \nearrow \\ \mu \\ \downarrow \\ a \end{array} &= \frac{1}{\mathcal{D}^3} \sum_{x,a} d_y d_x d_a \theta_x \theta_a \theta_b \begin{array}{c} y \\ \uparrow \\ \mu \\ \downarrow \\ y \end{array} \begin{array}{c} z \\ \nearrow \\ \mu \\ \downarrow \\ a \end{array} \\ &= \frac{1}{\mathcal{D}^3} \sum_{x,a} \theta_y^* d_y d_x d_a \theta_x \theta_a \theta_b \begin{array}{c} y \\ \swarrow \\ \mu \\ \uparrow \\ y \end{array} \begin{array}{c} z \\ \nearrow \\ \mu \\ \downarrow \\ a \end{array} \end{aligned} \quad (\text{B25})$$

Now we sum over x by using Eq.(B18). Then the above equation can be simplified as

$$\begin{aligned} (S^{(z)}T^{(z)})^3 \begin{array}{c} b \\ \swarrow \\ \mu \\ \uparrow \\ b \end{array} \begin{array}{c} z \\ \nearrow \\ \mu \\ \downarrow \\ a \end{array} &= \frac{1}{\mathcal{D}^2} \sum_{a,y} \Theta \cdot \theta_y^* d_y d_a \theta_a \theta_b (\theta_y^* \theta_a^*) \begin{array}{c} y \\ \swarrow \\ \mu \\ \uparrow \\ y \end{array} \begin{array}{c} z \\ \nearrow \\ \mu \\ \downarrow \\ a \end{array} \\ &= \Theta \cdot \sum_y \delta_{y,\bar{b}} \theta_y^* \theta_b \theta_y^* \begin{array}{c} y \\ \swarrow \\ \mu \\ \uparrow \\ y \end{array} \begin{array}{c} z \\ \nearrow \\ \mu \\ \downarrow \\ \bar{b} \end{array} = \Theta \cdot \theta_{\bar{b}}^* \begin{array}{c} \bar{b} \\ \swarrow \\ \mu \\ \uparrow \\ \bar{b} \end{array} \begin{array}{c} z \\ \nearrow \\ \mu \\ \downarrow \\ \bar{b} \end{array}, \end{aligned} \quad (\text{B26})$$

where in the last second step we have summed over a by using Eq.(B13). By comparing with Eq.(B23), one can find that $(S^{(z)}T^{(z)})^3 = \Theta(S^{(z)})^2$.

Similar to $S^{(z)}$, which corresponds to the S transformation of a punctured torus, one can generalize to the case of a torus with more than one punctures. For example, for a torus with two punctures, the corresponding twice-punctured S matrix

can be defined as

$$S^{(z_1, z_2)} := \frac{1}{\mathcal{D}} \sum_a d_a \begin{array}{c} \text{diagram} \end{array} \quad (\text{B27})$$

On the other hand, by using F -move and once-punctured S transformation, one has

$$\begin{array}{c} \text{diagram} \\ \text{diagram} \end{array} \xrightarrow{F} \begin{array}{c} \text{diagram} \\ \text{diagram} \end{array} \xrightarrow{S^{(w)}} \begin{array}{c} \text{diagram} \\ \text{diagram} \end{array} \quad (\text{B28})$$

By comparing Eqs.(B27) and (B28), one can find that the twice-punctured S -matrix and once-punctured S -matrix are related through the F -move as follows:

$$S^{(z_1, z_2)} = F \cdot S^{(w)} \cdot F^{-1}, \quad (\text{B29})$$

where we have neglected the indices of punctured S matrix and F symbols for brevity.

Based on the F moves, one can find the procedure above also applies to a multi-punctured S matrix. That is, a multi-punctured S matrix is related to the single-punctured S matrix through F moves.

a. Other punctured S matrices

In the main text, we have seen that the (gauge invariant) diagonal elements of certain $S^{(z)}$ can be used to distinguish different categories. In this subsection, we present the following two results on the punctured S matrix. (i) We summarize how $S_{B_{i,j}, B_{i,j}}^{(z)}$ are mapped between \mathcal{C}_u and $\mathcal{C}_{u'}$. We will consider $u = 1$ and $u' = 4$ for example, and the mapping between $\mathcal{C}_{u=2}$ and $\mathcal{C}_{u'=3}$ is similar. (ii) Not all punctured S matrices can distinguish different categories.

(i) *Mapping of $S_{B_{i,j}, B_{i,j}}^{(z)}$ between $\mathcal{C}_{u=1}$ and $\mathcal{C}_{u'=4}$.*

It is interesting that all the diagonal elements $S_{B_{i,j}, B_{i,j}}^{(z), u=1}$ can be mapped to $S_{B_{i',j'}, B_{i',j'}}^{(z'), u=4}$ by permuting anyons. This permutation is different from that of the modular T matrix in two aspects: (i) For $S^{(z)}$, we need to permute the anyons z in $\mathcal{C}_{u=1}$ to z' in $\mathcal{C}_{u'=4}$ where $\theta_z \neq \theta_{z'}$. For the T matrix, one can only permute anyons that have the same topological spin. (ii) Even for the permutation of type- B anyons in $S_{B_{i,j}, B_{i,j}}^{(z)}$, the permutations are different from that of T matrix. This is used to distinguish different categories in Sec.III C in the main text. The mappings from $S_{B_{i,j}, B_{i,j}}^{(z), u=1}$ to $S_{B_{i',j'}, B_{i',j'}}^{(z'), u=4}$ are summarized in Table XXVI.

| $u = 1$ | $u = 4$ |
|--|---|
| $S_{B_{1(4),i}, B_{1(4),i}}^{A_{1,1}(A_{2,6})}$ | $S_{B_{2(3),j}, B_{2(3),j}}^{A_{1,9}(A_{2,10})}$ |
| $S_{B_{2(3),i}, B_{2(3),i}}^{A_{1,1}(A_{2,6})}$ | $S_{B_{1(4),j}, B_{1(4),j}}^{A_{1,5}(A_{2,8})}$ |
| $S_{B_{1(4),i}, B_{1(4),i}}^{A_{1,2}(A_{2,1})}$ | $S_{B_{2(3),j}, B_{2(3),j}}^{A_{1,7}(A_{2,9})}$ |
| $S_{B_{2(3),i}, B_{2(3),i}}^{A_{1,2}(A_{2,1})}$ | $S_{B_{1(4),j}, B_{1(4),j}}^{B_{2(3),j}, B_{2(3),j}}$ |
| $S_{B_{1(4),i}, B_{1(4),i}}^{A_{1,3}(A_{2,7})}$ | $S_{B_{1(4),j}, B_{1(4),j}}^{A_{1,10}(A_{2,5})}$ |
| $S_{B_{2(3),i}, B_{2(3),i}}^{A_{1,3}(A_{2,7})}$ | $S_{B_{1(4),j}, B_{1(4),j}}^{A_{1,5}(A_{2,8})}$ |
| $S_{B_{1(4),i}, B_{1(4),i}}^{A_{1,4}(A_{2,2})}$ | $S_{B_{2(3),j}, B_{2(3),j}}^{A_{1,4}(A_{2,2})}$ |
| $S_{B_{2(3),i}, B_{2(3),i}}^{A_{1,4}(A_{2,2})}$ | $S_{B_{1(4),j}, B_{1(4),j}}^{A_{1,4}(A_{2,2})}$ |
| $S_{B_{1(4),i}, B_{1(4),i}}^{A_{1,5}(A_{2,8})}$ | $S_{B_{2(3),j}, B_{2(3),j}}^{A_{1,3}(A_{2,7})}$ |
| $S_{B_{2(3),i}, B_{2(3),i}}^{A_{1,5}(A_{2,8})}$ | $S_{B_{1(4),j}, B_{1(4),j}}^{A_{1,9}(A_{2,10})}$ |
| $S_{B_{1(4),i}, B_{1(4),i}}^{A_{1,6}(A_{2,3})}$ | $S_{B_{2(3),j}, B_{2(3),j}}^{A_{1,10}(A_{2,5})}$ |
| $S_{B_{2(3),i}, B_{2(3),i}}^{A_{1,6}(A_{2,3})}$ | $S_{B_{1(4),j}, B_{1(4),j}}^{B_{2(3),j}, B_{2(3),j}}$ |
| $S_{B_{1(4),i}, B_{1(4),i}}^{A_{1,7}(A_{2,9})}$ | $S_{B_{1(4),j}, B_{1(4),j}}^{A_{1,8}(A_{2,4})}$ |
| $S_{B_{2(3),i}, B_{2(3),i}}^{A_{1,7}(A_{2,9})}$ | $S_{B_{1(4),j}, B_{1(4),j}}^{A_{1,8}(A_{2,4})}$ |
| $S_{B_{1(4),i}, B_{1(4),i}}^{A_{1,8}(A_{2,4})}$ | $S_{B_{2(3),j}, B_{2(3),j}}^{A_{1,2}(A_{2,1})}$ |
| $S_{B_{2(3),i}, B_{2(3),i}}^{A_{1,8}(A_{2,4})}$ | $S_{B_{1(4),j}, B_{1(4),j}}^{A_{1,7}(A_{2,9})}$ |
| $S_{B_{1(4),i}, B_{1(4),i}}^{A_{1,9}(A_{2,10})}$ | $S_{B_{2(3),j}, B_{2(3),j}}^{A_{1,6}(A_{2,3})}$ |
| $S_{B_{2(3),i}, B_{2(3),i}}^{A_{1,9}(A_{2,10})}$ | $S_{B_{1(4),j}, B_{1(4),j}}^{B_{2(3),j}, B_{2(3),j}}$ |
| $S_{B_{1(4),i}, B_{1(4),i}}^{A_{1,10}(A_{2,5})}$ | $S_{B_{1(4),j}, B_{1(4),j}}^{A_{1,1}(A_{2,6})}$ |
| $S_{B_{2(3),i}, B_{2(3),i}}^{A_{1,10}(A_{2,5})}$ | $S_{B_{1(4),j}, B_{1(4),j}}^{A_{1,4}(A_{2,2})}$ |
| | $S_{B_{2(3),j}, B_{2(3),j}}^{A_{1,2}(A_{2,1})}$ |
| | $S_{B_{1(4),j}, B_{1(4),j}}^{A_{1,6}(A_{2,3})}$ |

TABLE XXVI. Mapping of the diagonal elements of $S^{(z)}$ between $\mathcal{C}_{u=1}$ and $\mathcal{C}_{u'=4}$. The concrete values of $S_{B_{i,j}, B_{i,j}}^{(z)}$ and the indices $i, j \in \{0, \dots, 4\}$ can be found in online materials.⁴⁷

More explicitly, in the first row of Table XXVI, the mapping between diagonal elements $S_{B_{1,i}, B_{1,i}}^{A_{1,1}}$ in $\mathcal{C}_{u=1}$ and $S_{B_{2,j}, B_{2,j}}^{A_{1,9}}$ in $\mathcal{C}_{u=4}$ means by considering the bijection of anyons $A_{1,1}^{(u=1)} \leftrightarrow A_{1,9}^{(u=4)}$, $B_{1,i}^{(u=1)} \leftrightarrow B_{2,j}^{(u=4)}$, $S_{B_{1,i}, B_{1,i}}^{A_{1,1}}$ in $\mathcal{C}_{u=1}$ can be sent to $S_{B_{2,j}, B_{2,j}}^{A_{1,9}}$ in $\mathcal{C}_{u=4}$, and vice versa. The mappings are similar for other diagonal elements in Table XXVI. The concrete values of $S_{B_{i,j}, B_{i,j}}^{(z)}$ and the indices $i(j)$ can be found in online materials.⁴⁷

(ii) *$S^{(z)}$ that cannot distinguish different categories.*

It is noted that not all punctured S matrices (together with the modular T matrix) can be used to distinguish different categories. This is as expected for $z = I_i$ with $i = 1, \dots, 4$. In this case, based on the fusion rules in Sec.III A, one can find that only type- I and type- A anyons are involved in $S^{(z)}$. Recalling that only type- B anyons carry the information of 3-cocycle ω^u , then $S^{(z)}$ with $z = I_i$ will be independent of u .

Here we want to emphasize that even for certain z which are type- A anyons, $S^{(z)}$ and T matrices may still not be enough to distinguish different categories. For example, let us consider $z = A_{1,0} (A_{2,0})$ in $\mathcal{C}_{u=1}$ and $\mathcal{C}_{u=4}$ categories.

For convenience, we write down the topological spins de-

two bases in (3.1) and (3.2) as $|\psi_{ab;z}^I\rangle$ and $|\psi_{ab;z}^{II}\rangle$, where we consider the case of multiplicity free for simplicity. Then one has

$$|\psi_{ab;z}^I\rangle = \sum_{z'} [F_{b\bar{a}}^{b\bar{a}}]_{(z,z')} |\psi_{ab;z'}^{II}\rangle, \quad (\text{B34})$$

with the F matrix defined in Eq.(B8). Then the overlap of two sets of basis vectors are $\langle \psi_{ab;z'}^{II} | \psi_{ab;z}^I \rangle = [F_{b\bar{a}}^{b\bar{a}}]_{(z,z')}$. Noting that the action of T_c on the basis $|\psi_{ab;z'}^{II}\rangle$ simply results in a phase, *i.e.*, $T_c |\psi_{ab;z'}^{II}\rangle = \theta_{z'} |\psi_{ab;z'}^{II}\rangle$, then transforming back to basis I, we have

$$\hat{T}_c |\psi_{ab;z}^I\rangle = \sum_{z',z''} [F_{b\bar{a}}^{b\bar{a}}]_{(z,z')} \cdot \theta_{z'} \cdot [F_{b\bar{a}}^{b\bar{a}}]_{(z',z'')}^{-1} |\psi_{ab;z''}^I\rangle. \quad (\text{B35})$$

Then the Dehn twist representation T_c in the basis in (1.2) has the form

$$\langle \psi_{ab;z''}^I | \hat{T}_c | \psi_{ab;z}^I \rangle = \sum_{z'} [F_{b\bar{a}}^{b\bar{a}}]_{(z,z')} \cdot \theta_{z'} \cdot [F_{b\bar{a}}^{b\bar{a}}]_{(z',z'')}^{-1}. \quad (\text{B36})$$

In general, T_c is not a diagonal matrix. However, if the theory is abelian, then one has $z = \mathbf{1}$ and $[F_{ab}^{ab}]_{\mathbf{1}z'} = N_{ab}^{z'}$. In this case, T_c is a diagonal matrix with the matrix elements

$$\langle \psi_{ab;z''}^I | \hat{T}_c | \psi_{ab;z}^I \rangle = \delta_{\mathbf{1},z} \delta_{\mathbf{1},z''} \theta_{z'} N_{b\bar{a}}^{z'}. \quad (\text{B37})$$

3. Mapping class group of genus-2 surface and knot/link invariants

As shown in Fig.1.1, $\text{MCG}(\Sigma_{2,0})$ can be generated by the five Dehn twists around the closed curves a_1, a_2, b_1, b_2 , and c . The modular relations of these generators can be found in Ref.29. In this appendix, with the surgery approach in TQFT, we give an intuitive picture why the representation of $\text{MCG}(\Sigma_{2,0})$ are related to the knots/links invariant that can distinguish MS MTCs.

In Ref.24, based on a computer search, it is found that the simplest knot invariant that can distinguish different MS MTCs with $G = \mathbb{Z}_{11} \rtimes \mathbb{Z}_5$ and the three-cocycle $\omega \in H^3(G, U(1))$ is the so-called figure-eight knot. In Ref.63, for some other motivations, the authors study how to use the representations of $\text{MCG}(\Sigma_{2,0})$ to construct a family of genus-2 pretzel knots including the figure-eight knot. Here we give a short review of this construction.

We consider a solid genus-2 manifold $\mathcal{M}_{g=2}^{3d}$, which is a 3-dimensional open manifold, with $\partial\mathcal{M}_{g=2}^{3d} = \Sigma_{2,0}$. Then we color $\mathcal{M}_{g=2}^{3d}$ by the trivalent graph in (1.2). In TQFT, this colored open 3-manifold represents the wavefunction $|\psi_{(a,\mu),(b,\nu),z}\rangle$. The first question is how to glue two $\mathcal{M}_{g=2}^{3d}$ to form a S^3 . This is fulfilled by gluing two solid genus-2 manifold with the operation:

$$I = T_{b_2} T_{a_2} T_c T_{a_1} T_{b_1}^{-1}, \quad (\text{B38})$$

where T_γ is the representation of Dehn twist around the closed curve γ with the direction labeled in (1.1). If we do Dehn twist

along the opposite direction, then one has $T_{\gamma^{-1}} = T_\gamma^{-1}$. With the operation in (B38), we have

$$\langle \mathcal{M}_{g=2}^{3d} | I | \mathcal{M}_{g=2}^{3d} \rangle = \mathcal{Z}(S^3), \quad (\text{B39})$$

or equivalently, $\langle \psi_{1,1,1} | I | \psi_{1,1,1} \rangle = \mathcal{Z}(S^3) = 1/\mathcal{D}$, where $\mathcal{Z}(S^3)$ denotes the partition function on S^3 , \mathcal{D} is the total quantum dimension of the theory, and the index '1' in $|\psi_{1,1,1}\rangle$ denotes the identity anyon.

Next, one can create a figure-eight knot in S^3 by starting from the following wavefunction defined on a solid genus-2 manifold:



$$(\text{B40})$$

which we denote as $|\psi_{\text{unknot}}^a\rangle$. Based on Eq.(B10), one can expand $|\psi_{\text{unknot}}^a\rangle$ with the complete basis vectors in (1.2) as $|\psi_{\text{unknot}}^a\rangle = \sum_{z,\mu} \sqrt{\frac{d_z}{d_a^2}} |\psi_{(a,\mu),(a,\mu),z}\rangle$. Then it is observed in Ref.63 that the figure-eight knot invariant can be created by

$$\mathcal{Z}(S^3, \text{figure-eight knot}) = \langle \psi_{1,1,1} | I \cdot U | \psi_{\text{unknot}}^a \rangle, \quad (\text{B41})$$

where $U = T_c T_{a_1}^{-1} T_{b_1}^{-1} T_{a_2}^{-1} T_{b_2}$, and $\mathcal{Z}(S^3, \text{figure-eight knot})$ denotes the partition function on S^3 with a figure-eight knot inserted. That is, with the basis vectors in (1.2) and the representations of $\text{MCG}(\Sigma_{2,0})$, one can construct certain nontrivial knot invariants that can distinguish MS MTCs. This illustrates why the $\text{MCG}(\Sigma_{2,0})$ representations can be used to distinguish MS MTCs beyond modular data.

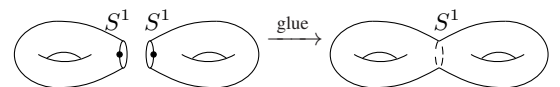
It will be interesting to study how to produce other non-trivial knot/link invariants with the generators of $\text{MCG}(\Sigma_{g,0})$. For example, if we can construct the Borromean ring with the genus- g basis (1.9) and the $\text{MCG}(\Sigma_{g,0})$ representations, then this will indirectly prove that the genus- g data will be able to distinguish *all* the MS MTCs.

Appendix C: More on topological lattice gauge theory

1. Topological invariants based on a punctured torus

For a lattice gauge theory on a manifold with punctures, the Hilbert space is discussed carefully in Ref.58 and 59. Different from the case of a closed manifold, now we need to fix the choice of group elements on the punctures.

The reason why we need to rigid the group elements on the punctures is due to the axiom of gluing in TQFTs. In TQFTs, the gluing of two punctured manifolds along the punctures is well defined only when we choose basepoints at the punctures.^{58,59} Let us consider gluing two punctured tori and gauge bundles along the punctures as follows:



$$(\text{C1})$$

where the punctures are represented by a circle $\partial\Sigma_{1,1} = S^1$. It is noted that the bundle over S^1 with a basepoint has a definite

holonomy $h \in G$. If no basepoint is chosen, the holonomy is determined only up to group conjugation. The two punctures in (C1) can be glued only when the holonomies along the two S^1 agree with each other.

The procedure in (C1) is more straightforwardly understood by considering the gluing in (4.38). In (4.38), the holonomies along the punctures are k and k' , respectively. The two punctured tori can be glued only when $k = k'$. Note this condition is different from $[k] = [k']$, where $[k]$ is the conjugacy class of k . Once we glue the two punctured tori along the puncture S^1 , we are supposed to forget the basepoint, and then the holonomy is only determined up to conjugacy. From this point of view, the gluing in (C1) corresponds to the map

$$\text{gluing} : G \rightarrow \text{Conj}(G) \quad (\text{C2})$$

for the holonomy around S^1 in (C1). This mapping assigns to each $k \in G$ its conjugacy class $[k]$.

Based on the flat connection condition in Eq.(4.26), one can find there are in total $|G|^2$ equivalence classes of bundles over $\Sigma_{1,1}$. That is, in the lattice gauge theory, we have $\dim \mathcal{H}(\Sigma_{1,1}) = |G|^2$. In addition, it is noted that for the modular transformation in Sec.IV B 2, since we need to rigid the holonomy around the puncture, one needs to choose the group element $t = 1$ in Eqs.(4.27) and (4.31). That is, no conjugacy is performed during the modular transformation.

Now let us compare with the result of quasi-particle basis calculation in Sec.III. The dimension of Hilbert space with a fixed anyon z at the puncture on $\Sigma_{1,1}$ has the expression

$$\dim \mathcal{H}(\Sigma_{1,1}, z) = \sum_a N_{a\bar{a}}^z, \quad (\text{C3})$$

where $N_{a\bar{a}}^z$ is the fusion coefficient. The meaning of the expression in (C3) is apparent. By fixing the anyon type z at the puncture, the dimension of the Hilbert space of degenerate ground states is the total number of fusion channels that a and \bar{a} fuse into z for all possible $a \in \Pi_C$. Now by including all the possible anyon types z , one can find the following relation

$$\sum_z \sum_a N_{a\bar{a}}^z d_z = |G|^2, \quad (\text{C4})$$

where on the right is the dimension of Hilbert space $\dim \mathcal{H}(\Sigma_{1,1})$ obtained from the lattice gauge theory of a finite group G . Considering that the integral quantum dimension d_z describes the internal degree of freedom for the anyon z at the puncture, the meaning of (C4) is also straightforward. Eq.(C4) can be rewritten as

$$\sum_z \dim \mathcal{H}(\Sigma_{1,1}, z) \cdot d_z = \dim \mathcal{H}(\Sigma_{1,1}). \quad (\text{C5})$$

This is as expected by considering that in defining $\dim \mathcal{H}(\Sigma_{1,1})$ we have to rigid the holonomy around the puncture without conjugacy. That is, the internal degree of freedom for anyon z at the puncture is included in this definition.

With the discussion above, now we are ready to compare the topological invariants obtained from the lattice gauge theory with those obtained from the quasi-particle basis calculation in Sec.III. It is noted that the $T_{x(y)}^t$ in Eqs.(4.27) and

(4.31) are used as building blocks for the genus-2 case, and therefore a gauge transformation is introduced. For $\Sigma_{1,1}$ itself, to have a definite holonomy around the puncture, we should not perform gauge transformation, and therefore the group elements t are fixed as $t = 1$. Denoting $T_{x(y)} := T_{x(y)}^{t=1}$, the punctured S and T matrices are obtained with the definition $T := T_x$, and $S := T_y \cdot T_x^{-1} \cdot T_y$. Then we can construct the topological invariants with the words in (3.55).

Depending on the holonomy k around the puncture [see (4.25)], the topological invariants for the MS MTCs with $G = \mathbb{Z}_{11} \rtimes \mathbb{Z}_5$ are grouped into three pieces:

$$W_{\Sigma_{1,1}} = W_{\Sigma_{1,1}}^I + W_{\Sigma_{1,1}}^{A_1} + W_{\Sigma_{1,1}}^{A_2}, \quad (\text{C6})$$

which are obtained by tracing over the basis vectors $|g_x, g_y; k\rangle$ in (4.25) with $k \in [1]$, $[a^1]$ and $[a^2]$, respectively.

| Quasi-particle basis result: | | | | |
|------------------------------|------------------------------|---------------------------------------|------------------------------------|----------------------------------|
| $W_1^{(z)}$ | $W_{\Sigma_{1,1}}^{I_0}$ | $\sum_{i=1}^4 W_{\Sigma_{1,1}}^{I_i}$ | $W_{\Sigma_{1,1}}^{I_5, I_6}$ | $W_{\Sigma_{1,1}}^{A_1, A_2}$ |
| $u = 0$ | 9 | -4 | 4 | 22 |
| $u = 1$ | $4 \cos \frac{2\pi}{5} + 5$ | -4 | $4 \cos \frac{2\pi}{5}$ | $22e^{\frac{2i\pi}{5} \times 1}$ |
| $u = 2$ | $4 \cos \frac{4\pi}{5} + 5$ | -4 | $4 \cos \frac{4\pi}{5}$ | $22e^{\frac{2i\pi}{5} \times 2}$ |
| $u = 3$ | $4 \cos \frac{4\pi}{5} + 5$ | -4 | $4 \cos \frac{4\pi}{5}$ | $22e^{\frac{2i\pi}{5} \times 3}$ |
| $u = 4$ | $4 \cos \frac{2\pi}{5} + 5$ | -4 | $4 \cos \frac{2\pi}{5}$ | $22e^{\frac{2i\pi}{5} \times 4}$ |
| Lattice gauge theory result: | | | | |
| $W_1^{(z)}$ | $W_{\Sigma_{1,1}}^I$ | $W_{\Sigma_{1,1}}^{A_1}$ | $W_{\Sigma_{1,1}}^{A_2}$ | |
| $u = 0$ | 45 | 110 | 110 | |
| $u = 1$ | $44 \cos \frac{2\pi}{5} + 1$ | $110 e^{\frac{2i\pi}{5} \times 1}$ | $110 e^{\frac{2i\pi}{5} \times 1}$ | |
| $u = 2$ | $44 \cos \frac{4\pi}{5} + 1$ | $110 e^{\frac{2i\pi}{5} \times 2}$ | $110 e^{\frac{2i\pi}{5} \times 2}$ | |
| $u = 3$ | $44 \cos \frac{4\pi}{5} + 1$ | $110 e^{\frac{2i\pi}{5} \times 3}$ | $110 e^{\frac{2i\pi}{5} \times 3}$ | |
| $u = 4$ | $44 \cos \frac{2\pi}{5} + 1$ | $110 e^{\frac{2i\pi}{5} \times 4}$ | $110 e^{\frac{2i\pi}{5} \times 4}$ | |

TABLE XXVIII. Comparison of the quasi-particle basis results in Table V and the lattice gauge theory results, for $W_{\Sigma_{1,1}}$ with the word $w_1^{(z)}$ in Eq.(3.55).

In comparison with the results obtained from the quasiparticle basis in Sec.III D 1, based on the relation in Eq.(C5), we have the following correspondence:

$$\begin{aligned} W_{\Sigma_{1,1}}^{I, \text{lattice}} &= \sum_{i=0, \dots, 6} W_{\Sigma_{1,1}}^{I_i, \text{q.p.}} \cdot d_{I_i}, \\ W_{\Sigma_{1,1}}^{A_1, \text{lattice}} &= W_{\Sigma_{1,1}}^{A_1, \text{q.p.}} \cdot d_{A_1}, \\ W_{\Sigma_{1,1}}^{A_2, \text{lattice}} &= W_{\Sigma_{1,1}}^{A_2, \text{q.p.}} \cdot d_{A_2}, \end{aligned} \quad (\text{C7})$$

where ‘q.p.’ means the results are obtained from the quasi-particle basis calculation. Let us take $u = 1$ in Table.XXVIII for example. Then we have $W_{\Sigma_{1,1}}^{I, \text{lattice}} = \sum_{i=0, \dots, 6} W_{\Sigma_{1,1}}^{I_i, \text{q.p.}} \cdot d_{I_i} = (4 \cos \frac{2\pi}{5} + 5) - 4 \times 1 + 4 \cos \frac{2\pi}{5} \times 2 \times 5 = 44 \cos \frac{2\pi}{5} + 1$, $W_{\Sigma_{1,1}}^{A_1, \text{lattice}} = W_{\Sigma_{1,1}}^{A_1, \text{q.p.}} \cdot d_{A_1} = 22 e^{\frac{2i\pi}{5} \times 1} \times 5 = 110 e^{\frac{2i\pi}{5} \times 1}$, and $W_{\Sigma_{1,1}}^{A_2, \text{lattice}} = W_{\Sigma_{1,1}}^{A_2, \text{q.p.}} \cdot d_{A_2} = 110 e^{\frac{2i\pi}{5} \times 1}$, where we have used the concrete value of quantum dimensions in Table II. The comparison of topological invariants for other words in Tables XXIX ~XXXIV can be made in a similar way.

| $W_2^{(z)}$ | $W_{\Sigma_{1,1}}^I$ | $W_{\Sigma_{1,1}}^{A_1}$ | $W_{\Sigma_{1,1}}^{A_2}$ |
|-------------|------------------------------|------------------------------------|------------------------------------|
| $u=0$ | 45 | 110 | 110 |
| $u=1$ | $44 \cos \frac{4\pi}{5} + 1$ | $110 e^{\frac{2i\pi}{5} \times 3}$ | $110 e^{\frac{2i\pi}{5} \times 3}$ |
| $u=2$ | $44 \cos \frac{2\pi}{5} + 1$ | $110 e^{\frac{2i\pi}{5} \times 1}$ | $110 e^{\frac{2i\pi}{5} \times 1}$ |
| $u=3$ | $44 \cos \frac{2\pi}{5} + 1$ | $110 e^{\frac{2i\pi}{5} \times 4}$ | $110 e^{\frac{2i\pi}{5} \times 4}$ |
| $u=4$ | $44 \cos \frac{4\pi}{5} + 1$ | $110 e^{\frac{2i\pi}{5} \times 2}$ | $110 e^{\frac{2i\pi}{5} \times 2}$ |

TABLE XXIX. $W_{\Sigma_{1,1}}$ with the word $w_2^{(z)}$ in Eq.(3.55), based on the lattice gauge theory calculation.

| $W_3^{(z)}$ | $W_{\Sigma_{1,1}}^I$ | $W_{\Sigma_{1,1}}^{A_1}$ | $W_{\Sigma_{1,1}}^{A_1}$ |
|-------------|----------------------|------------------------------------|------------------------------------|
| $u=0$ | 265 | 330 | 330 |
| $u=1$ | -65 | $330 e^{\frac{2i\pi}{5} \times 2}$ | $330 e^{\frac{2i\pi}{5} \times 2}$ |
| $u=2$ | -65 | $330 e^{\frac{2i\pi}{5} \times 4}$ | $330 e^{\frac{2i\pi}{5} \times 4}$ |
| $u=3$ | -65 | $330 e^{\frac{2i\pi}{5} \times 1}$ | $330 e^{\frac{2i\pi}{5} \times 1}$ |
| $u=4$ | -65 | $330 e^{\frac{2i\pi}{5} \times 3}$ | $330 e^{\frac{2i\pi}{5} \times 3}$ |

TABLE XXX. $W_{\Sigma_{1,1}}$ with the word $w_3^{(z)}$ in Eq.(3.55), based on the lattice gauge theory calculation.

| $W_4^{(z)}$ | $W_{\Sigma_{1,1}}^I$ | $W_{\Sigma_{1,1}}^{A_1}$ | $W_{\Sigma_{1,1}}^{A_2}$ |
|-------------|----------------------|------------------------------------|------------------------------------|
| $u=0$ | 265 | 220 | 220 |
| $u=1$ | 45 | $220 e^{\frac{2i\pi}{5} \times 3}$ | $220 e^{\frac{2i\pi}{5} \times 3}$ |
| $u=2$ | 45 | $220 e^{\frac{2i\pi}{5} \times 1}$ | $220 e^{\frac{2i\pi}{5} \times 1}$ |
| $u=3$ | 45 | $220 e^{\frac{2i\pi}{5} \times 4}$ | $220 e^{\frac{2i\pi}{5} \times 4}$ |
| $u=4$ | 45 | $220 e^{\frac{2i\pi}{5} \times 2}$ | $220 e^{\frac{2i\pi}{5} \times 2}$ |

TABLE XXXI. $W_{\Sigma_{1,1}}$ with the word $w_4^{(z)}$ in Eq.(3.55), based on lattice gauge theory calculation.

| $W_5^{(z)}$ | $W_{\Sigma_{1,1}}^I$ | $W_{\Sigma_{1,1}}^{A_1}$ | $W_{\Sigma_{1,1}}^{A_2}$ |
|-------------|------------------------------|------------------------------------|------------------------------------|
| $u=0$ | 45 | 110 | 110 |
| $u=1$ | $44 \cos \frac{4\pi}{5} + 1$ | $110 e^{\frac{2i\pi}{5} \times 2}$ | $110 e^{\frac{2i\pi}{5} \times 2}$ |
| $u=2$ | $44 \cos \frac{2\pi}{5} + 1$ | $110 e^{\frac{2i\pi}{5} \times 4}$ | $110 e^{\frac{2i\pi}{5} \times 4}$ |
| $u=3$ | $44 \cos \frac{2\pi}{5} + 1$ | $110 e^{\frac{2i\pi}{5} \times 1}$ | $110 e^{\frac{2i\pi}{5} \times 1}$ |
| $u=4$ | $44 \cos \frac{4\pi}{5} + 1$ | $110 e^{\frac{2i\pi}{5} \times 3}$ | $110 e^{\frac{2i\pi}{5} \times 3}$ |

TABLE XXXII. $W_{\Sigma_{1,1}}$ with the word $w_5^{(z)}$ in Eq.(3.55), based on the lattice gauge theory calculation.

| $W_6^{(z)}$ | $W_{\Sigma_{1,1}}^I$ | $W_{\Sigma_{1,1}}^{A_1}$ | $W_{\Sigma_{1,1}}^{A_2}$ |
|-------------|------------------------------|------------------------------------|------------------------------------|
| $u=0$ | 45 | 110 | 110 |
| $u=1$ | $44 \cos \frac{2\pi}{5} + 1$ | $110 e^{\frac{2i\pi}{5} \times 4}$ | $110 e^{\frac{2i\pi}{5} \times 4}$ |
| $u=2$ | $44 \cos \frac{4\pi}{5} + 1$ | $110 e^{\frac{2i\pi}{5} \times 3}$ | $110 e^{\frac{2i\pi}{5} \times 3}$ |
| $u=3$ | $44 \cos \frac{4\pi}{5} + 1$ | $110 e^{\frac{2i\pi}{5} \times 2}$ | $110 e^{\frac{2i\pi}{5} \times 2}$ |
| $u=4$ | $44 \cos \frac{2\pi}{5} + 1$ | $110 e^{\frac{2i\pi}{5} \times 1}$ | $110 e^{\frac{2i\pi}{5} \times 1}$ |

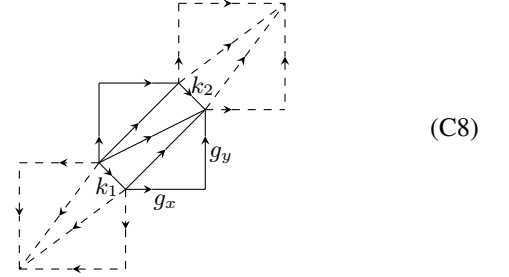
TABLE XXXIII. $W_{\Sigma_{1,1}}$ with the word $w_6^{(z)}$ in Eq.(3.55), based on lattice gauge theory calculation.

| $W_7^{(z)}$ | $W_{\Sigma_{1,1}}^I$ | $W_{\Sigma_{1,1}}^{A_1}$ | $W_{\Sigma_{1,1}}^{A_2}$ |
|-------------|------------------------------|------------------------------------|------------------------------------|
| $u=0$ | 45 | 110 | 110 |
| $u=1$ | $44 \cos \frac{4\pi}{5} + 1$ | $110 e^{\frac{2i\pi}{5} \times 2}$ | $110 e^{\frac{2i\pi}{5} \times 2}$ |
| $u=2$ | $44 \cos \frac{2\pi}{5} + 1$ | $110 e^{\frac{2i\pi}{5} \times 4}$ | $110 e^{\frac{2i\pi}{5} \times 4}$ |
| $u=3$ | $44 \cos \frac{2\pi}{5} + 1$ | $110 e^{\frac{2i\pi}{5} \times 1}$ | $110 e^{\frac{2i\pi}{5} \times 1}$ |
| $u=4$ | $44 \cos \frac{4\pi}{5} + 1$ | $110 e^{\frac{2i\pi}{5} \times 3}$ | $110 e^{\frac{2i\pi}{5} \times 3}$ |

TABLE XXXIV. $W_{\Sigma_{1,1}}$ with the word $w_7^{(z)}$ in Eq.(3.55), based on lattice gauge theory calculation.

2. More punctures

Now we give a brief sketch on how to generalize to the case of a torus with multiple punctures. This will be useful if we study the representations of $MCG(\Sigma_{g,0})$. For example, in the following is the triangulation for a torus with two punctures:



Here we embed this twice-punctured torus in a closed manifold $\Sigma_{3,0}$ of genus $g=3$ for simplicity. In fact, it is straightforward to check it is the building block for $\Sigma_{g,0}$ with $g>2$.

The generalization of the two Dehn twists T_x and T_y [see Eqs.(4.14) and (4.20)] to this case is straightforward, except that now g_x and g_y satisfy the following flat-connection condition (note the group elements are applied from right to left):

$$g_x g_y = k_2^{-1} g_y g_x k_1, \quad (C9)$$

where k_1 and k_2 denote the holonomy around the two punctures in (C8). In addition, the $U(1)$ phase associated to $T_{x(y)}$ transformation in (4.28) and (4.32) will be modified accordingly. There are now four triangular prisms $Y \times I$ as compared to three $Y \times I$ in (4.28) and (4.32). Once T_x and T_y are obtained, one can get the twice-punctured S matrix following the procedure in Sec.IV B.

3. Twisted quantum double of $G = \mathbb{Z}_p$

To illustrate the lattice gauge theory approach in the main text, we consider the example of a twisted quantum double of $G = \mathbb{Z}_p$, with $\omega \in H^3(\mathbb{Z}_p, U(1)) \cong \mathbb{Z}_p$.

There are two motivations for studying this simple example: one is that it mimics the calculation of modular data for MS MTCs with $G = \mathbb{Z}_q \rtimes \mathbb{Z}_p$ (as we mentioned in the main text, the modular data of MS MTCs that depend on the 3-cocyle ω^u are the same as those for $G = \mathbb{Z}_p$); the other is that one can see clearly how the modular transformations act on the genus-1 basis $|g_x, g_y\rangle$ as well as the wavefunction. It

is noted that the modular transformation acts on the basis and the wavefunction in an ‘opposite’ way.

On the manifold $\Sigma_{1,0}$, one can write down the quasi-particle basis in terms of group-element basis. Corresponding to the anyon-type in (2.6), the quasi-particle basis has the form⁵³

$$|g, \tilde{\chi}_m\rangle = \frac{1}{\sqrt{|G|}} \sum_{h \in G} \tilde{\chi}_m^g(h) |g, h\rangle. \quad (\text{C10})$$

where the character $\tilde{\chi}_m^g(h)$ is defined in Eq.(2.18), and has the explicit expression

$$\tilde{\chi}_m^g(h) = e^{\frac{2\pi i}{p^2}(pm+u[g]_p) \cdot [h]_p}, \quad (\text{C11})$$

here $[x]_p$ means $x \bmod p$. Now we consider the effect of Dehn twist $T_{x,y} := \frac{1}{|G|} \sum_{t \in G} T_{x,y}^t$. With some straightforward algebra, one can find that

$$T_x |g, \tilde{\chi}_m\rangle = \frac{1}{\sqrt{|G|}} \sum_{h \in G} \tilde{\chi}_m^g(h) \cdot \omega(g, g^{-1}h, g) |g, g^{-1}h\rangle. \quad (\text{C12})$$

By relabelling $g^{-1}h =: k$, one has

$$\begin{aligned} T_x |g, \tilde{\chi}_m\rangle &= \frac{1}{\sqrt{|G|}} \sum_{k \in G} \tilde{\chi}_m^g(gk) \omega(g, k, g) |g, k\rangle \\ &= \frac{1}{\sqrt{|G|}} \sum_{k \in G} e^{\frac{2\pi i}{p^2}(pm+u[g]_p) \cdot ([g]_p + [k]_p)} |g, k\rangle \\ &= \frac{1}{\sqrt{|G|}} \sum_{h \in G} e^{\frac{2\pi i}{p^2}(pm+u[g]_p) \cdot ([g]_p + [h]_p)} |g, h\rangle. \end{aligned} \quad (\text{C13})$$

Comparing the above equations, it is noted that T_x acts on the basis as $|g, h\rangle \rightarrow |g, g^{-1}h\rangle$, but acts on the wavefunction as $(g, h) \rightarrow (g, gh)$. It is similar for T_y . Eq.(C13) can be rewritten as

$$\begin{aligned} T_x |g, \tilde{\chi}_m\rangle &= e^{\frac{2\pi i}{p^2}(pm+u[g]_p) \cdot [g]_p} |g, \tilde{\chi}_m\rangle \\ &=: \theta_{g, \tilde{\chi}_m} |g, \tilde{\chi}_m\rangle. \end{aligned} \quad (\text{C14})$$

That is, the topological spin of anyon $(g, \tilde{\chi}_m)$ is $\theta_{(g, \tilde{\chi}_m)} = e^{\frac{2\pi i}{p^2}(pm+u[g]_p) \cdot [g]_p}$. Now let us check the effect of modular S transformation defined by $S := T_y \cdot T_x^{-1} \cdot T_y$. After some algebra, one can find that

$$S |g, \tilde{\chi}_m\rangle = \frac{1}{\sqrt{|G|}} \sum_{h \in G} \tilde{\chi}_m^g(h) W(g, h) |h^{-1}, g\rangle, \quad (\text{C15})$$

where one can check explicitly that $W(g, h) = 1$. Therefore, we can obtain

$$\begin{aligned} \langle g', \tilde{\chi}_{m'} | S |g, \tilde{\chi}_m\rangle &= \frac{1}{|G|} \sum_{h, h'} \delta_{g', h^{-1}} \delta_{h', g} [\chi_{m'}^{g'}(h')]^* \cdot \chi_m^g(h) \\ &= \frac{1}{p} [\chi_{m'}^{g'}(g)]^* \cdot \chi_m^g((g')^{-1}) \\ &= \frac{1}{p} [\chi_{m'}^{g'}(g)]^* \cdot [\chi_m^g((g')]^* \\ &= \frac{1}{p} e^{-\frac{2\pi i}{p^2}[p(m[g']_p + m'[g]_p) + 2u[g]_p [g']_p]}, \end{aligned} \quad (\text{C16})$$

where $[g, g'] = 1$ and $|G| = p$. One can find the modular data are the same as those for MS MTCs in (2.20) and (2.22). But as pointed out in the main text, for a prime number $p > 3$, there are only 3 inequivalent categories for $G = \mathbb{Z}_p$, while p inequivalent MS MTCs.

4. Some path integrals on 3-simplices

In this part, we present the expressions of some path integrals on 3-simplices for the cases of a punctured torus and a closed genus-2 manifold, which are used in Sec.IV.

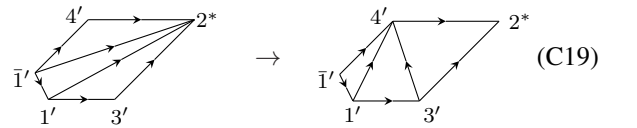
The phase associated to (4.28) is:

$$\begin{aligned} u_x^t(\Sigma_{1,1}) &= Y_{[\bar{1}24], [\bar{1}'4'2^*]} \cdot Y_{[\bar{1}14], [\bar{1}'1'2^*]} \cdot Y_{[134], [1'3'2^*]} \\ &\quad \cdot \omega([\bar{1}'1'], [1'4'], [4'2^*]) \cdot \omega([1'3'], [3'4'], [4'2^*]) \end{aligned} \quad (\text{C17})$$

The first three terms can be expressed in terms of $3 \times 3 = 9$ 3-cocycles as follows

$$\begin{aligned} &Y_{[\bar{1}24], [\bar{1}'4'2^*]} \cdot Y_{[\bar{1}14], [\bar{1}'1'2^*]} \cdot Y_{[134], [1'3'2^*]} \\ &= [\omega([2^* \bar{1}], [\bar{1}2], [24])^{-1} \cdot \omega([4'2^*], [2^* \bar{1}], [\bar{1}2])^{-1} \\ &\quad \cdot \omega([\bar{1}'4'], [4'2^*], [2^* \bar{1}])^{-1}] \cdot [\omega([2^* \bar{1}], [\bar{1}1], [14]) \\ &\quad \cdot \omega([\bar{1}'2^*], [2^* \bar{1}], [\bar{1}1]) \cdot \omega([\bar{1}'1'], [1'2^*], [2^* \bar{1}])] \\ &\quad \cdot [\omega([2^* \bar{1}], [13], [34]) \cdot \omega([3'2^*], [2^* \bar{1}], [13]) \\ &\quad \cdot \omega([1'3'], [3'2^*], [2^* \bar{1}])] \\ &= [\omega(g_y^{-1} g_x^{-1} t^{-1}, g_y, g_x)^{-1} \cdot \omega(t g_x t^{-1}, g_y^{-1} g_x^{-1} t^{-1}, g_y)^{-1} \\ &\quad \cdot \omega(t g_y t^{-1}, t g_x t^{-1}, g_y^{-1} g_x^{-1} t^{-1})^{-1}] \cdot [\omega(g_y^{-1} g_x^{-1} t^{-1}, k, g_y g_x) \\ &\quad \cdot \omega(t g_x g_y t^{-1}, g_y^{-1} g_x^{-1} t^{-1}, k) \cdot \omega(t k t^{-1}, t g_y g_x t^{-1}, g_x^{-1} g_y^{-1} t^{-1})] \\ &\quad \cdot [\omega(g_x^{-1} g_y^{-1} t^{-1}, g_x, g_y) \cdot \omega(t g_y t^{-1}, g_x^{-1} g_y^{-1} t^{-1}, g_x) \\ &\quad \cdot \omega(t g_x t^{-1}, t g_y t^{-1}, g_x^{-1} g_y^{-1} t^{-1})] \end{aligned} \quad (\text{C18})$$

The last two terms in Eq.(C17) come from the transformation as follows:



$$\begin{array}{ccc} \begin{array}{c} 4' \\ \nearrow \quad \searrow \\ 1' \quad 3' \end{array} & \rightarrow & \begin{array}{c} 4' \\ \nearrow \quad \searrow \\ 1' \quad 3' \end{array} \end{array} \quad (\text{C19})$$

and has the concrete expression

$$\begin{aligned} &\omega([\bar{1}'1'], [1'4'], [4'2^*]) \cdot \omega([1'3'], [3'4'], [4'2^*]) \\ &= \omega(t k t^{-1}, t g_y k^{-1} t^{-1}, t g_x t^{-1}) \cdot \omega(t g_x t^{-1}, t g_x^{-1} g_y t^{-1}, t g_x t^{-1}). \end{aligned} \quad (\text{C20})$$

The phase $u_y^t(\Sigma_{1,1})$ associated to (4.32) is

$$\begin{aligned} u_y^t(\Sigma_{1,1}) &= Y_{[\bar{1}24], [\bar{1}'2'3^*]} \cdot Y_{[\bar{1}14], [\bar{1}'1'3^*]} \cdot Y_{[134], [1'4'3^*]} \\ &\quad \cdot \omega([\bar{1}'1'], [1'2'], [2'3^*]) \cdot \omega([1'2'], [2'4'], [4'3^*])^{-1}. \end{aligned} \quad (\text{C21})$$

The first three terms can be expressed in terms of $3 \times 3 = 9$

3-cocycles as follows

$$\begin{aligned}
& Y_{[\bar{1}24],[\bar{1}'2'3^*]} \cdot Y_{[\bar{1}14],[\bar{1}'1'3^*]} \cdot Y_{[134],[1'4'3^*]} \\
&= [\omega([3^*\bar{1}], [\bar{1}2], [24])^{-1} \cdot \omega([2'3^*], [3^*\bar{1}], [\bar{1}2])^{-1} \\
&\quad \cdot \omega([\bar{1}'2'], [2'3^*], [3^*\bar{1}])^{-1}] \cdot [\omega([3^*\bar{1}], [\bar{1}1], [14]) \\
&\quad \cdot \omega([\bar{1}'3^*], [3^*\bar{1}], [\bar{1}1]) \cdot \omega([\bar{1}'1'], [1'3^*], [3^*1]) \\
&\quad \cdot \omega([3^*1], [13], [34]) \cdot \omega([4'3^*], [3^*1], [13]) \\
&\quad \cdot \omega([1'4'], [4'3^*], [3^*1])] \\
&= [\omega(g_y^{-1}g_x^{-1}t^{-1}, g_y, g_x)^{-1} \cdot \omega(tg_xt^{-1}, g_y^{-1}g_x^{-1}t^{-1}, g_y)^{-1} \\
&\quad \cdot \omega(tg_yt^{-1}, tg_xt^{-1}, g_y^{-1}g_x^{-1}t^{-1})^{-1}] \cdot [\omega(g_y^{-1}g_x^{-1}t^{-1}, k, g_yg_x) \\
&\quad \cdot \omega(tg_xg_yt^{-1}, g_y^{-1}g_x^{-1}t^{-1}, k) \cdot \omega(tkt^{-1}, tg_yg_xt^{-1}, g_x^{-1}g_y^{-1}t^{-1}) \\
&\quad \cdot \omega(g_x^{-1}g_y^{-1}t^{-1}, g_x, g_y) \cdot \omega(tg_yt^{-1}, g_x^{-1}g_y^{-1}t^{-1}, g_x) \\
&\quad \cdot \omega(tg_xt^{-1}, tg_yt^{-1}, g_x^{-1}g_y^{-1}t^{-1})]. \tag{C22}
\end{aligned}$$

Note that the above result is the same as that in Eq.(C18). Next, the last two terms in Eq.(C21) come from the the transformation as follows:

$$\begin{array}{ccc}
\begin{array}{c} 2' \\ \nearrow \\ 1' \end{array} & \rightarrow & \begin{array}{c} 2' \\ \nearrow \\ 1' \end{array} \\
\begin{array}{c} \nearrow \\ 1' \end{array} & & \begin{array}{c} \nearrow \\ 1' \end{array} \\
\begin{array}{c} \nearrow \\ 4' \end{array} & & \begin{array}{c} \nearrow \\ 4' \end{array} \\
\begin{array}{c} \nearrow \\ 3' \end{array} & & \begin{array}{c} \nearrow \\ 3' \end{array}
\end{array} \tag{C23}$$

and has the concrete expression as follows:

$$\begin{aligned}
& \omega([\bar{1}'1'], [1'2'], [2'3^*]) \cdot \omega([1'2'], [2'4'], [4'3^*])^{-1} \\
&= \omega(tkt^{-1}, t(g_yk^{-1})t^{-1}, tg_xt^{-1}) \\
&\quad \cdot \omega(t(g_yk^{-1})t^{-1}, t(g_y^{-1}g_x)t^{-1}, tg_yt^{-1})^{-1}. \tag{C24}
\end{aligned}$$

The phase associated to the gauge transformation in (4.41) is:

$$\begin{aligned}
\eta^t(\Sigma_{2,0}) &= Y_{[167],[1'6'7']} \cdot Y_{[\bar{1}17],[\bar{1}'1'7']} \cdot Y_{[\bar{1}57],[\bar{1}'5'7']} \\
&\quad \cdot Y_{[134],[1'3'4']} \cdot Y_{[\bar{1}14],[\bar{1}'1'4']} \cdot Y_{[\bar{1}24],[\bar{1}'2'4']}, \tag{C25}
\end{aligned}$$

The first (last) three terms correspond to the contribution of the left (right) punctured torus. Explicitly, we have

$$\begin{aligned}
& Y_{[167],[1'6'7']} \cdot Y_{[\bar{1}17],[\bar{1}'1'7']} \cdot Y_{[\bar{1}57],[\bar{1}'5'7']} \\
&= [\omega([1'1], [16], [67])^{-1} \cdot \omega([1'6'], [6'6], [67']) \\
&\quad \cdot \omega([1'6], [67'], [7'7])^{-1}] \cdot [\omega([\bar{1}'\bar{1}], [\bar{1}1], [17])^{-1} \\
&\quad \cdot \omega([\bar{1}'1'], [1'1], [17]) \cdot \omega([\bar{1}'1'], [1'7'], [7'7])^{-1}] \\
&\quad \cdot [\omega([\bar{1}'\bar{1}], [\bar{1}5], [57]) \cdot \omega^{-1}([\bar{1}'5'], [5'5], [57]) \\
&\quad \cdot \omega([\bar{1}'5'], [5'7'], [7'7])] \\
&= [\omega(t^{-1}, g_{2,y}, g_{2,x})^{-1} \cdot \omega(tg_{2,y}t^{-1}, t^{-1}, tg_{2,x}) \\
&\quad \cdot \omega(g_{2,y}t^{-1}, tg_{2,x}, t^{-1})^{-1}] \cdot [\omega(t^{-1}, k, g_{2,x}g_{2,y})^{-1} \\
&\quad \cdot \omega(tkt^{-1}, t^{-1}, g_{2,x}g_{2,y}) \cdot \omega(tkt^{-1}, tg_{2,x}g_{2,y}t^{-1}, t^{-1})^{-1}] \\
&\quad \cdot [\omega(t^{-1}, g_{2,x}, g_{2,y}) \cdot \omega(tg_{2,x}t^{-1}, t^{-1}, g_{2,y})^{-1} \\
&\quad \cdot \omega(tg_{2,x}t^{-1}, tg_{2,y}t^{-1}, t^{-1})]. \tag{C26}
\end{aligned}$$

and

$$\begin{aligned}
& Y_{[134],[1'3'4']} \cdot Y_{[\bar{1}14],[\bar{1}'1'4']} \cdot Y_{[\bar{1}24],[\bar{1}'2'4']} \\
&= [\omega([1'1], [13'], [3'4']) \cdot \omega([13'], [3'3], [34'])^{-1} \\
&\quad \cdot \omega([13], [34'], [4'4])] \cdot [\omega([\bar{1}'1'], [1'1], [14'])^{-1} \\
&\quad \cdot \omega([\bar{1}'\bar{1}], [\bar{1}1], [14']) \cdot \omega([\bar{1}1], [14'], [4'4]) \\
&\quad \cdot \omega([\bar{1}'\bar{1}], [\bar{1}2'], [2'4'])^{-1} \cdot \omega([\bar{1}2'], [2'2], [24']) \\
&\quad \cdot \omega([\bar{1}2], [24'], [4'4])^{-1}] \\
&= [\omega(t^{-1}, tg_{1,x}, tg_{1,y}t^{-1}) \cdot \omega(tg_{1,x}, t^{-1}, tg_{1,y})^{-1} \\
&\quad \omega(g_{1,x}, tg_{1,y}, t^{-1})] \cdot [\omega(tkt^{-1}, t^{-1}, tg_{1,y}g_{1,x})^{-1} \\
&\quad \cdot \omega(t^{-1}, k, tg_{1,y}g_{1,x}) \cdot \omega(k, tg_{1,y}g_{1,x}, t^{-1})] \\
&\quad \cdot [\omega(t^{-1}, tg_{1,y}, tg_{1,x}t^{-1})^{-1} \cdot \omega(tg_{1,y}, t^{-1}, t^{-1}g_{1,x}) \\
&\quad \cdot \omega(g_{1,y}, t^{-1}g_{1,x}, t^{-1})^{-1}] \tag{C27}
\end{aligned}$$

In the following we give the expression of $I_L^t(\Sigma_{1,1})$ in Eq.(4.46) [note the difference of ordering from that in (4.41)]:

$$\begin{aligned}
& Y_{[\bar{1}57],[\bar{1}'5'7']} \cdot Y_{[\bar{1}17],[\bar{1}'1'7']} \cdot Y_{[167],[1'6'7']} \\
&= [\omega([\bar{1}'\bar{1}], [\bar{1}5], [57]) \cdot \omega([\bar{1}'5'], [5'7'], [7'7]) \\
&\quad \cdot \omega([\bar{1}'5'], [5'5], [57])^{-1}] \cdot [\omega([\bar{1}'\bar{1}], [\bar{1}1], [17])^{-1} \\
&\quad \cdot \omega([\bar{1}'1'], [1'1], [17]) \cdot \omega([\bar{1}'1'], [1'7'], [7'7])^{-1}] \\
&\quad \cdot [\omega([1'1], [16], [67])^{-1} \cdot \omega([1'6'], [6'7'], [7'6])^{-1} \\
&\quad \cdot \omega([1'7'], [7'6], [67])] \\
&= [\omega(t^{-1}, g_{2,x}, g_{2,y}) \cdot \omega(tg_{2,x}t^{-1}, tg_{2,y}t^{-1}, t^{-1}) \\
&\quad \cdot \omega(tg_{2,x}t^{-1}, t^{-1}, tg_{2,y}t^{-1})^{-1}] \cdot [\omega(t^{-1}, k, g_{2,x}g_{2,y})^{-1} \\
&\quad \cdot \omega(tkt^{-1}, t^{-1}, g_{2,x}g_{2,y}) \cdot \omega(tkt^{-1}, tg_{2,x}g_{2,y}t^{-1}, t^{-1})^{-1}] \\
&\quad \cdot [\omega(t^{-1}, g_{2,y}, g_{2,x})^{-1} \cdot \omega^{-1}(tg_{2,y}t^{-1}, tg_{2,x}t^{-1}, g_{2,x}^{-1}t^{-1}) \\
&\quad \cdot \omega(tg_{2,x}g_{2,y}t^{-1}, g_{2,x}^{-1}t^{-1}, g_{2,x})]. \tag{C28}
\end{aligned}$$

Appendix D: Galois symmetry in the modular data

Galois symmetry plays an important role in proving the equivalence of modular data in MS MTCs. Here we give a brief review of the Galois symmetry in the modular data⁴¹⁻⁴³.

In Refs.41 and 42, it was found that the matrix element S_{ij} of the modular S matrix lies in the cyclotomic field $\mathbb{Q}(\zeta_n)$, which is a number field obtained by adjoining a complex primitive root of unity to \mathbb{Q} , the field of rational numbers. Here $\zeta_n = e^{\frac{2\pi i}{n}}$ is the n -th root of unity. More explicitly, $\mathbb{Q}(\zeta_n)$ can be thought of complex numbers of the form $a_0 + a_1\zeta_n + \dots + a_k\zeta_n^k$, where the coefficients a_i are real. In other words, each S_{ij} (with $i, j \in \Pi_C$) can be written as a polynomial in ζ_n with rational coefficients.

The proof of the above statement is based on the theorem in algebraic number theory that a field extension of \mathbb{Q} is contained in a cyclotomic field $\mathbb{Q}(\zeta_n)$ if the extension is normal and the corresponding Galois group is abelian.^{41,64}

First, let us consider the extension L of \mathbb{Q} generated by $\lambda_{ij} := \frac{S_{ij}}{S_{0j}}$, with $i, j \in \Pi_C$. It is noted that λ_{ij} with a fixed i is the solution of the polynomial equation:

$$\det(\lambda \mathbf{I} - N_i) = 0, \tag{D1}$$

where N_i is the fusion matrix $N_i = N_{ia}^b$. This indicates the extension of \mathbb{Q} is normal. Second, we consider the group element in the Galois group $\sigma \in \text{Gal}(L/\mathbb{Q})$. Since the fusion rules $\lambda_{ai}\lambda_{bi} = N_{ab}^c\lambda_{ci}$ are invariant under the Galois action, then one must have

$$\sigma\left(\frac{S_{ij}}{S_{0j}}\right) = \frac{S_{i\hat{\sigma}(j)}}{S_{0\hat{\sigma}(j)}}. \quad (\text{D2})$$

In other words, there is a group morphism from $\text{Gal}(L/\mathbb{Q})$ to permutations of anyons j with $j \in \Pi_C$. This sends a Galois automorphism σ to a bijection $j \rightarrow \hat{\sigma}(j)$ of Π_C .

Next, we need to generalize Eq.(D2) a little bit. Considering the modular S matrix is unitary and symmetric, and $S_{0j} = S_{0\bar{j}}$, one has $(\frac{1}{S_{0j}})^2 = \sum_i (\frac{S_{ij}}{S_{0j}}) \cdot (\frac{S_{i\bar{j}}}{S_{0\bar{j}}})$. Applying the automorphism σ to this equation, one can obtain

$$\sigma\left(\frac{1}{S_{0j}^2}\right) = \sum_i \left(\frac{S_{i\hat{\sigma}(j)}}{S_{0\hat{\sigma}(j)}}\right) \cdot \left(\frac{S_{i\overline{\hat{\sigma}(j)}}}{S_{0\overline{\hat{\sigma}(j)}}}\right) = \frac{\delta_{\hat{\sigma}(j),\overline{\hat{\sigma}(j)}}}{S_{0\hat{\sigma}(j)} \cdot S_{0\overline{\hat{\sigma}(j)}}}, \quad (\text{D3})$$

based on which we have $\hat{\sigma}(\bar{j}) = \overline{\hat{\sigma}(j)}$, and $\sigma(S_{0j}^2) = (S_{0\hat{\sigma}(j)})^2 = (S_{0\overline{\hat{\sigma}(j)}})^2$. Then one has $\sigma(S_{ij}^2) = \sigma\left(\frac{S_{ij}^2}{S_{0j}^2} \cdot S_{0j}^2\right) = (S_{i\hat{\sigma}(j)})^2$, and therefore

$$\sigma(S_{ij}) = \epsilon_\sigma(i) \cdot S_{\hat{\sigma}(i),j} = \epsilon_\sigma(j) \cdot S_{i,\hat{\sigma}(j)}. \quad (\text{D4})$$

with $\epsilon_\sigma(i), \epsilon_\sigma(j) = \pm 1$. The symmetric property of S matrix is used in Eq.(D4). One can find the extension of \mathbb{Q} generated by S_{ij} is finite and normal. In addition, considering $\sigma_a, \sigma_b \in$

$\text{Gal}(L/\mathbb{Q})$, it can be checked that $\sigma_a\sigma_b(S_{ij}) = \sigma_b\sigma_a(S_{ij})$. That is, $\text{Gal}(L/\mathbb{Q})$ is abelian. Till now, we have seen that the extension of \mathbb{Q} generated by S_{ij} is finite and $\text{Gal}(L/\mathbb{Q})$ is abelian. Then based on Kronecker-Weber theorem we arrive at the conclusion $S_{ij} \in \mathbb{Q}(\zeta_n)$.⁶⁴

The Galois group $\text{Gal}(\mathbb{Q}(\zeta_n)/\mathbb{Q})$ is defined to be the automorphisms of the field $\mathbb{Q}(\zeta_n)$ which fix \mathbb{Q} , and is *isomorphic* to the multiplicative group \mathbb{Z}_n^\times of integers coprime to n . In particular, for any $l \in \mathbb{Z}_n^\times$, we have an automorphism $\sigma_l \in \text{Gal}(\mathbb{Q}(\zeta_n)/\mathbb{Q})$ sending ζ_n to ζ_n^l . More explicitly, under the action of σ_l , $a_0 + a_1\zeta_n + \dots + a_k\zeta_n^k$ is sent to $a_0 + a_1\zeta_n^l + \dots + a_k\zeta_n^{lk}$.

Interestingly, for $\sigma \in \text{Gal}(\mathbb{Q}(\zeta_n)/\mathbb{Q})$, it is found that σ acts on the modular T matrix as follows⁶⁵

$$\sigma^2(T_{ii}) = T_{\hat{\sigma}(i)\hat{\sigma}(i)}. \quad (\text{D5})$$

For the S matrix, in general we have $\sigma^2(S_{ij}) = \epsilon_\sigma(i) \cdot \epsilon_\sigma(j) \cdot S_{\hat{\sigma}(i),\hat{\sigma}(j)}$, where $\epsilon_\sigma(i)$ and $\epsilon_\sigma(j)$ are the same as those in Eq.(D4). For the (twisted) quantum double of a finite group G as studied in this work, it is found that one always have $\epsilon_\sigma(i) = 1$ for arbitrary $i \in \Pi_C$.³⁹ That is, for a (twisted) quantum double of a finite group, we have

$$\sigma^2(S_{ij}) = S_{\hat{\sigma}(i)\hat{\sigma}(j)}. \quad (\text{D6})$$

The Galois action on modular matrices in Eqs.(D5) and (D6) turns out to be useful in proving the equivalence of modular data in MS MTCs (See also Sec.II B 1).

¹ Lev Davidovich Landau and Evgenii Mikhailovich Lifshitz, *Course of theoretical physics* (Elsevier, 1981).

² Xiao-Gang Wen, "Vacuum degeneracy of chiral spin states in compactified space," *Physical Review B* **40**, 7387 (1989).

³ Xiao-Gang Wen and Qian Niu, "Ground-state degeneracy of the fractional quantum hall states in the presence of a random potential and on high-genus riemann surfaces," *Physical Review B* **41**, 9377 (1990).

⁴ Frank Wilczek and Anthony Zee, "Appearance of gauge structure in simple dynamical systems," *Physical Review Letters* **52**, 2111 (1984).

⁵ Xiao-Gang Wen, "Topological orders in rigid states," *International Journal of Modern Physics B* **4**, 239–271 (1990).

⁶ Esko Keski-Vakkuri and Xiao-Gang Wen, "The ground state structure and modular transformations of fractional quantum hall states on a torus," *International Journal of Modern Physics B* **7**, 4227–4259 (1993).

⁷ Yi Zhang and Ashvin Vishwanath, "Establishing non-abelian topological order in gutzwiller-projected chern insulators via entanglement entropy and modular s-matrix," *Physical Review B* **87**, 161113 (2013).

⁸ W Zhu, Donna N Sheng, and F Duncan M Haldane, "Minimal entangled states and modular matrix for fractional quantum hall effect in topological flat bands," *Physical Review B* **88**, 035122 (2013).

⁹ Xiao-Gang Wen, "Topological orders and edge excitations in fractional quantum hall states," *Advances in Physics* **44**, 405–473

(1995).

¹⁰ Alexei Kitaev, "Anyons in an exactly solved model and beyond," *Ann. Phys.* **321**, 2–111 (2006), january Special Issue.

¹¹ Eric Rowell, Richard Stong, and Zhenghan Wang, "On classification of modular tensor categories," *Communications in Mathematical Physics* **292**, 343–389 (2009).

¹² Xiao-Gang Wen, "A theory of 2+ 1d bosonic topological orders," *National Science Review* **3**, 68–106 (2015).

¹³ Michal Mignard and Peter Schauenburg, "Modular categories are not determined by their modular data," *arXiv:1708.02796* (2017), 10.1103/PhysRevLett.99.220405.

¹⁴ Feng Luo, "Grothendieck's reconstruction principle and 2-dimensional topology and geometry," *arXiv preprint math/9904019* (1999).

¹⁵ Parsa Bonderson, Colleen Delaney, Csar Galindo, Eric C. Rowell, Alan Tran, and Zhenghan Wang, "On invariants of modular categories beyond modular data," *Journal of Pure and Applied Algebra* **223**, 4065–4088 (2019).

¹⁶ Gregory Moore and Nathan Seiberg, "Classical and quantum conformal field theory," *Commun.Math. Phys.* **123**, 177–254 (1989).

¹⁷ Daniel Friedan and Stephen Shenker, "The integrable analytic geometry of quantum string," *Phys. Lett. B* **175**, 287–296 (1986).

¹⁸ Cumrun Vafa, "Conformal theories and punctured surfaces," *Phys. Lett. B* **199**, 195–202 (1987).

¹⁹ Cumrun Vafa, "Toward classification of conformal theories," *Phys. Lett. B* **206**, 421–426 (1988).

²⁰ Hidenori Sonoda, "Sewing conformal field theories II,"

- Nucl. Phys. B **311**, 417–432 (1988).
- 21 Fangzhou Liu, Zhenghan Wang, Yi-Zhuang You, and Xiao-Gang Wen, “Modular transformations and topological orders in two dimensions,” arXiv:1303.0829.
 - 22 Paul Bruillard, Siu-Hung Ng, Eric C. Rowell, and Zhenghan Wang, “Rank-finiteness for modular categories,” J. Amer. Math. Soc. **29**, 857–881 (2015).
 - 23 Michal Mignard and Peter Schauenburg, “Morita equivalence of pointed fusion categories of small rank,” arXiv:1708.06538 (2017).
 - 24 Parsa Bonderson, Colleen Delaney, Csar Galindo, Eric C. Rowell, Alan Tran, and Zhenghan Wang, “On invariants of modular categories beyond modular data,” Journal of Pure and Applied Algebra **223**, 4065–4088 (2019).
 - 25 Ajinkya Kulkarni, Michal Mignard, and Peter Schauenburg, “A topological invariant for modular fusion categories,” arXiv:1806.03158 (2018), 10.1103/PhysRevLett.99.220405.
 - 26 P Bonderson, “Non-abelian anyons and interferometry PhD thesis California institute of technology,” Pasadena, California <http://thesis.library.caltech.edu/2447/2/thesis.pdf> (2007).
 - 27 Stephen P. Humphries, “Generators for the mapping class group,” in *Lecture Notes in Mathematics* (Springer Berlin Heidelberg, 1979) pp. 44–47.
 - 28 Bronislaw Wajnryb, “Mapping class group of a surface is generated by two elements,” Topology **35**, 377–383 (1996).
 - 29 Bronislaw Wajnryb, “A simple presentation for the mapping class group of an orientable surface,” Israel J. Math. **45**, 157–174 (1983).
 - 30 Benson Farb and Dan Margalit, *A Primer on Mapping Class Groups (PMS-49)* (Princeton University Press, 2017).
 - 31 Edward Witten, “Quantum field theory and the Jones polynomial,” Commun.Math. Phys. **121**, 351–399 (1989).
 - 32 Vladimir G. Turaev, *Quantum Invariants of Knots and 3-Manifolds*, Vol. 18 (DE GRUYTER, 2010).
 - 33 N. Reshetikhin and V. G. Turaev, “Invariants of 3-manifolds via link polynomials and quantum groups,” Invent Math **103**, 547–597 (1991).
 - 34 N. Y. Reshetikhin and V. G. Turaev, “Ribbon graphs and their invariants derived from quantum groups,” Commun.Math. Phys. **127**, 1–26 (1990).
 - 35 Wade Bloomquist and Zhenghan Wang, “On topological quantum computing with mapping class group representations,” J. Phys. A: Math. Theor. **52**, 015301 (2018).
 - 36 Erik Verlinde, “Fusion rules and modular transformations in 2D conformal field theory,” Nucl. Phys. B **300**, 360–376 (1988).
 - 37 It is known that there exist exactly two non-isomorphic groups of order pq . One is the cyclic group \mathbb{Z}_{pq} which is Abelian, and the other is a non-Abelian group, which is a semidirect product $\mathbb{Z}_q \rtimes \mathbb{Z}_p = \mathbb{Z}_q \rtimes_n \mathbb{Z}_p$.
 - 38 S Mac Lane, “Homology, classics in mathematics springer-verlag, berlin,” Reprint of the 1975 edition (1995).
 - 39 Antoine Coste, Terry Gannon, and Philippe Ruelle, “Finite group modular data,” Nucl. Phys. B **581**, 679–717 (2000).
 - 40 We thank P. Schauenburg for comments on this point.
 - 41 Jan de Boer and Jacob Goeree, “Markov traces and III factors in conformal field theory,” Commun.Math. Phys. **139**, 267–304 (1991).
 - 42 A. Coste and T. Gannon, “Remarks on Galois symmetry in rational conformal field theories,” Phys. Lett. B **323**, 316–321 (1994).
 - 43 Pavel Etingof, Dmitri Nikshych, and Viktor Ostrik, “On fusion categories,” Ann. Math. **162**, 581–642 (2005).
 - 44 A.N. Schellekens and S. Yankielowicz, “Extended chiral algebras and modular invariant partition functions,” Nucl. Phys. B **327**, 673–703 (1989).
 - 45 Denis Bernard, “String characters from kac-moody automorphisms,” Nucl. Phys. B **288**, 628–648 (1987).
 - 46 M. Kreuzer and A.N. Schellekens, “Simple currents versus orbifolds with discrete torsion — a complete classification,” Nucl. Phys. B **411**, 97–121 (1994).
 - 47 See online materials at, <https://sites.google.com/view/mtc-bey>
 - 48 Robbert Dijkgraaf and Edward Witten, “Topological gauge theories and group cohomology,” Commun.Math. Phys. **129**, 393–429 (1990).
 - 49 Michael A. Levin and Xiao-Gang Wen, “String-net condensation: a physical mechanism for topological phases,” Phys. Rev. B **71**, 045110 (2005).
 - 50 Xie Chen, Zheng-Cheng Gu, Zheng-Xin Liu, and Xiao-Gang Wen, “Symmetry protected topological orders and the group cohomology of their symmetry group,” Phys. Rev. B **87**, 155114 (2013).
 - 51 Andrej Mesaros and Ying Ran, “Classification of symmetry enriched topological phases with exactly solvable models,” Phys. Rev. B **87**, 155115 (2013).
 - 52 R. Dijkgraaf, V. Pasquier, and P. Roche, “Quasi hope algebras, group cohomology and orbifold models,” Nucl. Phys. B Proc. Suppl. **18**, 60–72 (1991).
 - 53 Yuting Hu, Yidun Wan, and Yong-Shi Wu, “Twisted quantum double model of topological phases in two dimensions,” Phys. Rev. B **87**, 125114 (2013).
 - 54 Ling-Yan Hung and Xiao-Gang Wen, “Universal symmetry-protected topological invariants for symmetry-protected topological states,” Phys. Rev. B **89**, 075121 (2014).
 - 55 Juven C. Wang and Xiao-Gang Wen, “Non-abelian string and particle braiding in topological order: Modular(3,z)representation and(3+1)-dimensional twisted gauge theory,” Phys. Rev. B **91**, 035134 (2015).
 - 56 Shenghan Jiang, Andrej Mesaros, and Ying Ran, “Generalized modular transformations in (3 + 1)D topologically ordered phases and triple linking invariant of loop braiding,” Phys. Rev. X **4**, 031048 (2014).
 - 57 William S Massey, *A basic course in algebraic topology* (Springer Science & Business Media, 1991).
 - 58 Daniel S. Freed and Frank Quinn, “Chern-simons theory with finite gauge group,” Commun.Math. Phys. **156**, 435–472 (1993).
 - 59 Daniel S. Freed, “Lectures on topological quantum field theory,” in *Integrable Systems, Quantum Groups, and Quantum Field Theories* (Springer Netherlands, 1993) pp. 95–156.
 - 60 Semeon Arthamonov and Shamil Shakirov, “Refined chern-simons theory in genus two,” arXiv:1504.02620 10.1103/PhysRevLett.99.220405.
 - 61 Parsa Bonderson, Lukasz Fidkowski, Michael Freedman, and Kevin Walker, “Twisted interferometry,” arXiv preprint arXiv:1306.2379 (2013).
 - 62 C. McMullen, “Riemann surfaces, dynamics and geometry,” 2018 10.1103/PhysRevLett.99.220405.
 - 63 Semeon Arthamonov and Shamil Shakirov, “Refined chern-simons theory in genus two,” arXiv preprint arXiv:1504.02620 (2015).
 - 64 Daniel A Marcus, *Number fields*, Vol. 8 (Springer, 1977).
 - 65 Chongying Dong, Xingjun Lin, and Siu-Hung Ng, “Congruence property in conformal field theory,” Algebra & Number Theory **9**, 2121–2166 (2015).